

https://dspace.org/

Novel CD4-immunoglobulin fusion proteins as HIV-1 immunotherapeutics

Sojane, Katlego

2013-03-19
http://hdl.handle.net/10539/12558

Downloaded from a DSpace repository. https://dspace.org/

Novel CD4-immunoglobulin fusion proteins as HIV-1 immunotherapeutics

Katlego Sojane

Dissertation submitted to the Faculty of Health Sciences, University of the Witwatersrand, in fulfilment of the requirements for the degree of the Master of Science in Medicine.

Johannesburg, 2012

Declaration

I, Katlego Sojane declare that this dissertation is my own work. It is being submitted for the degree of Master of Science in Medicine in the University of the Witwatersrand, Johannesburg. It has not been submitted before for any degree or examination at this or any other university.

Katlego Sojane

October 2012

Abstract

The initial step of HIV entry into host cells involves the specific binding of gp120 envelope glycoprotein to the cell-surface CD4 protein, expressed by antigen-presenting cells. Extensive systemic infection of host cells by HIV leads to immune dysfunction and ultimately the demise of infected individuals due to AIDS.

The gp120-CD4 interaction (K_D of approximately 2 X 10^{-9} M) is of primary importance to the infection process of HIV and poses a validated therapeutic target. Mutational analyses of CD4 show that residues in domains 1 and 2 of CD4 contribute to gp120 binding. Soluble CD4 protein, composed of domains 1 and 2 or 1 to 4 only, has been shown to compete with cell-surface CD4 for gp120 binding and inhibit host cell infection. Soluble CD4 achieves viral inhibition by uncoating HIV of its envelope proteins, reducing the amount of cell-surface CD4 recognition by gp120 and preventing the cell-to-cell spread of HIV by syncytium formation. Due to the short serum-lifetime of soluble CD4 in the blood, modified forms of it have been generated which contain life-time extending immunoglobulin portions attached to them. The attachment of soluble CD4 in place of immunoglobulin variable regions may increase the valence of CD4 available for gp120 binding and may contribute extra immune effector functions depending on the Fc portion type.

PRO 542 (CD4-IgG2), composed of four two-domain CD4 molecules replacing the variable regions of antibody IgG2, was found to have greater valence and effector functions than soluble CD4. Like soluble CD4, PRO 542 was deemed safe at all concentrations tested during clinical trials; however tests were halted as it could not significantly reduce viral load in patients. In this study, we designed constructs which produced a PRO 542-like protein (kCD4-IgG2^{wt}) in a novel way. Constructs encoding a mutant S60C PRO 542-like molecule (kCD4-IgG2^{S60C}) were also generated to produce a heterotetramer intended to bind gp120 with even higher affinity by virtue of intermolecular redox-disulphide exchange. The uniquely produced heterotetrameric kCD4-IgG2^{wt} and kCD4-IgG2^{S60C} proteins were expressed in Human Embryonic Kidney 293T cells and collected in culture supernatant. Purification of kCD4-IgG2^{wt} and kCD4-IgG2^{S60C} was of limited success; however both proteins could bind Protein-A agarose beads like NIH PRO 542 implying that

their Fc portions were fully folded. Immunoprecipitation tests showed the ability of kCD4-IgG2^{wt} to bind gp120 from HIV-1$_{Bal}$ like PRO 542 confirming the high structural and functional integrity of kCD4-IgG2^{wt}. Finally, surface plasmon resonance studies (SPR) were conducted to evaluate the ability of supernatant-contained kCD4-IgG2^{wt} and kCD4-IgG2^{S60C} to bind six different gp120 molecules from genetically diverse viruses. SPR studies included purified PRO 542 obtained from the National Institutes of Health (NIH), two-domain CD4 (2dCD4^{wt}) and an S60C mutant two-domain CD4 (2dCD4^{S60C}) as positive controls. The culture supernatant from mock transfections was used as a negative control. According to SPR data, supernatant-containing kCD4-IgG2^{wt} binds specifically to gp120 of HIV-1$_{CN54}$, HIV-1$_{SF162}$, HIV-1$_{IN25925}$, HIV-1$_{ZA706010164}$, HIV-1$_{96ZM651}$ and HIV-1$_{Bal}$ like NIH PRO 542, 2dsCD4^{wt} and 2dsCD4^{S60C}. Monoclonal antibody 17b, which binds the co-receptor binding site of gp120 was observed to bind gp120 from HIV-1$_{SF162}$, HIV-1$_{IN25925}$, HIV-1$_{ZA706010164}$ and HIV-1$_{Bal}$, after the gp120s co-receptor binding site was exposed by supernatant-contained kCD4-IgG2^{wt}, NIH PRO 542, 2dsCD4^{wt} and 2dsCD4^{S60C}. Low concentrations of expressed kCD4-IgG^{S60C} did not permit the observation of kCD4-IgG2^{S60C} binding to any of the tested gp120s.

Results obtained from this study showed that the novel strategies employed to produce heterotetrameric kCD4-IgG2^{wt}, which was identical in structure and function to NIH PRO 542, were successful. Novel and functional CD4-based molecules with activity against HIV gp120 may be generated using the strategies described in this study.

Acknowledgements

Sincere thanks to my supervisors, Prof. Maria Papathanasopoulos and Dr. Alexio Capovilla, for guidance and support with this project. I appreciate the opportunity given to me to work in the HIV Pathogenesis Research Laboratory.

Mr. Mark Killick and Mrs. Nichole Cerutti for their advice and assistance in the laboratory.

Members of the HIV Pathogenesis Research Laboratory.

My loving family for moral support.

The Poliomyelitis Research Foundation and the National Research Foundation for financial support.

Table of Contents

Declaration ii

Abstract iii

Acknowledgements v

Table of Contents vi

List of Figures x

List of Tables xii

List of Abbreviations xiii

Chapter 1: Introduction 16

1.1 History of HIV and AIDS 17

1.2 Structural organisation of HIV 17

1.3 HIV life-cycle 18

1.4 Genetic variation of HIV 19

1.5 Clinical progression of individuals infected with HIV-1 20

1.6 Treatment options against HIV-1 infection 22

1.6.1 Reverse transcriptase inhibitors 22

1.6.2 Protease inhibitors 23

1.6.3 Integrase inhibitors 23

1.6.4 Entry inhibitors 23

1.6.5 Highly active antiretroviral treatment (HAART) 25

1.7 Novel strategies to prevent viral entry 25

1.7.1 Cell-surface CD4 25

1.7.2 Structure of gp120-CD4 complexes 26

1.7.3 HIV-1 neutralising antibodies to prevent CD4 mediated viral entry 28

1.7.3.1 Antibody IgG1 b12 31

1.7.3.2 Antibody F105 31

1.7.3.3 Antibody HJ16 32
1.7.3.4 Antibody VRCO1 32
1.7.4 Molecular mimics of cell-surface CD4 to prevent viral entry 33
1.7.4.1 Recombinant soluble CD4-immunoglobulin fusion molecules 34
1.7.4.2 PRO 542 35
1.7.4.3 Chalcogen substitutions in 2dsCD4 38
1.8 Aims of the study 39
Chapter 2: Materials and Methods 40
2.1 Reagents used in this study. 41
2.2 Computer-modelling of the gp120-2dsCD4 interaction 42
2.3 Design of kCD4-IgG2^{wt} and kCD4-IgG2^{S60C} encoding recombinant plasmids. 43
2.4 Transformation of *E. coli* DH5α cells with pcDNA 3.1 (+) constructs. 46
2.4.1 Glycerol stocks production 46
2.4.2 Plasmid preparation, isolation and purification 46
2.5 Agarose gel electrophoresis 47
2.5.1 Characterization of recombinant plasmids (Plasmid DNA digestion with Eco R1) 48
2.6 Optimization of recombinant protein expression in Human Embryonic Kidney 293T cells (HEK293T) 48
2.6.1 HEK293T mammalian cells 48
2.6.1.1 Feeding and passaging of HEK293T mammalian cells 48
2.6.1.2 Preparation of HEK293T frozen cell stocks and thawing 49
2.6.1.3 Quantification of HEK293T mammalian cells 49
2.6.2 Optimization of transient transfections of HEK293T cells 49
2.6.2.1 Optimization of single-transient transfections of HEK293T cells using Lipofectamine™ transfection reagent 50
2.6.2.2 Optimization of single-transient transfections of HEK293T cells using different DNA concentrations and Polyfect transfection reagent 51
2.6.3 SDS-PAGE 51
2.6.4 Western blotting 52

2.6.5 Optimization of transient co-transfections for expression of heterotetrameric kCD4-IgG2^{wt} and heterotetrameric kCD4-IgG2^{S60C} in HEK293T cells 53

2.7 Large scale expression of heterotetrameric kCD4-IgG2^{wt} and heterotetrameric kCD4-IgG2^{S60C} in HEK293T cells 54

2.8 Purification of heterotetrameric kCD4-IgG2^{wt} and heterotetrameric kCD4-IgG2^{S60C} 54

2.8.1 Purification of heterotetrameric kCD4-IgG2^{wt} using the Äkta FPLC system 54

2.8.2 Purification of heterotetrameric kCD4-IgG2^{wt} and heterotetrameric kCD4-IgG2^{S60C} using Protein-A agarose beads 55

2.9 Immunoprecipitation of HIV gp120 with heterotetrameric kCD4-IgG2^{wt} 56

2.9.1 Optimal binding of heterotetrameric kCD4-IgG2^{wt} to Protein-A agarose beads 56

2.9.2 Immunoprecipitation of HIV gp120 by heterotetrameric kCD4-IgG2^{wt} 58

2.10 Surface plasmon resonance (SPR) studies 58

Chapter 3: Results 62

3.1 Computer-modelling of the gp120-2dsCD4 interaction 63

3.2 Design of kCD4-IgG2^{wt} and kCD4-IgG2^{S60C} encoding constructs and the generation of recombinant plasmid stocks 63

3.3 Analysis of purified and digested pcDNA 3.1 (+) recombinant constructs 66

3.4 Single-transfections for optimal transient expression of each construct in HEK293T cells 66

3.4.1 Optimized expression of kCD4-IgG2^{wt} LC in HEK293T cells using different DNA carriers 67

3.4.2 Optimization of protein expression by varying concentrations of pKH^{wt}, pKH^{S60C}, pKL^{wt} and pKL^{S60C} with Polyfect transfection reagent 69

3.5 Co-transfections for transient expression of kCD4-IgG2^{wt} and kCD4-IgG2^{S60C} heterotetrameric proteins 70

3.6 Purification of heterotetrameric kCD4-IgG2^{wt} and heterotetrameric kCD4-IgG2^{S60C} 74

3.6.1 Purification of heterotetrameric kCD4-IgG2^{wt} from serum-free conditioned medium using the Äkta FPLC system 74

3.6.2 Purification of heterotetrameric kCD4-IgG2^{wt} and heterotetrameric kCD4-IgG2^{S60C} using Protein-A agarose beads 74

3.7 Immunoprecipitation of HIV gp120 by heterotetrameric kCD4-IgG2^{wt} bound to Protein-A agarose beads 77

3.7.1 Optimal binding of kCD4-IgG2^{wt} to Protein-A agarose beads 77

3.7.2 Immunoprecipitation of HIV gp120 by heterotetrameric kCD4-IgG2^{wt} bound to Protein-A agarose beads 78

3.8 SPR analysis of gp120 binding to heterotetrameric kCD4-IgG2^{wt} and heterotetrameric kCD4-IgG2^{S60C} 80

Chapter 4: Discussion 88

4.1 The design and synthesis of the kCD4-IgG2^{wt} and kCD4-IgG2^{S60C} encoding expression vectors 89

4.2 Single-expression studies of pKH^{wt}, pKH^{S60C}, pKL^{wt} and pKL^{S60C} 91

4.3 Co-transfection of pKH^{wt} with pKL^{wt} to produce heterotetrameric kCD4-IgG2^{wt}, as well as the co-transfection of pKH^{S60C} with pKL^{S60C} for the production of heterotetrameric kCD4-IgG2^{S60C} 92

4.4 Purification of heterotetrameric kCD4-IgG2^{wt} and heterotetrameric kCD4-IgG2^{S60C} 94

4.5 The immunoprecipitation of gp120 by heterotetrameric kCD4-IgG2^{wt} adsorbed to Protein-A agarose beads 96

4.6 SPR studies 97

Chapter 5: Conclusion 100

Chapter 6: References 103

Chapter 7: Appendices 124

Appendix 1: Nucleic acid analyses reagents and protocols 125

Appendix 2: Protein expression and characterisation related reagents 127

List of Figures

1.1	Structural organisation of an HIV virion, image obtained from Papathanasopoulos (2009) [10]	18
1.2	The disease progression profile of HIV infected individuals obtained from Fauci (1993) [43]	22
1.3	Structure of HIV-1_{HXBC2} gp120 in complex with 2dsCD4 and antibody 17b.	27
1.4	The structure of PRO 542.	36
2.1 A	The structure of kCD4-IgG2^{wt} and kCD4-IgG2^{S60C}.	44
2.1 B	The pcDNA 3.1 (+) vector (5428 bp) used to express the chains of kCD4-IgG2^{wt} or kCD4-IgG2^{S60C}.	45
2.2	The GLC sensor chip used for SPR experiments.	61
3.1	Computer-modelling of the gp120-2dsCD4^{wt} (A) and gp120-2dsCD4^{S60C} (B) interactions.	64
3.2	Amino acid sequence alignments of the kCD4-IgG2^{wt} and kCD4-IgG2^{S60C} heavy (A) and light chains (B).	65
3.3	Agarose gel electrophoresis analyses of *EcoRI* digested and undigested pKH^{wt}, pKH^{S60C}, pKL^{wt} and pKL^{S60C} constructs after purification.	67
3.4	Western blot image showing the protein expression levels of 4 µg and 10 µg of kCD4-IgG2^{wt} LC using Polyfect transfection reagent and Lipofectamine™, respectively.	68
3.5	Western blot image showing the protein expression levels of 2 µg and 4 µg of pKL^{wt}, pKL^{S60C}, pKH^{wt} and pKH^{S60C} transfected with Polyfect transfection reagent into HEK293T cells in 25 cm^3 flasks.	70

3.6 Western blot image showing expressed amounts of kCD4-IgG2^{wt}, NIH PRO 542 standards and control expression culture supernatant, under non-reducing (A) and reducing conditions (B). 72

3.7 Western blot image showing expressed amounts of kCD4-IgG2^{S60C} with an NIH PRO 542 standard and control expression culture supernatant under non-reducing conditions. 73

3.8 A Western blot image showing samples of the steps during the purification process of kCD4-IgG2^{wt}. 76

3.8 B Western blot image showing the analysis of the samples collected during the purification of kCD4-IgG2^{S60C}. 77

3.9 Western blot image showing the binding capacity of Protein-A agarose beads to kCD4-IgG2^{wt} using anti-CD4 antibodies (A) and detection of gp120 using anti-gp120 antibodies (B). 79

3.10 Western blot image of the immunoprecipitation of HIV-1 gp120 Bal by kCD4-IgG2^{wt} adsorbed to Protein-A agarose beads. 80

3.11 The interactions of selected analytes with various immobilised gp120 from HIV clades B and C (A-F), as well as the binding of MAb 17b to the CD4i of various gp120s exposed by the selected analytes (G-L). 83-86

List of Tables

2.1 All the reagents obtained from the NIH AIDS Research and Reference Reagents programme used in this study. 42

List of Abbreviations

2dsCD4	Two-domain soluble CD4
4dsCD4	Four-domain soluble CD4
Å	Angstroms
AIDS	Acquired immunodeficiency syndrome
APS	Ammonium persulphate
BIS	Bisacrylamide
BnMAbs	Broadly neutralising monoclonal antibodies
bp	Base pairs
Cat. no.	Catalogue number
CD4bs	CD4 binding site
CD4bp	CD4 binding pocket
CD4i	CD4 induced epitope
cDNA	Complementary DNA
CDR	Complementary determining region
CoRbs	Co-receptor binding site
CTL	Cytotoxic T-lymphocyte
DMEM	Dulbecco's modified Eagle's medium
DNA	Deoxyribonucleic acid
E. coli	*Escherichia coli*
Env	Envelope glycoprotein
FBS	Fetal bovine serum

Fc	Constant heavy chain regions
FDA	Food and Drug Administration
GALT	Gut associated lymphoid tissue
HAART	Highly active-antiretroviral treatment
HBS	Hepes buffered saline
HC	heavy chains
HCl	Hydrochloric acid
HIV	Human immunodeficiency virus
HTLV	Human T-lymphotropic virus
IN	Indian
KCl	Potassium chloride
kDa	Kilodaltons
kbp	Kilobase pairs
LC	Light chains
MAb	Monoclonal antibody
M	Molar concentration
MPER	Membrane-proximal external region
M-tropic	Macrophage tropic
NaCl	Sodium chloride
ng	Nanograms
NHS	N-hydroxysuccinimide
NIH	National Institutes of Health

nm	Nanometers
nM	Nanomolar
PAGE	Polyacrylamide gel electrophoresis
PBS	Phosphate buffered saline
RU	Response units
ZA	South African
s	Seconds
SFM	Serum free medium
SDS	Sodium dodecyl sulphate
SPR	Surface plasmon resonance
TEMED	N, N, N’, N’-tetramethylethylenediamine
Tris	Tris(hydroxymethyl)aminomethane
wt	Wild-type
ZM	Zambian
µ	Micro

Chapter 1: Introduction

1.1 History of HIV and AIDS

Acquired immunodeficiency syndrome (AIDS), first described in 1981, is a unique disease state which arises when CD4+ T-lymphocytes are severely depleted in persons infected with the human immunodeficiency virus (HIV). Over time, the reduction in CD4+ T-lymphocytes leaves the infected individual highly susceptible to a variety of opportunistic infections and or malignancies which, if left untreated, eventually leads to their death [1, 2]. Within a few years after the first reports in 1981, HIV infection was described in most countries in the world, and was classified as a pandemic. The latest data shows that by the end of 2009, 32.8 million people world-wide were estimated to be living with HIV and approximately 68% of them were from Sub-Saharan Africa (www.unaids.org) [3, 4].

1.2 Structural organisation of HIV

The overall shape of HIV is spherical, with a diameter of between 100 and 120 nm [5, 6]. HIV belongs to the family *Retroviridae*, as it has a genome consisting of two single-stranded plus RNA molecules, which are reverse transcribed to DNA molecules by the viral enzyme reverse transcriptase (Figure 1.1). The RNA genome is encapsulated in a capsid (p24). Surrounding the p24 is the p17 (an outer matrix protein), which is further encased within the viral membrane comprised of the viral gp120 and gp41 envelope glycoproteins and host derived membrane [7-10].

To fulfil other requirements for successful infection of host cells, HIV carries three enzymes within the capsid; protease, integrase and reverse transcriptase derived from the *pol* gene (Figure 1.1). The protease enzyme is essential for the cleavage of Gag-Pol polyproteins during the assembly and maturation of virions while reverse transcriptase and integrase are necessary for viral DNA synthesis and integration, respectively. The regulatory Tat and Rev proteins are critical for regulating the infection processes, along with Nef, Vif and Vpu as accessory proteins that function as virulence factors [8, 10, 11].

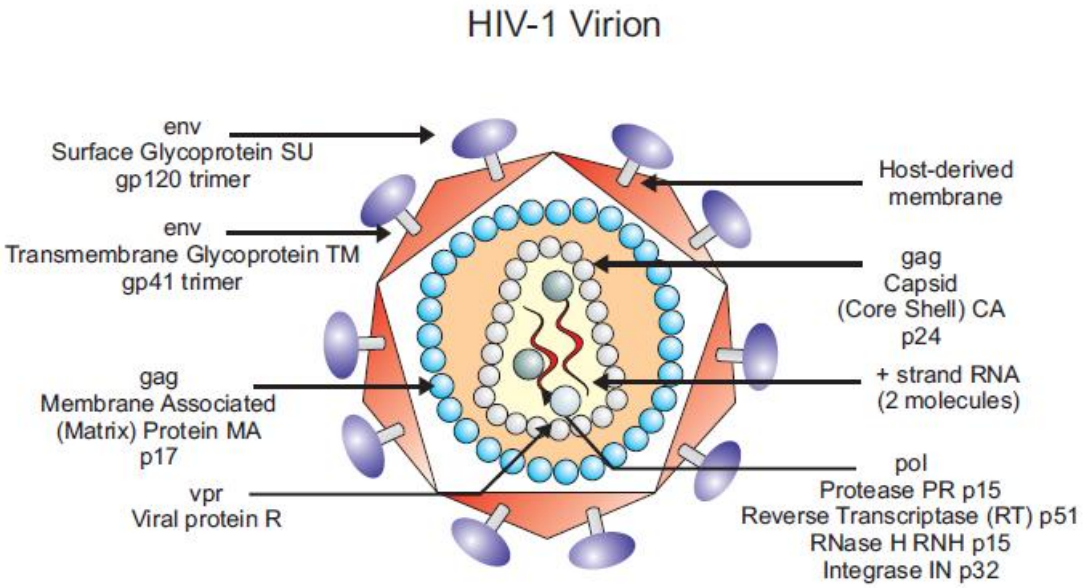

Figure 1.1: Structural organisation of an HIV virion, image obtained from Papathanasopoulos (2009) [10].

1.3 HIV life-cycle

Generally, individuals acquire HIV through sexual (heterosexual and homosexual) contact with an HIV infected person. Other modes of transmission include mother to child transmission, and contact with infected blood. In sexual transmission, HIV is passed through the genito-urinary mucosal surfaces of the infected person to an uninfected person, allowing virus particles access and attachment to CD4+ T-lymphocytes, dendritic cells or macrophages [12]. To initiate entry, the viral surface envelope glycoprotein gp120 sequentially binds CD4 and a co-receptor, either CCR5 or CXCR4, on the surface of the host cell. Following attachment to the host receptors, the formation of the six helix bundle in the transmembrane glycoprotein gp41 and subsequent fusion of the viral and host membranes occurs [13-17].

The viral p24 capsid core is then introduced into the host cell cytoplasm where it uncoats to release the error-prone reverse transcriptase (among other proteins) for commencement of viral cDNA generation [18]. After the viral cDNA is synthesized;

integrase, Vpr and a range of host proteins assemble to form the pre-integration complex. The pre-integration complex moves into the nucleus where the viral cDNA is irreversibly integrated into the host cell genome by the integrase enzyme. When the cell with integrated viral cDNA becomes transcriptionally active, all viral mRNAs are efficiently exported to the cytoplasm where viral proteins are synthesized. The Gag-pol polyprotein is cleaved by the viral protease as required, whereas the viral envelope glycoprotein (env) is produced as a hyperglycosylated gp160 precursor that undergoes proteolytic cleavage in the Golgi apparatus by host proteases to generate gp120 and gp41 subunits, which then assemble into non-covalently attached heterotrimers [14, 19, 20].

Immature virions are ultimately assembled and bud out taking a portion of the host membrane with them, within which the gp120 and gp41 subunits are embedded [17, 21, 22]. Subsequently, the viral protease completes the Gag cleavage sequence to form mature virions capable of new rounds of infection. If the host cell is not transcriptionally active, the viral DNA remains embedded in the host genome and acts as a reservoir for latent infections. One replication cycle takes approximately 2.5 days, and one infected cell can produce up to 130 000 new virions [23-28].

1.4 Genetic variation of HIV

The inability of the reverse transcriptase enzyme to proof-read the cDNA sequences it generates, results in the generation of diverse forms of the virus during each replication cycle. Coupled with the high replicative capacity and immune selective pressures of the host, one finds the diversity of HIV increasing over time. There are two types of HIV: HIV type 1 (HIV-1) and HIV type 2 (HIV-2). Within HIV-1, there are four major groups of HIV-1 , namely M (major), N (non-major), O (outlier) and P, while HIV-2 is subdivided into groups A to G (http://www.hiv.lanl.gov) [3, 4]. Infection with HIV-1 group M is responsible for the major pandemic worldwide [29].

Within group M alone there are 9 subtypes: A to D, F to H, J and K. The *gag* genes of all the subtypes within HIV-1 group M have approximately 15% differences in sequence and approximately 25% differences in their env gene sequences on average between each other [30-36]. Some subtypes are closer in sequence identity than others and even within subtypes; sub-groups can be distinguished, namely sub-subtypes A1 and A2 and sub-subtypes F1 and F2. Notably, subtypes are geographically dispersed. For instance; subtype A of HIV-1 has been isolated around Central Africa, subtype B in North America and Europe, whereas subtype C predominates in Southern Africa and India. Some subtypes are generally found within single countries such as subtypes F, G, J and K; which are found in Romania, Russia, Democratic Republic of Congo and Cameroon, respectively [3, 37]. A small number of subtypes have been identified within group O, but an even lesser amount has been found within group N [38].

Because retroviruses have high propensity to recombine, numerous viruses composed of genetic structures from two or more separate subtypes have often been identified. If these are found in only one dually-infected (or multiply-infected) individual, they are called a unique recombinant form (URF). If an inter-subtype recombinant is transmitted to many individuals, and eventually infects three or more persons who are not epidemiologically related, they become one of the circulating recombinant forms (CRF). To date, 51 CRFs have been characterised within group M isolates of HIV-1 alone, and one CRF within HIV-2 (http://www.hiv.lanl.gov/content/sequence) [3, 4, 37, 39-42].

1.5 Clinical progression of individuals infected with HIV-1

Throughout the course of HIV infection, a number of different stages of disease progress are observed (Figure 1.2) [43].

After transmission of HIV, the stage of acute HIV infection commences and may last a minimum of two weeks and a maximum of approximately 6 months. HIV infected persons experience similar symptoms to person infected with the Influenza virus [44]. In this phase, the virus replicates vigorously and depletes the number of CD4+

T-lymphocytes in the gut-associated lymphoid tissue (GALT), the primary HIV replication site [12]. The expansion of the viral population is curtailed somewhat by the action of cytotoxic T-lymphocytes (CTLs) and HIV-specific antibodies which are recruited by the body to fight the infection [43, 45-47].

The period that follows after acute infection is the clinically asymptomatic stage. In this stage, infected person may recover a large number of their CD4+ T-lymphocytes and establish a viral load set-point [10]. The level of the viral load set-point has been regarded as an important determinant in the progression of infected persons to AIDS. Infected person with lower viral load set-points tend to survive longer than those with higher set-points. Infected individuals may remain in this stage of infection for up to 10 years while remaining infectious (Clinical latency) (Figure 1.2). Towards the end of the asymptomatic stage, large numbers of CD4+ T cells are once again reached [10, 47, 48].

Once the levels of CD4+ T cells are severely reduced, the infected person experiences symptoms from opportunistic infections or malignancies such as Tuberculosis, Candidiasis and Kaposi sarcoma. This stage of immune vulnerability is referred to as the symptomatic stage, with persons generally having a CD4 count of less than 200 CD4+ T cells per cubic millilitre of blood (a normal CD4 count is 1000) and indicates the onset of AIDS [10, 49]. The host immune system then boosts the fight against HIV infection using humoral or cellular responses; however these interventions arise too late in the infection process and rarely suppress the infection completely [43]. In this late stage of infection, virions arise which may employ an alternative chemokine co-receptor, CXCR4, or both CXCR4 and CCR5, further establishing the AIDS state [22, 50]. If the infected persons are not provided with highly active-antiretroviral therapy (HAART) before the symptomatic stage is reach, they generally have increased morbidity and mortality. It is observed that the earlier infected persons are placed on HAART, the slower the progression to AIDS will be. Person entering the AIDS stage of infection rarely survive more than two years without treatment [10, 51-53].

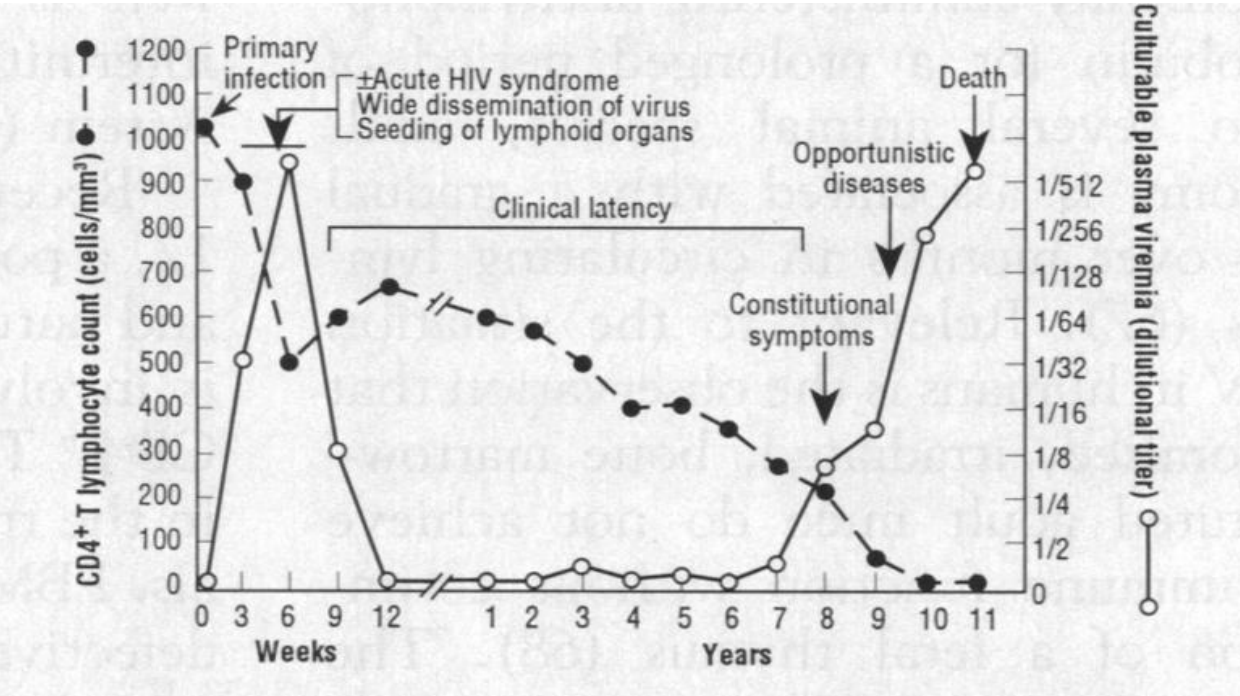

Figure 1.2: The disease progression profile of HIV infected individuals obtained from Fauci (1993) [43].

1.6 Treatment options against HIV-1 infection

To date, there is no cure for HIV-1 infection, however over twenty-five different agents have obtained FDA approval for clinical use in the fight against HIV. The twenty-five compounds could be divided into six different categories according to the targets they act upon [54].

1.6.1 Reverse transcriptase inhibitors

The nucleoside reverse transcriptase inhibitors (Zidovudine, Didanosine, Zalcitabine, Stavudine, Lamivudine, Abacivir and Emtricitabine), non-nucleoside reverse transcriptase inhibitors (Nevirapine, Delavirdine, Efavirenz and Etravirine), and the nucleotide reverse transcriptase inhibitor Tenofovir target and suppress the functioning of HIV reverse transcriptase enzyme [54-57].

1.6.2 Protease inhibitors

To counteract the functioning of the protease enzyme, the inhibitors; Saquinavir, Ritonavir, Indinavir, Nelfinavir, Amprenavir, Lopinavir, Atazanavir, Fosamprenavir, Tipranavir and Darunavir are available [54-56].

1.6.3 Integrase inhibitors

There is only one clinically available drug targeting the HIV integrase enzyme, which is Raltegravir [54-58].

1.6.4 Entry inhibitors

Two entry inhibitors currently have FDA approval: Enfuvirtide, a fusion inhibitor, and Maraviroc, a CCR5 antagonist (www.fda.gov/oashi/aids/virals.html) [59-64].

The G-protein coupled transmembrane CCR5 receptor acts a high affinity receptor for the RANTES and MIP1α, but also assists HIV in entering host cells by acting as a secondary receptor for gp120. The non-peptidic Maraviroc molecule is the first FDA approved CCR5 antagonist, having the ability to prevent HIV gp120 from using the co-receptor binding site (CoRbs) of CCR5 for viral entry processes in a non-competitive manner [65]. Only treatment experienced individuals, harbouring R5 viruses are eligible for salvage treatment with Maraviroc [54, 59, 65-72]. Patients with combinations of R5 and X4 viruses are barred from using Maraviroc as it is feared that they will develop selective pressures in favour of X4 viruses, which are not antagonised by Maraviroc. It is unclear if Maraviroc has the potential to induce a change in co-receptor preferences of HIV itself [54, 59, 61, 65, 72-78]. It has not been investigated if long-term usage of Maraviroc may have oncologic and immunologic disadvantages, however this HIV inhibitor has encouraged the development of other CCR5 antagonists such as Vicriviroc (currently in phase 3 clinical trials) [54-57, 67, 69].

The gp41 subunit of env responsible for HIV fusing to host cells is approximately 345 amino acids in length and is organised into three major substructures. The fusion

protein is composed of an ectodomain, a transmembrane domain and a C-terminal domain. The ectodomain contains a hydrophobic fusion peptide, a polar region, two heptad repeat regions (HR1 and HR2) and a membrane proximal exterior region (MPER) [79]. The HR1 and HR2 regions which are connected together by a disulphide bond within a hydrophilic region between them. The conformational changes induced by gp120 binding to CD4 ultimately lead to the bundling together of three HR1 regions. Thereafter, a hydrophobic groove between the HR1 and HR2 regions folds upon itself which allows the two regions to associate in an anti-parallel fashion, promoting the formation of a six-helical bundle. The formation of the six-helical bundle drives the fusion of host cell and viral membranes [79-81].

Enfuvirtide (T-20) is another drug approved by the FDA which prevents HIV entry into host cells [54, 58]. T-20 is generated by synthesizing a peptide which has the same sequence as the HR2 region of gp120. When the six-helical bundle starts to form during the fusion process, T-20 disrupts the association of the bundles by binding to the HR1 regions [63, 82]. There were no cytotoxic effects observed in *in vitro* tests of T-20 against HIV. In association with an optimized antiretroviral regime, T-20 provides treatment experienced patients with greater than 1. 6 $\log_{10}$ reductions in viral load compared to control groups who only had a 0.764 $\log_{10}$ reduction [63, 64, 82-92]. Resistance to T-20 is known to occur, however the viruses that are resistant to T-20 are generally less fit [63]. In order to reduce the potential of T-20 strains arising, one needs to design peptides which bind more stably to gp41 HR1 and suppress replication of virus greatly. Oligomers or peptides that target the six-helical bundle have been shown to have greater viral suppression activity against HIV. The oligomers have improved helical stabilization motifs making binding to the HR1 regions stronger, in some cases 3600 fold better than the activity of T-20 on the same target. In future, oligomeric gp41 antagonists may improve our armamentarium of entry inhibitors [93].

1.6.5 Highly active antiretroviral treatment (HAART)

Drug regimens comprised of a minimum of three antiretroviral drugs from the different aforementioned categories, given to AIDS patients to extend their lifetime is known as HAART [54-58]. For example, first line regimens will incorporate two nucleoside reverse transcriptase inhibitors, and one non-nucleoside reverse transcriptase inhibitor. Notwithstanding the large amount of therapies available to treat and extend the lives of HIV positive patients, drug resistance and treatment failures still arise. Unfortunately, HAART requires the patient to adhere stringently to the therapy for the rest of their lives, may provide harmful side-effects and the potential to allow drug-resistant variants to arise [72, 87]. Other treatments are being developed to provide more sterilizing and functional cures of HIV [10, 54, 56, 57, 94].

1.7 Novel strategies to prevent viral entry

An improved understanding of the interaction between the viral envelope glycoprotein and the host cell has implications for vaccine immunogen design as well as novel antiretroviral drug design. The attachment process of HIV to host cells is largely dependent on gp120 interacting with CD4 to reveal the gp120 co-receptor binding site (CoRbs), so that it may interact with a chemokine receptor, either CCR5 or CXCR4. All HIV-1 strains require CD4 to initiate entry (with the exception of viruses infecting neural tissue) [95-98], making the CD4-gp120 interaction an important antiretroviral drug target.

1.7.1 Cell-surface CD4

Cell-surface CD4 receptors naturally interact with major histocompatibility complex II (MHC II) in antigen recognition processes facilitated by thymus derived lymphocytes (T-lymphocytes). Monocytes and macrophages also have CD4 receptors on their surfaces, but are distributed in lesser amounts relative to T-lymphocytes [99]. Distinct features of the non-polymorphic 55 kDa CD4 protein are the four tandem extracellular domains which comprise of 372 amino acids, resembling the domains of immunoglobulins and twenty-three transmembrane amino acids that are connected to a thirty-eight amino acid cytoplasmic segment [100, 101]. HIV subverts the normal functioning of CD4 as an antigen-presenting agent and uses it as a

primary receptor for attachment to host cells [102]. The affinity and avidity of gp120 for CD4 is high, providing the interaction with a relatively low dissociation constant of approximately 10^{-9} M [103, 104].

1.7.2 Structure of gp120-CD4 complexes

The gp120 molecule is composed of five variable regions and five constant regions. There are nine or ten possible disulphide bonds in the gp120 molecule which assist in the folding and or functioning of the protein. The C1 region of gp120 has a disulphide bond between residues 54 and 57; region C2 has disulphide bonds between residues 218-247 and 228 and 239. One disulphide bond links the C3 and C4 regions while a disulphide bond is found at the base of V3 and V4 regions also [105]. Loops of the gp120 molecule comprise of 3 disulphide bonds between residues 119 and 205, residues 129 and 196 as well as residues 131 and 157 [105-107]. Not all the disulphide bonds of gp120 are important for functioning. In fact, only five disulphides are important for the functioning of gp120 while the other four or five disulphides contribute to the structural integrity of the protein only. Two disulphide bonds of gp120 do not contribute to the replication or the functioning of the virus and those are between residues 119 and 205 as well as 378-445, however; the disulphide bonds of residues 57-74, 218-247, 228-239 and 296-331 are important for proper functioning and replication of viruses. Mutation of the disulphides between residues 126-196, 131-157 and 598-604 allow the protein to fold properly, however removal of any of these three disulphides do not provide the virus with the capability of replicating [105, 107].

The crystal structure of core gp120, derived from an HIV-1 clade B HXBC2 strain, in complex with 2dsCD4 and antibody 17b was solved in 1998 by Kwong *et al* (Figure 1.3) [106]. The structure elucidated how the conformational changes of gp120 protein are induced post-CD4 engagement and how the co-receptor binding site may be exposed for interaction with a chemokine receptor [106, 108, 109]. The gp120 protein that was crystallised with CD4 and antibody 17b was extensively modified, however, with variable regions and termini severely truncated, and glycosylation sites altered [22, 106].

Created by the interface of the inner and outer domains of gp120 is a hydrophobic binding pocket that is specific for binding CD4 protein (Figure 1.3), which provides HIV with the capability of attaching to CD4+ T-lymphocytes, monocytes, dendritic cells and brain microglia [106]. Upon binding, phenylalanine 43 of CD4 enters deep inside the gp120 binding pocket, making extensive contacts with a number of gp120 residues. The contacts made by CD4 within the CD4 binding site (CD4bs) equate to approximately 800 $Å^2$ of the gp120 surface [106]. Following CD4 binding the V2 loop of gp120 moves from occluding the CD4 induced epitope (CD4i), the V3 loop and the bridging sheet mini-domain. The V2 and V3 loops move in such a way as to expose and stabilize the chemokine receptor binding site, after CD4 binding. Monoclonal antibody 17b was found to bind the CD4i more readily after CD4 had bound gp120 (Figure 1.3), however minimal binding may still be accomplished without the conformational changes induced by CD4 binding to gp120 [22, 106, 110].

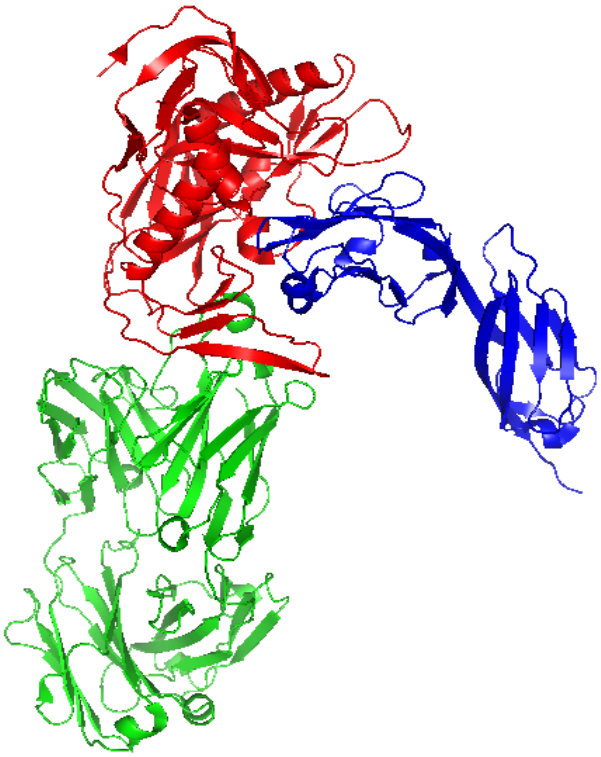

Figure 1.3: Structure of HIV-1_{HXBC2} gp120 in complex with 2dsCD4 and antibody 17b. The crystal structure of 2dsCD4 and the CD4i antibody 17b bound to gp120 (PDB ID: 1G9M) was generated by Kwong *et al* (1998) [106]. The image was viewed

using The PyMOL Molecular Graphics System, evaluation version 1. 2. 8, Schrodinger, LCC. The gp120 protein is coloured red whilst 2dsCD4 and antibody 17b are coloured blue and green respectively.

Several other models, crystal structures and cryoEM tomography structures have been published of unliganded gp120 and gp120 in complex with antibodies, which have assisted with the elucidation of the conformation changes undertaken by gp120 during host cell attachment [6, 14, 17, 21, 106, 108, 111-117]. The structures have further helped elucidate the conformations and epitopes within gp120 that are necessary for the entry process, as well as the mechanisms of antibody mediated neutralization.

1.7.3 HIV-1 neutralising antibodies to prevent CD4 mediated viral entry

In time, it may be possible to reduce HIV infection by virtue of a vaccine; however current attempts at eliciting vigorous antibody responses against HIV have been disappointing. HIV has the ability to mask multiple conserved epitopes with a glycan shield in its outer domain and evolve its sequences by mutations [14, 118]. It is, therefore, difficult for the adaptive immune response to combat the virus effectively. Pre-exposure prophylaxes seem to be attractive interventions to reduce HIV infection as they protect individuals from contracting the virus or prime their immune systems for the infection [119-126]. A comprehensive, tiered categorization of HIV-1 isolates has been created to organise viral strains and subtypes according to their sensitivities of neutralisations. Tier 1 isolates are most susceptible, tier 2 viruses moderately susceptible and tier 3 viruses are least susceptible to neutralisation by known antibodies. It is envisioned that vaccine design will be based on antibodies that neutralise a large amount of tier 1 and tier 2 HIV-1 viruses as those viruses are most prevalent [127]. HIV-1 infected patients with broadly neutralising sera are found to produce anti-gp120 CD4bs site antibodies more than antibodies targeting other regions. Because of the conservation of the CD4bs sequence and the accessibility of the epitope by antibodies, it may be profitable to create immunogens with high structural and chemical similarity to the CD4bs epitopes for vaccine purposes. The

current array of anti-CD4bs antibodies also provide one with a scaffold for designing anti-gp120 antagonist [128-134].

Walker *et al* (2010) assessed the serum neutralising antibody specificities in non-clade B carriers of HIV. All the patients studied had displayed strong, broad and potent serum neutralising activity against recombinant gp120 (rgp120) and trimeric gp140. One third of the patients had unidentifiable neutralising specificity; however it is presumed that those neutralising antibodies target quaternary structural epitopes of env trimers [135]. A group of patients had antibodies recognising recombinant trimeric gp140 much better than rgp120 indicating that those antibodies are more efficient at targeting a trimeric gp120 foldon than single rgp120 or that they recognise gp41 epitopes. It was also presumed that the recognition efficacy of epitopes by these antibodies would vary amongst isolates and trimeric gp140 foldons. Even though 30% of the donors participating in the study had sera containing antibodies that target the membrane-proximal external region (MPER), these antibodies did not considerably affect the overall activity of the sera [128, 129, 135]. The data suggested that antibodies targeting the MPER are rare and not generated in large amounts compared to antibodies that target other regions. Predominantly, broadly neutralising monoclonal antibody (bnMAbs) that target the CD4-binding site (CD4bs) and CoRbs are most abundant in the donor serum [128, 135]. Donors displaying serum with low neutralisation breadth and activity may have numerous antibody types of varying specificity, while some donors have fewer antibody types and less specificity, but with great neutralisation breadth and potency [129, 135, 136]. Moreover, some patients have different antibodies that target the same or overlapping epitope and their sera generally provide greatest neutralising breadth and potency. Twenty one percent of antibodies generated amongst donors targeted either the same or overlapping epitopes of those of monoclonal antibody PG9 and PG16, 26% of serum antibodies targeted the N-glycan of residue 332 of Env, 26% of antibodies targeted the CD4bs and/or CoRbs and another 21% of the antibodies were sensitive to the I165A mutation of env. Interestingly, the remaining 6% of antibodies generated were directed at unknown (cryptic) epitopes, presumably arising from quaternary structures of full length env trimers [135]. Another strategy that may be employed is identifying cryptic, conserved epitopes and finding ways to elicit antibodies against those epitopes [137].

It has been shown that priming the immune systems of non-human primates with neutralizing antibodies may have a protective effect against HIV acquisition (passive immunisation) [138-140]. Alternatively, the neutralising antibodies may be used as templates to generate molecules with enhanced anti-HIV activity. A large number of antibodies have been found to be elicited after infection with HIV which target conserved and variable regions of HIV envelope protein [128]. Some antibodies are capable of neutralising HIV from many different subtypes and are referred to as broadly neutralising monoclonal antibodies (bnMAbs). It is unknown when bnMAbs will be developed by patients and which regions of env they would target. It is predicted that after approximately 2.5 years post HIV infection, bnMAbs are generated and in some case just after 1 year. If the patient does not generate bnMAbs within 2 years of infection, it is unlikely that they will generate bnMAbs [135]. The bnMAbs generated target conserved motifs of env such as the CD4bs of the env trimers [117, 120, 141]. It is unclear, however, why some antibodies show limited neutralising potential for various strains and why others are broadly neutralising [142].

The angle of recognition is one factor which may determine how potent two antibodies, with the same epitope will be, if they have different neutralization breath [14, 116, 117]. Notably, antibodies that recognize more variable regions of env may be rendered ineffective after some time as the variable regions increase in length or gain mutations due to viral evolution. These antibodies, targeting variable regions, are usually generated early on in infection, but they have limited neutralising capacity compared to those antibodies in late infection [135]. Patients who generate antibodies to variable regions of env are more susceptible to viral escape than those having antibodies that target conserved regions [143]. Recently, bnMAbs that target variable regions and show great potency have been discovered. These antibodies which target quaternary env epitopes of HIV display comparable efficacy to antibodies targeting the CD4bs [113, 135, 144-147].

1.7.3.1 Antibody IgG1 b12

Understanding how anti-HIV antibodies are elicited by the body will improve vaccine design initiatives. As highlighted before, it is observed that most anti-HIV antibodies which are elicited by patients recognize conserved regions of env. One of the antibodies that recognize the CD4 binding site of gp120 is antibody b12 which was isolated from the bone marrow of a patient who was asymptomatic but seropositive for 6 years [148, 149]. When tested against a variety of HIV strains belonging to subtype B, b12 was shown to neutralize 75% of the strains, it also reacted with more than 50% of strains belonging to subtypes A-D and one strain of subtype E [149]. Passive immunization of human peripheral blood leukocytes in severe combined immunodeficient mice (hu-PBL-SCID) with b12 can protect these mice from viral challenge even several hours post treatment [150]. The global structure of b12 is asymmetric; it has an 18 amino acid long CDR H3 region with a tryptophan residue at the tip [120]. According to the crystal structure of gp120 in complex with b12, b12 targets the outer domain of gp120 like CD4, but also contacts V1 and V3 regions of gp120, thus allowing it to neutralize approximately 40% of all known HIV-1 subtypes [120, 148, 151, 152]. Other anti-CD4bs antibodies or agents may act as CD4 analogues, binding in such a way as to permit gp120 to refold and expose its co-receptor binding site [6, 153-156]. Antibody b12, however, does not allow gp120 to reveal its co-receptor binding site after binding [157]. Notwithstanding the breadth and potency of neutralization displayed by b12, more efficacious CD4bs bnMAbs are being discovered.

1.7.3.2 Antibody F105

Antibodies F105 and b12 target overlapping epitopes; however the degree of neutralisation between them differs [14]. Antibody b12 neutralises a wider panel of HIV-1 strains and more potently. Both F105 and b12 have relatively long complementary determining region (CDR) H3 regions, but that of b12 is longer consisting of 18 residues compared to F105 with 15 residues [158-160]. The longer length of b12 CDR H3 region may account for its better neutralising capacity as it accesses the hydrophobic CD4 binding pocket deeper than the F105 CDR H3. Unlike b12, F105 has an apical CDR H3 phenylalanine 100A residue that accessed

the CD4bs much like phenylalanine 43 of CD4. Antibody b12 uses an apical CDR H3 tryptophan 100A to access the CD4 phenylalanine 43 binding pocket instead [160]. F105 binds to the CD4bs of gp120 with its heavy chain residues in a similar way to CD4. In fact, arginine 59 of CD4 and arginine 100F of F105 both interact with aspartic acid 368 of gp120 analogously [14]. The CD4 and F105 bound states of gp120 are highly similar; overlaying CD4 bound or F105 bound states of gp120 provides an RMSD of approximately 1.97 angstroms (Å). B-cells generating b12 have undergone more affinity maturation (by somatic hypermutation) than those producing F105, evident in the greater amount of germ-line V and J region mutations experienced by b12 producing B-cells (F105 has 13 mutations whereas b12 has 45 mutations) [160].

1.7.3.3 Antibody HJ16

An antibody molecule that provides similar breadth of neutralisation and activity to antibody b12 against HIV is HJ16 [126, 129]. Unlike antibody b12, HJ16 was isolated from a patient infected with HIV of clade C. Antibody HJ16 neutralises approximately one third of all HIV-1 virus and targets the region proximal to the CD4bs [129]. Interestingly, HJ16 selectively neutralises multiple tier-2 pseudoviruses, making it a candidate employable for vaccine design strategies. It has been shown to inhibit the binding of soluble CD4 (sCD4) to HIV gp120, but shows incomplete inhibition of antibody b12 to gp120. HJ16 and b12 are found to recognise non-overlapping, discontinuous epitopes of the CD4bs which are proximal to each other [126, 129]. Other CD4bs antibodies along with b12 are unable to neutralise D368R gp120 mutants, however the mutation does not affect the activity of HJ16 making it a viable option for viruses resistant to most anti-CD4bs antibodies. Moreover, the D368R gp120 mutants are bound more tightly by HJ16 compared to wild-type gp120 [14, 129, 151].

1.7.3.4 Antibody VRCO1

Another antibody that recognizes the CD4 binding site (CD4bs) of gp120 is VRC01. No other known antibody shows more potency and breadth in neutralisation than

VRC01, which neutralises 91% of HIV-1 subtypes. Using computer-assisted protein design, recombinant env probes were generated to specifically identify CD4bs antibodies from a population of B-cells [116, 117, 141]. Wu *et al* (2010) successfully isolated a somatic variant of VRC01 and named it VRC02 as well as a unique IgG1 clone named VRC03 using the same computer-assisted protein design strategy [141]. Interestingly, VRC01 and VRC02 have identical CDR H3 sequences and both are highly somatically mutated. Compared to the putative germ-line sequences, VRC01 and VRC02 nucleotide sequences are 32% divergent in the variable heavy encoding (VH) region and 17-19% in the variable kappa encoding (VK) region. Much of VRC01 neutralisation success is based on its ability to mimic the binding of CD4 to gp120. B-cells producing VRC01 have undergone extensive affinity maturation processes to enhance the binding capacity of the VRC01 to gp120, evident in the unique structure of the antibody [116]. Crystal structural data shows the structures of gp120 post VRC01 or CD4 binding are almost identical, deviating from each other minimally [117]. In spite of the great activity of VRC01 against HIV-1, the env probes used to generate the antibody were modified to have residues homologous to SIV gp120 and some residues not related to gp120 sequences. The probes also had variable regions 1 and 3 regions removed, so it is unclear how the variable regions of gp120 would affect the actions of VRC01, 2 or 3 [116, 117]. It remains to be seen if a patient can generate VRCO1-like antibodies, independently, with similar potency to env trimers.

1.7.4 Molecular mimics of cell-surface CD4 to prevent viral entry

Considering that HIV generally requires CD4 for virion attachment to host cells, molecules that resemble cell-surface CD4 (structurally and chemically) would compete for binding to gp120 protein and reduce the amount of virus attaching to host cells [153, 161-167]. Molecular mimics of cell-surface CD4 such as recombinant 2dsCD4 or 4dsCD4 do not have a transmembrane peptide and cytoplasmic tail and have been used as immunotherapeutic agents against HIV infections. These soluble versions of CD4 behave as ‘molecular decoys’, because they have the ability to mimic the CD4-gp120 interaction, disrupt the non-covalent associations of env subunits and cause the premature shedding of virion env proteins [164, 165, 168-

181]. The differences in activity between 2dsCD4 and 4dsCD4 against HIV are negligible, because domains 3 and 4 of CD4 or 4dsCD4 do not contribute significantly or directly to gp120 binding [182]. Both forms of soluble CD4 have the gp120-binding amino-terminal domain 1 of CD4 (amino acids 1-92) which shares 32% homology with immunoglobulin variable regions and domain 2 which is intimately associated [183].

Several groups have described targeting HIV-1 by using recombinant, soluble CD4-based therapies [171, 173-177, 184-191]. Ongoing research in the field aims to discover new ways of generating the CD4-based therapies and improving their pharmacokinetic properties.

1.7.4.1 Recombinant soluble CD4-immunoglobulin fusion molecules

Soluble CD4 portions were genetically fused to IgG1 and IgM constant portions to block HIV infectivity and reduce syncytia formation [162, 163, 182, 192]. Arthos *et al* (2002) later improved the avidity of CD4-IgG1 by creating polymeric fusions thereof [193]. A large number of CD4-immunoglobulin fusion variants have been described with different effector functions and avidity levels [153, 162, 165, 166, 168, 193-195]. Allaway *et al* (1993) and have shown that a smaller bivalent CD4-γ2 fusion protein can act synergistically with drugs that target other regions of gp120 and prevent HIV-1 mediated cell fusion [196]. It is predicted that patients who are capable of producing antibodies against the V3 region of gp120 and gp41 subunits would therefore have an enhanced ability of neutralizing HIV-1 when supplemented with a CD4-based immunotherapeutic. Syncytia formations have been found to catalyse the spread of HIV-1 virions between uninfected and infected cells. To this end, combination therapies that incorporate CD4-based molecules and other entry inhibitors would considerably reduce HIV infection of host cells, syncytia formation and delay the onset of AIDS [119, 153, 196-198].

1.7.4.2 PRO 542

PRO 542 (CD4-IgG2) is a chimeric molecule composed of two-domain soluble CD4s (2dsCD4) attached to the Fc and light chain kappa portions of human IgG2 (Figure 1.4). PRO 542 is able to bind to the discontinuous CD4bs epitope of gp120 which naturally recognizes cell-surface CD4 [153, 181, 196, 199]. In comparison with 2dsCD4 or 4dsCD4, PRO 542 is significantly more effective in neutralizing HIV-1 plasma, *ex vivo*, and can also neutralize T-cell line-adapted viruses and primary isolates of HIV-1 [6, 153, 200-205]. The tetrameric PRO 542 resembles naturally occurring antibodies structurally, due to the soluble CD4 moieties having immunoglobulin-like structure [6, 153]. To date, there is no crystal structural information showing the full structure of PRO 542 or PRO 542-gp120 complexes. When observing immunoelectron microscopy images of PRO 542-HIV complexes, however, one may identify four irregular shaped lobes around a smaller structure. The lobes are presumed to be gp120 and the centre structure being an Fc portion of PRO 542. Therefore, one PRO 542 molecule has the capacity to bind to four gp120 molecules as it has four 2dsCD4 domains that contain gp120 binding sites which extend flexibly into the solvent environment [6, 153, 196-200, 204].

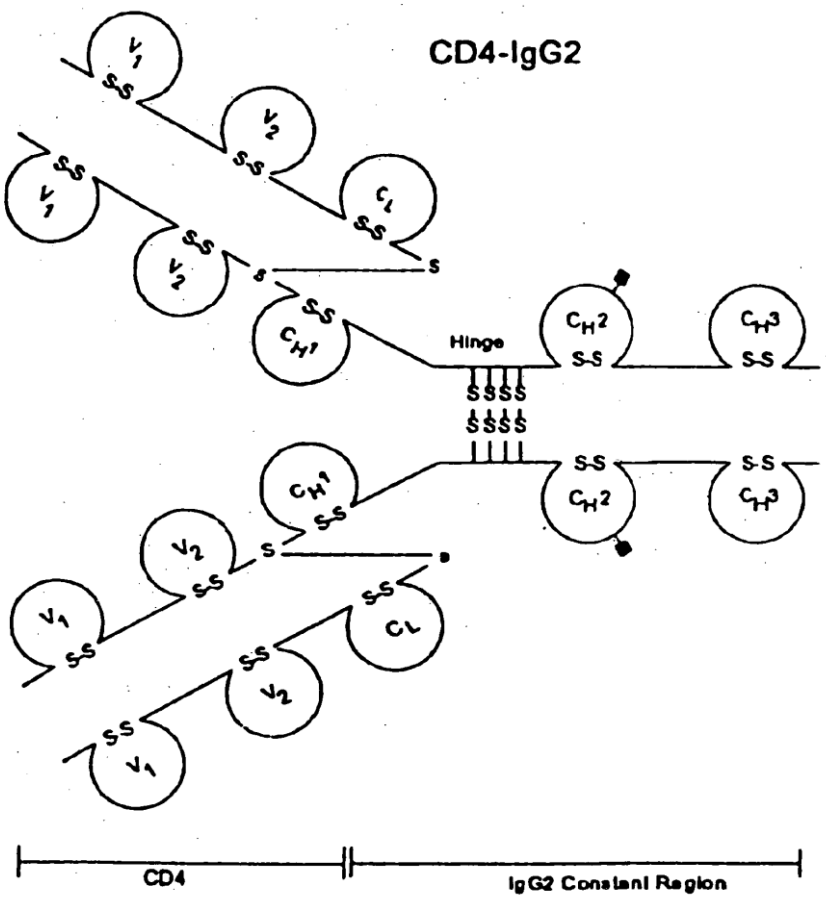

Figure 1.4: The structure of PRO 542. The structure of PRO 542 (CD4-IgG2) was obtained from Allaway *et al* (1995) [153].

The human IgG2 Fc portion plays a number of structural and functional roles in PRO 542 molecules. Structurally; the Fc portion acts as a scaffold that holds the 2dsCD4 moieties in relatively close proximity to each other and allows increased potential of the tetrameric molecule to bind more than one gp120 molecule [6, 119, 153, 162, 166, 199]. Functionally; the Fc portion reduces the rate of the 2dsCD4 catabolism in the human body, thus extending the half-life of 2dsCD4 moieties by three to four days, compared to minutes without the Fc portion [153, 166, 181, 196, 199, 202, 206-208]. Depending on the Fc portion used, one may change the type antibody-dependent cell-mediated cytotoxicity (ADCC) against HIV or other immune effector responses [162, 163, 199]. Another benefit of attaching 2dsCD4 moieties to IgG2 Fc portions is the potential transfer of immune responses between mother and foetus

using Fc dependent receptors (passive immunity via the transcytosis mechanism) [162, 166, 199]. The high affinity Fc receptor 1 (FcR1) binds monomeric IgG as well as antigen-IgG complexes. Although FcR1 interacts with IgG isotopes 1, 3 and 4, it is inert to IgG2. The low affinity FcR2, however, does interact with IgG2, but not as efficiently as it does with IgG1 or 3 [199, 209].

PRO 542 displayed cross-clade neutralization of HIV-1 and is more effective than some human monoclonal antibodies (huMabs) in neutralizing primary HIV-1 isolates [198, 202, 205]. All HIV-1 subtype B primary isolates were neutralized by PRO 542 with a median IC_{50} of 6.2 µg/mL, but non-subtype B viruses that were tested were more susceptibility to neutralization, having a median IC_{50} of 4.8 µg/mL [198, 205]. One human monoclonal antibody (huMab) tested alongside PRO 542, IgG1 b12 which binds to an epitope overlapping that of PRO 542 in the CD4 binding site of HIV-1, showed lower cross-neutralizing activity than PRO 542 [198]. A separate *in vivo* study, using the human peripheral blood leukocyte severe combined immunodeficient (hu-PBL-SCID) mouse model injected with peripheral blood mononuclear cells (PBMCs) and HIV-1 showed that PRO 542 can reduce HIV-1 viral loads in animal models. On average, HIV-1 titres were lowered by 5- to 625-fold when PRO 542 was administered to the infected SCID-mouse. At a dose level of 10 mg/kg, four out of six mice tested, were effectively protected from HIV-1_{JR-CSF}, but were vulnerable to HIV-1_{AD6}. The dose levels of PRO 542 were then increased 5-fold and four of the five mice were protected from HIV-1_{JR-CSF} and HIV-1_{AD6} [197].

In phase 1/2 clinical testing involving paediatrics of different race and gender, PRO 542 showed impressive pharmacokinetics in HIV-1 neutralization, as well as low toxicity to patients. PRO 542 was the primary contributor of reduced viral loads in the tested patients [153, 197, 198, 201, 204]. An adult cohort with variable demographics was also treated with PRO 542 and they also did not show adverse side effects from PRO 542 infusions, at all doses tested. PRO 542 was not found to react with any other epitopes on the virion surface besides the CD4bs. High anti-viral activity was achieved by PRO 542 as marked decreases in HIV RNA and plasma viremia were

detected. One patient who was infused with 10 mg/kg of PRO 542 showed greater than 2 log reduction in HIV RNA level 2 weeks post-infusion. It was hypothesised that such rapid clearance of PRO 542 coated virus was attained by the reticuloendothelial system. Although the Fc portion of PRO 542 has limited effector function, it is believed that its ability to opsonise virus by cross-linking may increase the clearance of virus efficiently. PRO 542 was, however, discontinued from clinical trial after the log drop in patient viral load was not significant enough to warrant further human clinical trials. [82, 153, 197, 200, 202, 210].

When patients were infused with PRO 542 and T-20 (Enfuvirtide), synergistic neutralization of HIV-1 was achieved, which countered the multi-step entry processes of HIV-1 [82]. T-20 is unable to recognize its gp41 epitope before gp120 has attached to cell surface CD4, but can bind transiently exposed gp41 pre-fusion intermediates. PRO 542 can cause viral env shedding and exposure of gp41 epitopes, allowing it to work collaboratively with T-20 and consecutively in preventing viral attachment and fusion. Both drugs are individually capable of neutralizing a broad range of genetically diverse strains of HIV-1 as they bind to conserved regions of gp120 that are imperative for viral attachment and entry. Due to the potency of the synergy between PRO 542 and T-20; lower doses of the drugs may be employed in synergistic combination therapies compared to monotherapy, thus reducing drug toxicity in patients [82, 119]. PRO 542 and other CD4-based therapies are good templates for the design of gp120 CD4bs antagonists [196, 199].

1.7.4.3 Chalcogen substitutions in 2dsCD4

Cerutti *et al* (2010) showed that introducing a cysteine residue in the vicinity of a gp120 disulphide may increase the affinity and avidity of CD4 for gp120. By substituting CD4 serine 60 with a cysteine residue, a CD4 thiol group interacts with the gp120 disulphide C126-196C by virtue of a redox-exchange reaction. Unlike wild-type 2dsCD4 which binds to gp120 non-covalently, the $2dsCD4^{S60C}$ binds covalently to gp120 and may reduce the potential of gp120 dissociating from CD4 [180]. We hypothesize that the addition of the S60C mutation to a CD4-IgG2 protein will bind HIV-1 gp120 covalently, thereby increasing the molecules therapeutic potential. This

study details the development of a wild-type CD4-IgG2 protein as well as a S60C mutant CD4-IgG2 protein, which is intended to bind more tightly to HIV gp120 than the wild-type protein.

1.8 Aims of the study

The overall aim of this study was to construct a modified PRO 542-like fusion protein containing the D1D2 domains of CD4 and an IgG2 Fc portion and compare it to wild-type PRO 542 (PRO 542^{wt}) in its ability to bind HIV-1 gp120. The 'mutant' PRO 542 (PRO 542^{mt}) would be designed based on the patented chalcogen substitution (patent: **PCT/IB2009/051287**, described in section 1.7.4.3) to bind to HIV-1 gp120 covalently. The chalcogen substitution in the D1D2 CD4 domains of PRO 542^{mt} is expected to increase the bond strength between the PRO 542^{mt} and HIV-1 gp120. If the PRO 542^{mt} proves to have superior binding and activity against HIV-1 gp120, it would warrant further preclinical investigation as an attachment inhibitor.

This was achieved by the following objectives:

1.8.1. To construct mammalian expression vectors, each containing cDNA inserts which encode for heterotetrameric kCD4-$IgG2^{wt}$ (PRO 542^{wt}) and kCD4-$IgG2^{S60C}$ (PRO 542^{mt}) chains.

1.8.2. To express and purify the heterotetrameric kCD4-$IgG2^{wt}$ and kCD4-$IgG2^{S60C}$ recombinant proteins.

1.8.3. To characterize and compare the biochemical activities (binding specificity) of heterotetrameric kCD4-$IgG2^{wt}$ and kCD4-$IgG2^{S60C}$ against HIV-1 gp120.

Chapter 2: Materials and Methods

2.1 Reagents used in this study.

All reagents obtained through the NIH AIDS Research and Reference Reagent Programme, division of AIDS, NIAIDS, and NIH (https://www.aidsreagent.org) are listed in Table 2.1.

The CD4-IgG2 (PRO 542) protein was used as a positive control in sodium dodecyl sulphate polyacrylamide gel electrophoresis (SDS-PAGE)/Western blot analyses and surface plasmon resonance (SPR) binding experiments. The recombinant HIV-1_{CN54} gp120 (gp120 CN54), HIV-1_{SF162} gp120 (gp120 SF162) were available from the NIH AIDS Research and Reference Reagent Programme (Table 2.1), whereas HIV-$1_{96ZM651}$ gp120 (gp120 ZM), HIV-1_{Bal} gp120 (gp120 Bal), HIV-$1_{IN25925}$ gp120 (gp120 IN) and HIV-$1_{ZA706010164}$ gp120 (gp120 ZA) were available in our laboratory. All recombinant gp120 were used as ligands in SPR experiments. Two-domain CD4 ($2dsCD4^{wt}$) and two-domain CD4 S60C mutant ($2dsCD4^{S60C}$) were available in our laboratory and used as positive controls in SPR experiments. Monoclonal antibody 17b (MAb 17b) was used to confirm the exposure of CD4 induced epitopes (CD4i) in SPR experiments. The HIV-$1_{93TH975}$ gp120 (gp120 93TH975) and gp120 Bal were used as positive controls in immunoprecipitation experiments. The Chessie 13-39.1 (Chessie) supernatant, ID6 and NEA-9301 anti-gp120 antibodies (Perkin Elmer; Waltham, Massachusetts) were used as the primary antibodies in Western blotting for gp120 protein detection in immunoprecipitation experiments. The anti-CD4 antibody (clone MT310; Santa Cruz Biotechnology INC; California, USA) was used as a primary antibody and an anti-mouse Ig horseradish peroxidase-linked whole antibody (GE Healthcare; Buckinghamshire, England) was used a secondary antibody in all Western blotting experiments. The pCI-neo mammalian expression vector with an insert encoding four-domain soluble CD4 with an S60C mutation ($4dsCD4^{S60C}$) ($p4dsCD4^{S60C}$) used for single transfection optimization was available in our laboratory. Monomer solution and TEMED used in SDS-PAGE were purchased from Sigma-Aldrich (St. Louis, USA).

Table 2.1 All the reagents obtained from the NIH AIDS Research and Reference Reagents programme used in this study.

Catalogue Number	Name of reagent	Source
4091	Antibody 17b	Dr. James E. Robinson
11780	CD4-IgG2 (PRO 542)	Progenics Pharmaceuticals
7749	HIV-1 CN54 gp120	Dr. Ian Jones
7363	HIV-1 SF162 gp120	DAIDS, NIAID
990	Chessie 13-39.1 supernatant	Dr. George K. Lewis
2343	Antibody ID6	Dr. Kenneth Ugen and Dr. David Weiner
3234	HIV-1 gp120 93TH975	BioMolecular Technology

2.2 Computer-modelling of the gp120-2dsCD4 interaction

Previous studies conducted in our laboratory showed that mutating CD4 serine 60 to cysteine allows the introduction of a thiol group within the vicinity of the gp120 126C-196C disulphide, which allows for a stabilized inter-molecular redox exchange reaction to occur [106, 180, 211]. The crystal structure coordinates of gp120 in complex with CD4 and antibody 17b were obtained from the Protein Data Bank (PDB), PDB ID 1G9M [106]. The structures were viewed using the PyMOL Molecular Graphics System, evaluation version 1. 2. 8, Schrodinger, LCC and Swiss PDB viewer (version 4.0.4) [211].

2.3 Design of kCD4-IgG2^{wt} and kCD4-IgG2^{S60C} encoding recombinant plasmids.

A total of four constructs were designed to generate a wild-type (wt) and mutant S60C tetravalent chimeric antibody, consisting of four two-domain soluble CD4 (2dsCD4)-like moieties grafted onto an IgG2 scaffold (Figure 2.1 A). The wild-type chimeric antibody (kCD4-IgG2^{wt}) heavy chain (HC) gene sequence was similar to that of the PRO 542 HC sequence (ATCC no. 75193). It contained all the exons coding for the human CD4 leader/signal sequence and the first two domains of human CD4 (amino acids 1-179) fused to the Fc portion of human IgG2, but excluded all the introns. Similarly, the kCD4-IgG2^{wt} light chain (LC) gene sequence was identical to that of the PRO 542 LC sequence (ATCC no. 75194) and contained all the exons coding for the human CD4 leader/signal sequence and the first two domains of human CD4 (amino acids 1-179) joined to the first codon of the constant portion of the human IgG2 kappa LC sequence (Figure 2.1 A) [199]. The constructs composed of kCD4-IgG2^{wt} HC and LC cDNA cloned into pcDNA 3.1 (+) were called pKH^{wt} and pKL^{wt}, respectively. The mutant kCD4-IgG2^{S60C} HC and kCD4-IgG2^{S60C} LC encoding constructs (pKH^{S60C} and pKL^{S60C}) were identical to the wild-type constructs with the exception of a serine to cysteine mutation at position 60 of the CD4 portions. The four constructs were ordered from GeneArt (Regensburg, Germany), and cloned into pcDNA3.1 (+) (Invitrogen; Figure 2.1 B).

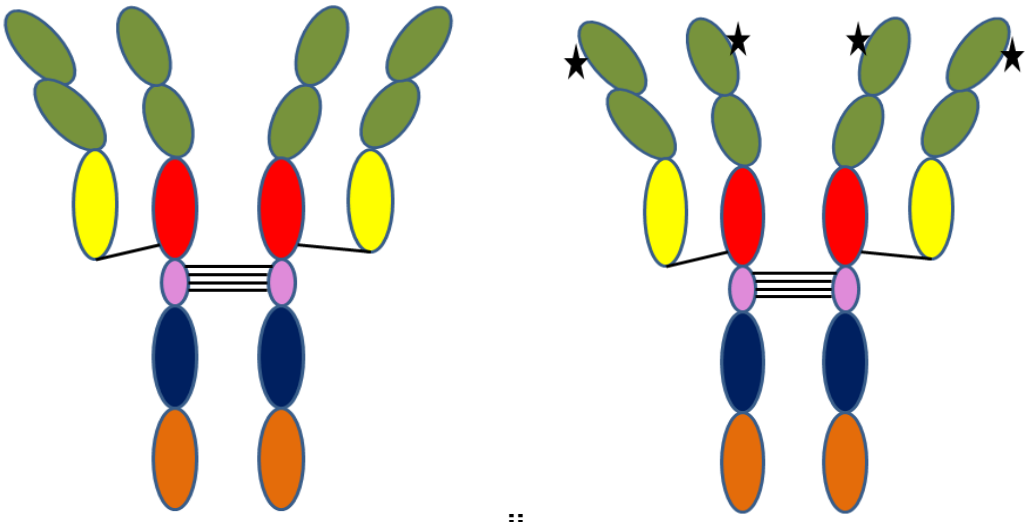

i: ii

Figure 2.1 A: The structure of kCD4-IgG2^{wt} and kCD4-IgG2^{S60C}. The images numbered with Roman numerals 1 and 2 display the structure of kCD4-IgG2^{wt} and kCD4-IgG2^{S60C}, respectively. In both images, the green ovals represent the domains of 2dsCD4; the yellow ovals represent the constant light chain kappa regions of IgG2; the red ovals represent the CH1 domain of IgG2; the pink ovals represent the hinge region of IgG2; the blue ovals represent the CH2 regions of IgG2; the orange ovals represent the CH3 regions of IgG2 and the black lines represent interchain disulphide binds. In the image of kCD4-IgG2^{S60C}, the black stars show the approximate location of the serine to cysteine mutation at residue position 60.

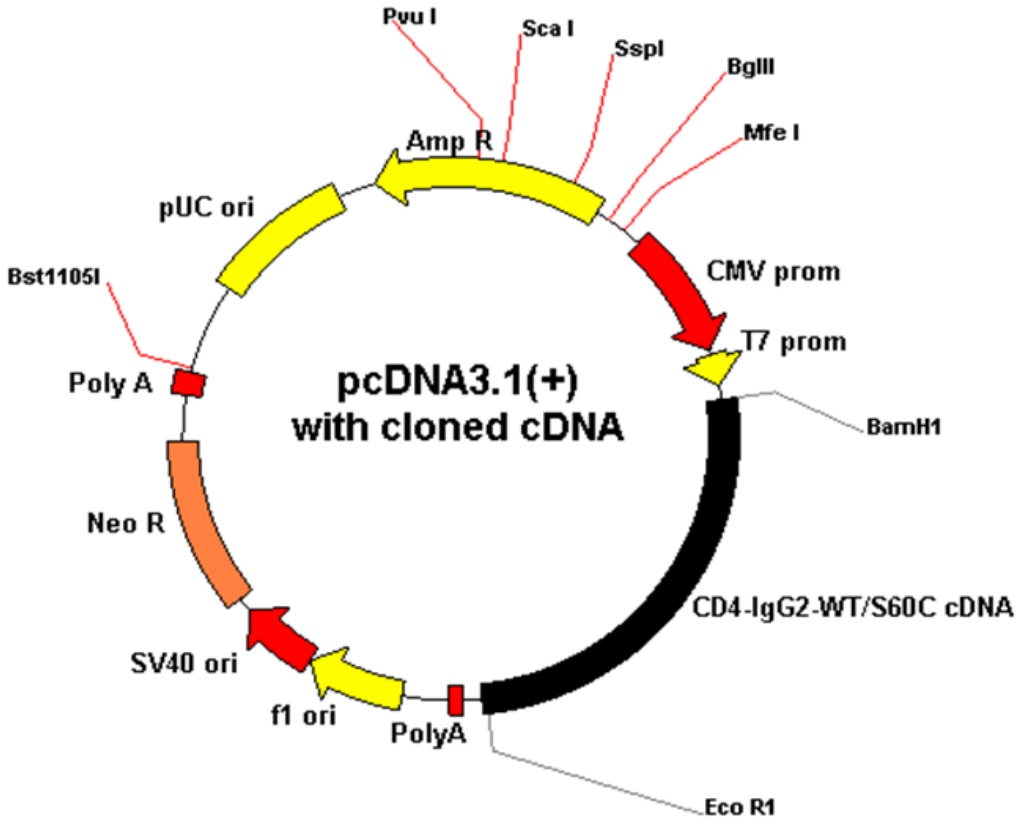

Figure 2.1 B: The pcDNA 3.1 (+) vector (5428 bp) used to express the chains of kCD4-IgG2^{wt} or kCD4-IgG2^{S60C}. The cDNA sequences of the recombinant proteins were cloned into the mammalian expression vector using BamH1 and Eco R1 restrictions sites.

2.4 Transformation of *E. coli* DH5α cells with pcDNA 3.1 (+) constructs.

Upon arrival from GeneArt, the four lyophilized recombinant constructs were resuspended in sterile distilled water (dH_2O) to a concentration of 0.25 µg/µL. Chemically competent *Escherichia coli* (*E. coli*) DH5α cells (available in our laboratory) were removed from -80 °C storage conditions and allowed to thaw on ice. Ten microlitres of each recombinant construct were added to separate 100 µL aliquots of *E. coli* DH5α cells and placed on ice for 30 minutes. Thereafter, the bacterial cells were heat shocked for 90 seconds at 42 °C and then placed immediately on ice. The now transformed bacterial cells were then provided with 100 µL of LB broth (Appendix 1.1) and shaken at 250 rpm in a 37 °C incubator for 1 hour. After incubation, the bacterial cells were plated out onto LB agar plates (Appendix 1.2) with 10 µL of ampicillin (Merck; Darmstadt, Germany; Appendix 1.3) at a concentration of 100 µg/mL. The plates were then incubated at 37 °C for 24 hours.

2.4.1 Glycerol stocks production

A single colony of transformed bacterial cells was isolated from LB agar plates (Appendix 1.2), inoculated into 50 mL LB broth containing 1X of ampicillin (Appendix 1.3) and incubated in a 37 °C incubator on an orbital shaker at 250 rpm for 16 hours. Thereafter, aliquots of 800 µL cultured transformed bacterial cells were added to 200 µL of glycerol (Saarchem, South Africa) and these were stored in a -80 °C freezer for long-term storage. Before use, the aliquots were thawed on ice to 4 °C.

2.4.2 Plasmid preparation, isolation and purification

Glycerol stocks of transformed bacterial cells (harbouring one of the recombinant constructs) (refer to 2.4.1) were thawed on ice for 20 minutes. Ten µL of cultured transformed bacterial cells were then added to 500 mL of sterile LB broth with 1 g of ampicillin (Merck, Darmstadt, Germany; Appendix 1.3) and shaken in a 37 °C incubator at 250 rpm for 16 hours. The bacterial culture was then centrifuged at 6000 rpm and 4 °C for 20 minutes using an Avanti J-E centrifuge (Beckman Coulter; California, USA). To extract the recombinant plasmid from the bacterial cells, a Qiafilter Maxi Prep Plasmid Kit (Qiagen; Venlo, Netherlands) was used according to the manufacturer's instructions. In brief, the bacterial pellet was homogenously resuspended in 10 mL of buffer P1 (containing 1 mg/mL of ribonuclease), before 10

mL of buffer P2 was added to lyse the cells under alkaline conditions. The resulting mixture was inverted six times and allowed to incubate at 20 °C for 5 minutes. Following that, 10 mL of Buffer P3 was added and the mixture was inverted another 6 times to neutralise the cells and lysate. The lysate and cells were then transferred to a Qiafilter cartridge (provided in the kit) and allowed to incubate for 10 minutes at 20 °C. To separate the lysate from the cells, a plunger was inserted into the Qiafilter cartridge, allowing the lysate to filter out from the cells. The lysate was collected in a Qiagen-tip (provided in the kit), which was previously equilibrated with buffer QBT to commence gravity-flow anion-exchange chromatography. Once the lysate had entered the Qiagen-tip resin; proteins, RNA and genomic DNA were washed out using buffer QC and the plasmid DNA was eluted using buffer QF. To precipitate the plasmid DNA from the elution, 0.7 volumes of 70% isopropanol (Appendix 1.8) was added and the mixture was centrifuged at 4000 rpm for 1 hour and 4 °C using an Eppendorf centrifuge 5810 R (Eppendorf; Hamburg, Germany). The resultant supernatant was discarded whilst the pelleted plasmid DNA was washed with 70% ethanol (Appendix 1.9). The plasmid DNA was pelleted out by centrifugation at 4000 rpm for 1 hour and at 4 °C using the Eppendorf centrifuge 5810 R (Eppendorf; Hamburg, Germany). The resultant supernatant was discarded and the plasmid DNA was allowed to air-dry for 1 hour before being resuspended in 500 µL of sterile dH_2O. The amounts and purity of plasmid DNA collected were determined using a Nanodrop ND1000 spectrophotometer (Thermo Fisher Scientific; Massachusetts, USA).

2.5 Agarose gel electrophoresis

The purity, homogeneity and size of the constructs were assessed using agarose gel electrophoresis. One microlitre of ethidium bromide (Promega; Madison, USA) at a concentration of 10 mg/mL was dissolved in 100 mL of a 0.7% agarose gel (Appendix 1.11). One microlitre of each purified construct was diluted with 5 µL 6X loading buffer (Appendix 1.12) before the mixture was loaded in the well. The O'GeneRuler DNA ladder mix (Fermentas, Massachusetts, USA) was run as a molecular weight standard. Electrophoresis of the samples was conducted at 77 V using a Bio-Rad powerpack (Bio-Rad laboratories, Hercules, USA) for 2 hours. The

agarose gel was subsequently visualised by UV light, using a UV transilluminescence machine**.**

2.5.1 Characterization of recombinant plasmids (Plasmid DNA digestion with Eco R1)

Each of the four recombinant plasmids was characterized by restriction enzyme digestion to ensure they were of the correct size. One µL of each purified recombinant plasmid (refer to 2.4.2) was placed in a separate reaction tube containing 2 µL of Eco R1 supporting buffer (Fermentas; Massachusetts, USA), 1 µL of Eco R1 (Fermentas, Massachusetts, USA) at a concentration of 10 U/µL and 14 µL of sterile double deionised H_2O (ddH_2O). The four reaction tubes were then incubated in a 37 °C water-bath for 1 hour and 30 minutes to catalyse the reactions. The reaction was stopped by placing the reaction tubes on ice. Thereafter, a 5 µL sample from each reaction tube was analyzed by agarose gel electrophoresis (see section 2.5).

2.6 Optimization of recombinant protein expression in Human Embryonic Kidney 293T cells (HEK293T)

2.6.1 HEK293T mammalian cells

2.6.1.1 Feeding and passaging of HEK293T mammalian cells

HEK293T cells (available in our laboratory) were grown in 75 cm^3 dishes (Thermo Fisher Scientific; Massachusetts, USA) in 14 mL of Dulbecco's Modified Eagle Medium (DMEM) (Sigma-Aldrich; St. Louis, USA) supplemented with 10 mM Glutamax™ L-glutamine (Invitrogen; California, USA) and 10% fetal bovine serum (FBS) (Sigma-Aldrich, St. Louis, USA) (complete DMEM) in a 37 °C and 5% CO_2 incubator. Once the cells had grown to 80% confluence; the culture supernatant was discarded and the adherent cells were rinsed with 10 mL of 1X phosphate buffered saline (PBS) (Sigma-Aldrich; St. Louis, USA) and split by incubating them with 500 µL of 0.25% trypsin: EDTA mix (Sigma-Aldrich; St. Louis, USA) for less than five

minutes at 37 °C. The trypsin: EDTA solution was then discarded and 10 mL of fresh complete DMEM was added to the cells. Cells were split ten-fold and placed into new tissue culture flasks with appropriate amounts of fresh complete DMEM. Once the cells had been passaged twenty times, they were discarded and replaced with thawed cell stocks.

2.6.1.2 Preparation of HEK293T frozen cell stocks and thawing

Split cells were supplied with 10% dimethyl sulphoxide (DMSO) (Fluka chemika; Buchs, Switzerland) in fresh complete DMEM. The cells were stored at -80 °C and thawed on ice before use.

2.6.1.3 Quantification of HEK293T mammalian cells

Twenty microlitres of the split HEK293T cells was combined with 80 µL of Hyclone trypan blue (Thermo Fisher Scientific; Massachusetts, USA), and placed on a haemocytometer (Neubauer, West Germany) slide for counting on an Olympus CKX41 microscope (Olympus America Inc; USA).

To calculate the total number of cells (N): the formula N= (m) (tb) (V) (10^4) was employed where 'N' is the number of cells in suspension, 'm' is the mean of cell counts per 0.1 mm^3, 'tb' is the correction for the trypan blue dilution, 'V' is the volume of the original cell suspension in millilitres and '10^4' is for the volume in the original cell suspension in millilitres.

2.6.2 Optimization of transient transfections of HEK293T cells

For all transfection experiments, HEK293T cells that were 80% confluent were split, counted, and seeded at 1.2 X 10^6 or 3.6 X 10^6 cells per 25 cm^3 or 75 cm^3 tissue culture flask, respectively in complete DMEM, and incubated overnight in a 37 °C, 5% CO_2 incubator. When the HEK293T cells from the overnight flasks reached 40-80% confluence, they were ready for use in transfection experiments.

Optimal transfection conditions for single and co-transfections were established for selected/each construct by testing different DNA concentrations, transfection reagents, and post transfection harvest times.

2.6.2.1 Optimization of single-transient transfections of HEK293T cells using Lipofectamine™ transfection reagent

Transfections involving the use of Lipofectamine™ (Invitrogen; California, USA) transfection reagent as the DNA carrier were conducted according to the Lipofectamine™ Reagent Handbook, in 25 cm^3 tissue culture flasks.

Ten micrograms of pKL^{wt} at a ratio of 1 part purified plasmid DNA to 5 parts Opti-Mem® (µL) (Invitrogen; California, USA) (without additives) was prepared. In a separate reaction tube, a ratio of 1 part Lipofectamine™ (Invitrogen; California, USA 1 µg DNA: 1 µL Lipofectamine™) to 5 parts Opti-Mem® (µL) (Invitrogen; California, USA) (without additives) was prepared. The two mixtures were incubated separately for 5 minutes at room temperature, combined and incubated for a further 20 minutes at room temperature, to allow complex formation. Transfection reagent with no DNA added was used as a negative transfection control.

The complete DMEM from the overnight tissue culture flasks was then replaced with fresh complete DMEM, and the transfection mix was added to the cells, and incubated in a 37 °C, 5% CO_2 incubator for up to 48 hours post-transfections. The culture supernatant containing the transfection mix was replaced with fresh complete DMEM at 16-24 hours post transfection, and kept for SDS-PAGE and Western blot analyses (see section 2.6.3). At 48 hours post-transfection, the culture supernatant and cells were harvested and stored at 4 °C for subsequent SDS-PAGE and Western blot analyses.

2.6.2.2 Optimization of single-transient transfections of HEK293T cells using different DNA concentrations and Polyfect transfection reagent

Transfections involving the use of Polyfect transfection reagent as the DNA carrier (Qiagen; Venlo, Netherlands) were conducted according to the Polyfect Transfection Reagent Handbook (Qiagen; Venlo, Netherlands) in 25 cm^3 tissue culture flasks.

Two and four micrograms of all the purified recombinant plasmids (section 2.4.2) were diluted in 150 µL of DMEM (Sigma-Aldrich; St. Louis, USA; no additives) and incubated at room temperature for 5 minutes. Twenty or forty millilitres of Polyfect transfection reagent (1 µg DNA: 10 µL Polyfect; Qiagen; Venlo, Netherlands) was then added to the 2 µg and 4 µg DNA solutions, respectively, and incubated for a further 20 minutes at room temperature to allow for complex formation. The transfection mix was added to the overnight cultures and supernatant and cells were harvested and analysed as described in section 2.6.2.1.

2.6.3 SDS-PAGE

To assess the sizes of proteins expressed after transfections were conducted, a discontinuous SDS-PAGE system was employed [212]. A stacking and resolving gel, containing 4 and 8.75% acrylamide, respectively, were cast using a Bio-Rad system, having a thickness of 1.5 mm each (Hercules, USA). The resolving gel solution was poured first (Appendix 2.3) and a thin layer of running gel overlay (Appendix 2.3) was applied over it to assist polymerization. Upon completion of resolving gel polymerisation, the running gel overlay was decanted. Sterile dH_2O was used to wash the resolving gel. Stacking gel solution (Appendix 2.3) was poured on top of the resolving gel. The height of the stacking gel solution poured was twice the height of the volume of sample to be applied.

All culture supernatant samples were clarified by centrifugation at 3900 rpm, 4 °C using an Eppendorf 5810 R centrifuge (Eppendorf; Hamburg, Germany) using Amicon® Ultra Centrifugal Filter Units (Millipore, Massachusetts, USA). Clarified samples were combined with 2X treatment buffer (Appendix 2.3) in a 1:1 volumetric ratio to give a final volume of 50 µL, placed in boiling water for 3

minutes and loaded into the polymerised stacking gel. NIH PRO 542 was used as the positive protein control, unless otherwise stated. The gels were run with a constant current of 10 milliamps for approximately 45 minutes, before an increased current of 20 milliamps was applied until the dye front had migrated to 1 cm from the bottom of the gel.

2.6.4 Western blotting

Following SDS-PAGE, gels were immersed in transfer buffer (Appendix 2.4) for 15 minutes and transferred to Hybond-C extra nitrocellulose membrane (Amersham Biosciences; Bucks, England) using a Transblot semi-dry transfer system (Bio-Rad laboratories, Hercules, USA) with a constant current of 4 milliamps per gel for 1 hour and 30 minutes. After the transfer process, the nitrocellulose membrane was placed in 5% non-fat skimmed milk (Bio-Rad; Hercules, USA) dissolved in 1X tris-buffered saline at pH 7.4 supplemented with 0.1% tween-20 (1X TTBS) (Sigma-Aldrich; St. Louis, USA (Appendix 2.4)) and stored at 4 °C for 24 hours. The nitrocellulose membrane was then rinsed with 50 mL of 1X TTBS three times before MT310 antibody (Santa Cruz Biotechnology INC; California, USA) at a concentration of 1:1000 in 3 mL was applied to the membrane on a flat surface for 1 hour. Following incubation with the MT310 antibody, the nitrocellulose membrane was washed with 50 mL of 1X TTBS three times before anti-mouse Ig horseradish peroxidase-linked whole antibody (GE Healthcare; Buckinghamshire, England) at a concentration of 1:1000 in 3 mL was applied to the blot on a flat surface for 1 hour. The membrane was washed three times with 50 mL of 1X TTBS to remove any unbound antibodies or non-specifically bound antibodies. SuperSignal West Pico Chemiluminescent Substrate (Thermo Fisher Scientific; Massachusetts, USA) was then applied to the membrane according to manufacturer's instructions. Results of this experiment were analysed by monitoring the enzymatic reaction using a Chemidoc (Bio-Rad; Hercules, USA) and employing the Chemi-high sensitivity setting.

2.6.5 Optimization of transient co-transfections for expression of heterotetrameric kCD4-IgG2^{wt} and heterotetrameric kCD4-IgG2^{S60C} in HEK293T cells

To determine whether kCD4-IgG2^{wt} HC and LC were able to assemble a fully folded, functional heterotetrameric kCD4-IgG2^{wt} protein, the pKH^{wt} and pKL^{wt} plasmids were co-transfected into HEK293T cells.

Co-transfection experiments of varying DNA concentrations with Polyfect transfection reagent was performed in 25 cm^3, 75 cm^3 and 175 cm^3 tissue culture flasks seeded with 1.2 X 10^6, 3.6 X 10^6, or 6 X 10^6 HEK293T cells, respectively. A total of 4 µg (2 µg pKH^{wt}; 2 µg pKL^{wt} LC), 12 µg (6 µg pKH^{wt}; 6 µg pKL^{wt}) and 28 µg (14 µg pKH^{wt}; 14 µg pKL^{wt}) of plasmid DNA was transfected into the 25 cm^3, 75 cm^3 and 175 cm^3 tissue culture flasks, respectively. Transfection controls were flasks inoculated with DNA carrier only.

Sixteen to 24 hours post transfections, the serum containing medium was decanted, cells were washed with 1X PBS and supplied with serum-free medium (SFM II) supplement with 10 mM of Glutamax™ L-glutamine (both Invitrogen; California, USA; complete SFM II). Every 24 hours for 4 days thereafter, the serum-free supernatant was collected (stored at 4 °C) and replaced with the same volume of fresh medium. At 96 hours, culture supernatant and cells were harvested and stored at 4 °C. All the culture supernatants were then clarified and concentrated using Amicon® Ultra Centrifugal Filter Units (Millipore; Massachusetts, USA). Samples were analysed by SDS-PAGE and Western Blotting as described in section 2.6.3 and 2.6.4, respectively.

To determine whether kCD4-IgG2^{S60C} HC and kCD4-IgG2^{S60C} LC were able to assemble a fully folded, functional heterotetrameric kCD4-IgG2^{S60C} protein, the pKL^{S60C} and pKH^{S60C} plasmids were co-transfected into HEK293T cells grown in 175 cm^3 tissue culture flasks, and analysed as described above.

2.7 Large scale expression of heterotetrameric kCD4-IgG2^{wt} and heterotetrameric kCD4-IgG2^{S60C} in HEK293T cells

Culture supernatant from co-transfection experiments of several 175 cm^3 tissue culture flasks were clarified, pooled, filtered through 0.22 micron filters (Millipore, Massachusetts, USA), and used for subsequent purification experiments. Pooled supernatant was used immediately or stored at 4 °C.

2.8 Purification of heterotetrameric kCD4-IgG2^{wt} and heterotetrameric kCD4-IgG2^{S60C}

Protein-A affinity chromatography was used to purify kCD4-IgG2^{wt} and kCD4-IgG2^{S60C} from culture supernatants harvested from section 2.7.

2.8.1 Purification of heterotetrameric kCD4-IgG2^{wt} using the Äkta FPLC system

A one-step purification protocol for heterotetrameric kCD4-IgG2^{wt} using a 1 mL Hitrap Protein-A HP column (GE Healthcare; Buckinghamshire, England), as per manufacturer's instructions was performed on the Äkta FPLC system (GE Healthcare; Buckinghamshire, England). Briefly, the 1mL Hitrap Protein-A HP column was equilibrated with 1X PBS (Sigma-Aldrich; St. Louis, USA) at a flow-rate of 2 mL/minute for 5 minutes, before the filtered culture supernatant was applied to it at a flow-rate of 1 mL/minute. The flow-through was collected, and stored. The column was then washed with 1X PBS at a flow-rate of 2 mL/minute for 2 minutes, to remove unbound or non-specifically bound material and flow-through was collected. To elute the bound proteins, 0.1 M citric acid buffer at pH 3.6 (Appendix 2.7) was passed through the column at a flow-rate of 1 mL/minute, and directly collected in tubes containing 200 µL of 1 M tris-HCl at pH 9 to neutralize the eluted fraction. Absorbance readings at 280 nm were monitored throughout the purification process. The UNICORN 5.2 (Build 500) software by GE Healthcare (Buckinghamshire, England) was used to monitor the purification steps.

The sample flow-through, washes and eluate were each concentrated to 500 µL using Amicon® Ultra Centrifugal Units (Millipore, Massachusetts, USA), and 30 µL thereof was used for SDS-PAGE and Western blot analysis.

2.8.2 Purification of heterotetrameric kCD4-IgG2^{wt} and heterotetrameric kCD4-IgG2^{S60C} using Protein-A agarose beads

Culture supernatants containing kCD4-IgG2^{wt} or kCD4-IgG2^{S60C} (section 2.7) were analysed by SDS-PAGE and Western blot analysis to confirm protein expression, and then purified using Protein-A agarose beads (Bio-Rad; Hercules, USA; Appendix 2.5).

The Protein-A agarose beads were stored in 1X PBS containing 0.1% sodium azide (both from Sigma-Aldrich; St. Louis, USA). Before use, the beads were washed thoroughly with 1X PBS without sodium azide. Culture supernatant was then incubated with 0.5 mL (kCD4-IgG2^{S60C}) and 1 mL (kCD4-IgG2^{wt}) of washed Protein-A agarose beads (Bio-Rad; Hercules, USA) (Appendix 2.5) in a 50 mL Nunc tube (Roskilde, Denmark), and shaken at 250 rpm at 4 °C for 72 hours.

To pellet the Protein-A agarose beads with kCD4-IgG2^{wt} or kCD4-IgG2^{S60C} adsorbed, the 50 mL tubes were centrifuged at 3900 rpm, 4 °C for 10 minutes using an Eppendorf 5810 R centrifuge (Eppendorf; Hamburg, Germany). The supernatant was removed and stored at 4 °C. The beads were then washed by the addition of 1 bead volume of 0.02 M sodium phosphate buffer at pH 6.5 (binding buffer) (Appendix 2.6) five times, and centrifuged at 13 000 rpm in an Eppendorf 5415 R centrifuge (Eppendorf; Hamburg, Germany) at 4 °C. All subsequent centrifugation steps were carried out under these conditions. The resultant washes were pooled, concentrated to 500 µL and stored at 4 °C. The elution step involved adding 1 bead volume of 0.1 M sodium citrate buffer at pH 3.5 (elution buffer) (Appendix 2.7) twice to the washed beads. The eluate was immediately transferred to a new reaction tube containing 200 µL of 1M tris-HCl at pH 9 (Appendix 2.8) to neutralize the elution solution and then concentrated to 200 µL before being stored at 4 °C.

The beads were subsequently washed with 2 bead volumes of binding buffer (Appendix 2.6) and regenerated with 2 bead volumes of regeneration buffer (Appendix 2.9). The regeneration flow-through was collected and concentrated to 500 µL and stored at 4 °C. All solutions were concentrated using the Amicon® Centrifugal Filter Units, centrifuged in an Eppendorf 5810 R centrifuge (Eppendorf; Hamburg, Germany) at 3900 rpm at 4 °C.

Thirty microlitres of the initial unbound material, concentrated wash steps, concentrated eluate and concentrated regeneration supernatant were each analysed by SDS-PAGE and Western Blotting as described in section 2.6.3 and 2.6.4, respectively.

2.9 Immunoprecipitation of HIV gp120 with heterotetrameric kCD4-IgG2^{wt}

To assess whether the expressed kCD4-IgG2^{wt} was fully assembled and had a functional CD4 and Fc portion, kCD4-IgG2^{wt} adsorbed to Protein-A agarose beads was incubated with purified monomeric HIV gp120 Bal.

2.9.1 Optimal binding of heterotetrameric kCD4-IgG2^{wt} to Protein-A agarose beads

Varying amounts of kCD4-IgG2^{wt} were incubated with the Protein-A agarose beads to identify optimal binding conditions/capacity, and analysed by SDS-PAGE and Western blot analysis. Ninety microlitres of beads was washed with 500 µL of 1X PBS four times to remove storage buffer (0.1% sodium azide in 1X PBS). Thirty microlitre aliquots of the beads were placed in three separate Eppendorf tubes. One of the reaction tubes containing 30 µL of beads was incubated with 1 µg of NIH PRO 542; the second reaction tube containing 30 µL of beads was incubated with 250 µL of control supernatant, and the third reaction tube containing 30 µL of beads was incubated with 250 µL (approximately 500 ng) of kCD4-IgG2^{wt} containing supernatant. The three reaction tubes were then shaken at 250 rpm and 4 °C on an orbital shaker for 16 hours. The beads were pelleted using an Eppendorf Centrifuge 5415 R (Eppendorf; Hamburg, Germany) and the supernatants of the reaction tubes

were stored at 4 °C for SDS-PAGE-Western blot analysis as described in section 2.6.3 and 2.6.4, respectively. The pelleted beads were washed five times with 1 mL of 1X PBS to remove non-specifically bound material. Beads were analysed using SDS-PAGE and Western blotting techniques. NIH PRO 542, gp120 93TH975 and gp120 Bal recombinant proteins were included on the SDS-PAGE and Western blot as positive controls. The blot was analysed using the MT310 antibody as a primary antibody and the anti-mouse Ig horseradish peroxidase-linked whole antibody as a secondary antibody. Following that, the blot was stripped, and then had the anti-gp120 cocktail (Appendix 2.10) applied to it as a primary antibody and the anti-mouse Ig horseradish peroxidase-linked whole antibody as a secondary antibody.

Optimal supernatant-bead volumes were used in all subsequent immunoprecipitation experiments.

The Protein-A agarose beads were prepared by washing 150 µL of beads with 500 µL of binding buffer (Appendix 2.6), pelleting the beads by centrifugation in an Eppendorf 5415 R centrifuge at 13 000 rpm and 4 °C and discarding the binding buffer supernatant. The wash step was repeated five times before all the beads were divided into 50 µL aliquots that were placed in 3 separate Eppendorf reaction tubes (Eppendorf; Hamburg, Germany). The three reaction tubes with beads were treated with 1 µg of NIH PRO 542 (positive control), 250 µL of the aforementioned concentrated kCD4-IgG2^{wt} culture supernatant, or untreated (negative control). The three reaction tubes were then shaken at 250 rpm at 4 °C for 24 hours. The unbound materials from the three reaction tubes were kept as the flow-through samples for SDS-PAGE and Western blotting analysis. The beads in all the reaction tubes were washed with 500 µL of binding buffer 5 times each to remove non-specific binders.

.

2.9.2 Immunoprecipitation of HIV gp120 by heterotetrameric kCD4-IgG2^{wt}

Two micrograms of HIV gp120 Bal was added to each of the three aforementioned reaction tubes (Protein-A agarose beads-kCD4-IgG2^{wt}; bead-NIH PRO 542; beads alone) and incubated for 72 hour on a shaker at 250 rpm and 4 °C. The bead-bound proteins were then washed with 500 µL binding buffer (refer to appendix 2.6) 5 times and pelleted using an Eppendorf 5415 R centrifuge (Eppendorf; Hamburg, Germany). Thirty microlitres of the beads, and supernatant (containing unbound protein) from each reaction tube were then analysed by SDS-PAGE and Western Blotting techniques (refer to 2.7). The primary antibody used in the SDS-PAGE and Western blotting analyses was a cocktail of anti-gp120 antibodies (ID6, Chessie supernatant and NEA; refer to Table 2.1; Appendix 2.10), whilst the secondary antibody used was the anti-mouse Ig horseradish peroxidase-linked whole antibody (GE Healthcare; Buckinghamshire, England) as described in section 2.6.4 (Appendix 2.4).

2.10 Surface plasmon resonance (SPR) studies

Surface plasmon resonance was used to further characterize the binding of the kCD4-IgG2^{wt} and kCD4-IgG2^{S60C} to gp120 using the ProteOn XPR36™ (Bio-Rad; Hercules, USA) at 25 °C, with recommended Bio-Rad reagents, unless otherwise stated.

The GLC sensor chip employed for the SPR experiment was pre-conditioned by sequentially passing 0.5% SDS, 50 mM NaOH and 100 mM HCl over all thirty-six flow cells of the sensor chip at a flow-rate of 30 µL/minute and a contact time of one minute. To commence binding studies (activation), a 1:1 ratio of 1-ethyl-3-(3-dimethylaminopropyl) carbodiimide hydrochloride (EDC) and N-hydroxysuccinimide (NHS) was mixed and passed over the sensor chip surface to activate surface carboxyl groups at a flow rate of 30 µL/minute for a period of two minutes.

The following six recombinant gp120 proteins: CN54, SF162, ZA706010164, 96ZM651 (ZM), IN25925 (IN) and Bal (Section 2.1) were individually dissolved in 10 mM sodium acetate buffer at pH 5.5 to a concentration of 5 µg/mL. Each

gp120 type was passed over its dedicated flow channel (Figure 2.2) at a flow-rate of 25 µL/minute for a duration of six minutes, until immobilisation (amine coupling) levels had reach a minimum of 2000 response units (RU). To remove gp120 molecules which were uncoupled to the sensor surface or gp120 dimers that had formed on the surface, 10 mM glycine at pH 3.5 was passed over every flow cell of immobilised gp120 at a flow rate of 100 µL/minute for a period of 18 seconds. The flow-channels were then washed with hepes buffered saline (HBS; Appendix 2.11) at a flow-rate of 25 µL/minutes for four minutes and a new baseline was reached. Excess carboxyl groups were then capped using ethanolamine.

For each gp120, six flow cells were available for reactions with the following 6 analytes (Figure 2.2): kCD4-IgG2^{wt} supernatant (section 2.6.4), kCD4-IgG2^{S60C} supernatant (section 2.6.4), negative control supernatant (section 2.6.4), NIH PRO 542, 2dsCD4^{wt} and 2dsCD4^{S60C}. The purified analytes NIH PRO 542, 2dsCD4^{wt} and 2dsCD4^{S60C} were dissolved in HBS to a final concentration of 500 nM. The kCD4-IgG2^{wt} culture supernatants contained approximately 5-10 µg recombinant protein, whereas the kCD4-IgG2^{S60C} culture supernatant contained approximately 25 ng (estimated by Western blot analyses and densitometry). All the analytes were passed over each of the six immobilised gp120 types individually at a flow-rate of 25 µL/minute for six minutes. The reaction surfaces were then washed again with HBS, to remove non-specific binding or unbound material from immobilised gp120 at a flow-rate of 25 µL/minute for a period of 15 minutes and dissociation of the analytes was monitored.

To further confirm the specificity of gp120 binding to CD4 containing molecules, the monoclonal antibody 17b was passed over the gp120 cells to detect whether CD4 induced epitopes (CD4i) were exposed. The monoclonal antibody 17b was diluted in HBS to a concentration of 500 nM and passed over all reaction surfaces at a flow-rate of 25 µL/minutes for four minutes. Unbound or non-specifically bound

17b was removed by washing HBS over the reaction surfaces at a flow-rate of 25 µL/minute for four minutes and the dissociation of 17b was monitored.

In order to repeat the injection of analytes, 10 mM glycine at pH 2.5 was passed over all flow-channels at a flow-rate of 100 µL/minute for a period of 18 seconds to regenerate the gp120 ligand binding sites. The initial injection of analytes to ligands was repeated at a flow-rate of 25 µL/minute for five minutes to confirm specificity of the CD4 containing proteins for gp120 (data not shown). Data for the SPR studies was analysed using the ProteOn Manager Software (Bio-Rad; Hercules, USA) and Microsoft Excel 2007 was used for fitting SPR data. The signals obtained from the interspots and control expression culture supernatant was subtracted from signals of other analyte-ligand reactions. All sensorgrams showing an RU level greater than 3 fold that of the reference sample suggested the occurrence of specific binding.

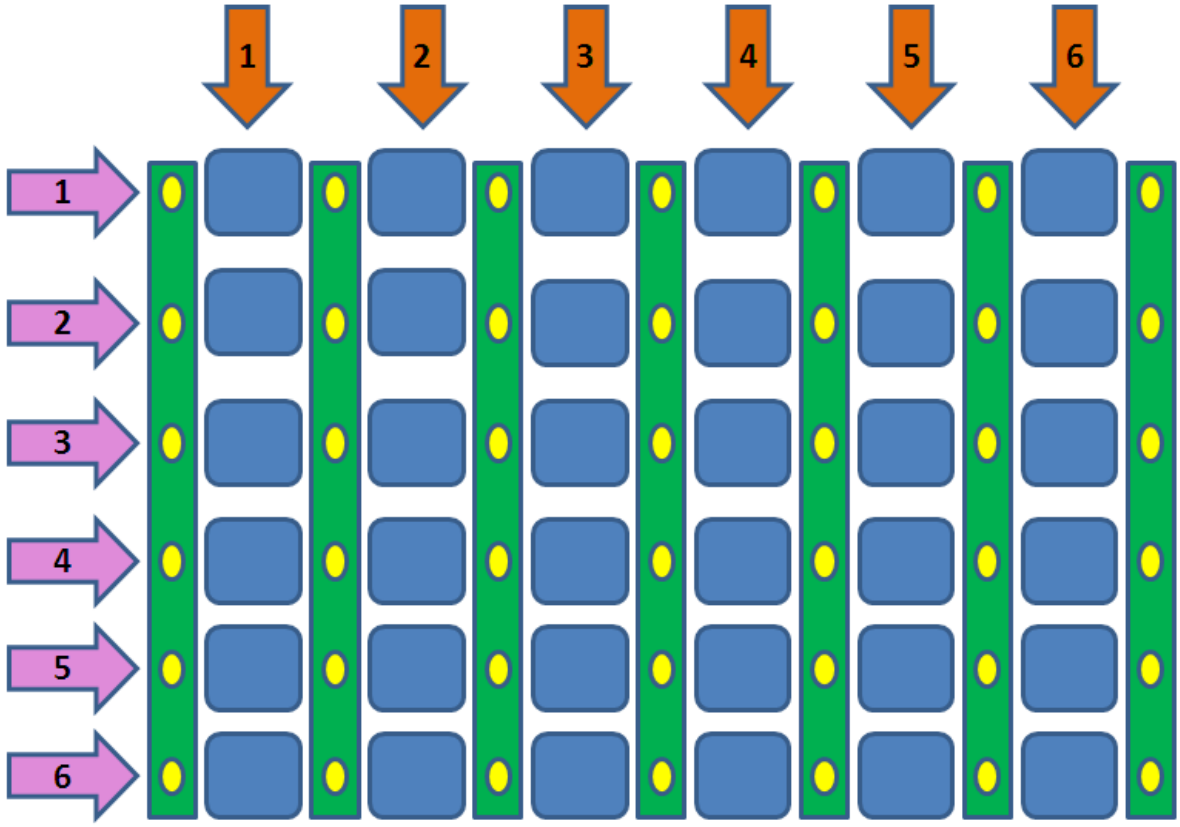

Figure 2.2: The GLC sensor chip used for SPR experiments. The blue squares represent the 36 interaction spots and the yellow ovals represent the 84 interspot references. The orange arrows numbered 1 to 6 represent the horizontal flow channels in which gp120s CN54, SF162, ZM, ZA, IN and Bal; respectively, were immobilised on the chip. The pink arrows numbered 1 to 6 represent the analytes NIH PRO 542, kCD4-IgG2^{wt} containing supernatant, kCD4-IgG2^{S60C} containing supernatant, 2dsCD4^{wt}, 2dsCD4^{S60C} and control expression supernatant, respectively, injected into the vertical flow channels.

Chapter 3: Results

3.1 Computer-modelling of the gp120-2dsCD4 interaction

Molecular modelling of the gp120-2dsCD4 interaction confirmed the presence of a CD4 serine 60 molecule within 4.85 Å distance of a gp120 disulphide (C126-C196) (Figure 3.1 A). By mutating the CD4 serine 60 residue to a cysteine residue, a thiol group was placed in the vicinity of the gp120 (C126-196C) disulphide, allowing a redox exchange reaction to occur between the two proteins (Figure 3.1 B) [180, 211]. This mutation was used to design two of the four the constructs used in this study.

3.2 Design of kCD4-IgG2^{wt} and kCD4-IgG2^{S60C} encoding constructs and the generation of recombinant plasmid stocks

The amino acid sequence alignment of kCD4-IgG2^{wt} and kCD4-IgG2^{S60C} heavy and light chain sequences, respectively, are shown in Figure 3.2. The kCD4-IgG2^{wt} and kCD4-IgG2^{S60C} HC cDNA inserts encode proteins composed of 530 amino acids (1599 bp), whereas the kCD4-IgG2^{wt} and kCD4-IgG2^{S60C} LC cDNA inserts encode proteins composed of 310 amino acids (939 bp).

Each of the cDNA sequences were separately inserted in a pcDNA 3.1 (+) plasmid synthesized by GeneArt (Regensburg, Germany), successfully transformed into *E.coli* DH5α and glycerol stocks were generated. The recombinant plasmids were then purified on a large scale (Figure 3.3, lanes 9-12).

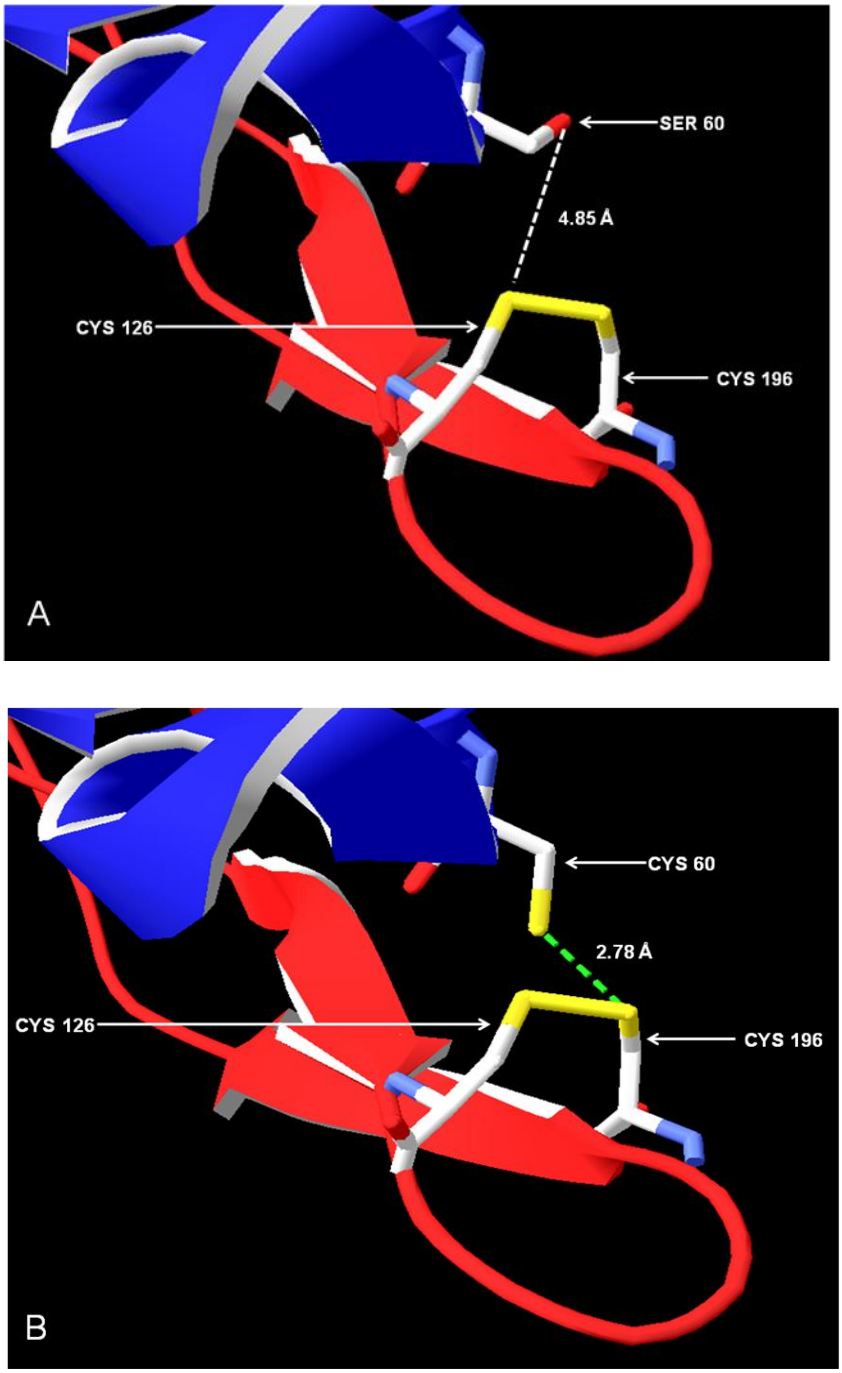

Figure 3.1: Computer-modelling of the gp120-2dsCD4^{wt} (A) and gp120-2dsCD4^{S60C} (B) interactions. The structures of CD4 (blue) and gp120 (red) are displayed in ribbon configuration. The atomic structures of the CD4 serine 60, the mutant CD4 cysteine 60, gp120 cysteine 126 and 196 residues are shown in stick configuration (yellow represents sulphur atoms, red represents oxygen atoms, blue represents a nitrogen atom and white represents carbon atoms). The image was viewed with Swiss PDB viewer (version 3.7) [106, 211].

A

```
                    *       20        *       40        *       60        *       80
kCD4-IgG2 wt:    MNRGVPFRHLLLVLQLALLPAATQGKKVVLGKKGDTVELTCTASQKKSIQFHWKNSNQIKILGNQGSFLTKGPSKLNDRA :  80
kCD4-IgG2 S60c:  ................................................................................ :  80

                    *       100       *       120       *       140       *       160
kCD4-IgG2 wt:    DSRRSLWDQGNFPLIIKNLKIEDSDTYICEVEDQKEEVQLLVFGLTANSDTHLLQGQSLTLTLESPPGSSPSVQCRSPRG : 160
kCD4-IgG2 S60c:  .C.............................................................................. : 160

                    *       180       *       200       *       220       *       240
kCD4-IgG2 wt:    KNIQGGKTLSVSQLELQDSGTWTCTVLQNQKKVEFKIDIVVLAFASTKGPSVFPLAPCSRSTSESTAALGCLVKDYFPEP : 240
kCD4-IgG2 S60c:  ................................................................................ : 240

                    *       260       *       280       *       300       *       320
kCD4-IgG2 wt:    VTVSWNSGALTSGVHTFPAVLQSSGLYSLSSVVTVPSSNFGTQTYTCNVDHKPSNTKVDKTVERKCCVECPPCPAPPVAG : 320
kCD4-IgG2 S60c:  ................................................................................ : 320

                    *       340       *       360       *       380       *       400
kCD4-IgG2 wt:    PSVFLFPPKPKDTLMISRTPEVTCVVVDVSHEDPEVQFNWYVDGVEVHNAKTKPREEQFNSTFRVVSVLTVVHQDWLNGK : 400
kCD4-IgG2 S60c:  ................................................................................ : 400

                    *       420       *       440       *       460       *       480
kCD4-IgG2 wt:    EYKCKVSNKGLPAPIEKTISKTKGQPREPQVYTLPPSREEMTKNQVSLTCLVKGFYPSDIAVEWESNGQPENNYKTTPPM : 480
kCD4-IgG2 S60c:  ................................................................................ : 480

                    *       500       *       520       *
kCD4-IgG2 wt:    LDSDGSFFLYSKLTVDKSRWQQGNVFSCSVMHEALHNHYTQKSLSLSPGK : 530
kCD4-IgG2 S60c:  ................................................... : 530
```

B

```
                    *       20        *       40        *       60        *       80
kCD4-IgG2 wt:    MNRGVPFRHLLLVLQLALLPAATQGKKVVLGKKGDTVELTCTASQKKSIQFHWKNSNQIKILGNQGSFLTKGPSKLNDRA :  80
kCD4-IgG2 S60c:  ................................................................................ :  80

                    *       100       *       120       *       140       *       160
kCD4-IgG2 wt:    DSRRSLWDQGNFPLIIKNLKIEDSDTYICEVEDQKEEVQLLVFGLTANSDTHLLQGQSLTLTLESPPGSSPSVQCRSPRG : 160
kCD4-IgG2 S60c:  .C.............................................................................. : 160

                    *       180       *       200       *       220       *       240
kCD4-IgG2 wt:    KNIQGGKTLSVSQLELQDSGTWTCTVLQNQKKVEFKIDIVVLAFTVAAPSVFIFPPSDEQLKSGTASVVCLLNNFYPREA : 240
kCD4-IgG2 S60c:  ................................................................................ : 240

                    *       260       *       280       *       300       *
kCD4-IgG2 wt:    KVQWKVDNALQSGNSQESVTEQDSKDSTYSLSSTLTLSKADYEKHKVYACEVTHQGLSSPVTKSFNRGEC : 310
kCD4-IgG2 S60c:  ............................................................... : 310
```

Figure 3.2: Amino acid sequence alignments of the kCD4-IgG2^{wt} and kCD4-IgG2^{S60C} heavy (A) and light chains (B). Dots indicate identity to the top sequence. The amino acids not highlighted represent the CD4 portions of the proteins, amino

acids highlighted blue represent the IgG2 portions of the proteins and the S60C mutation is highlighted in yellow.

3.3 Analysis of purified and digested pcDNA 3.1 (+) recombinant constructs

Single restriction enzyme digest analyses of the pKH^{wt}, pKH^{S60C}, pKL^{wt} and pKL^{S60C} constructs loaded in a 0.7% agarose gel are shown in Figure 3.3.

After digestion with Eco R1, pKH^{wt} and pKH^{S60C} constructs showed the expected size of approximately 7100 bp (actual size of 7027 bp) (Figure 3.3, lane 2 and 4 respectively). The digested pKL^{wt} and pKL^{S60C} constructs display a size of approximately 6500 bp (actual size of 6367 bp) (Figure 3.3, lane 6 and 8 respectively).

The purified recombinant plasmids were used in all subsequent transient transfection experiments.

3.4 Single-transfections for optimal transient expression of each construct in HEK293T cells

Different transfection reagents, recombinant plasmid concentrations and post-transfection harvest times were successfully compared to establish optimal transient expression protocols for each of the four constructs in HEK293T cells.

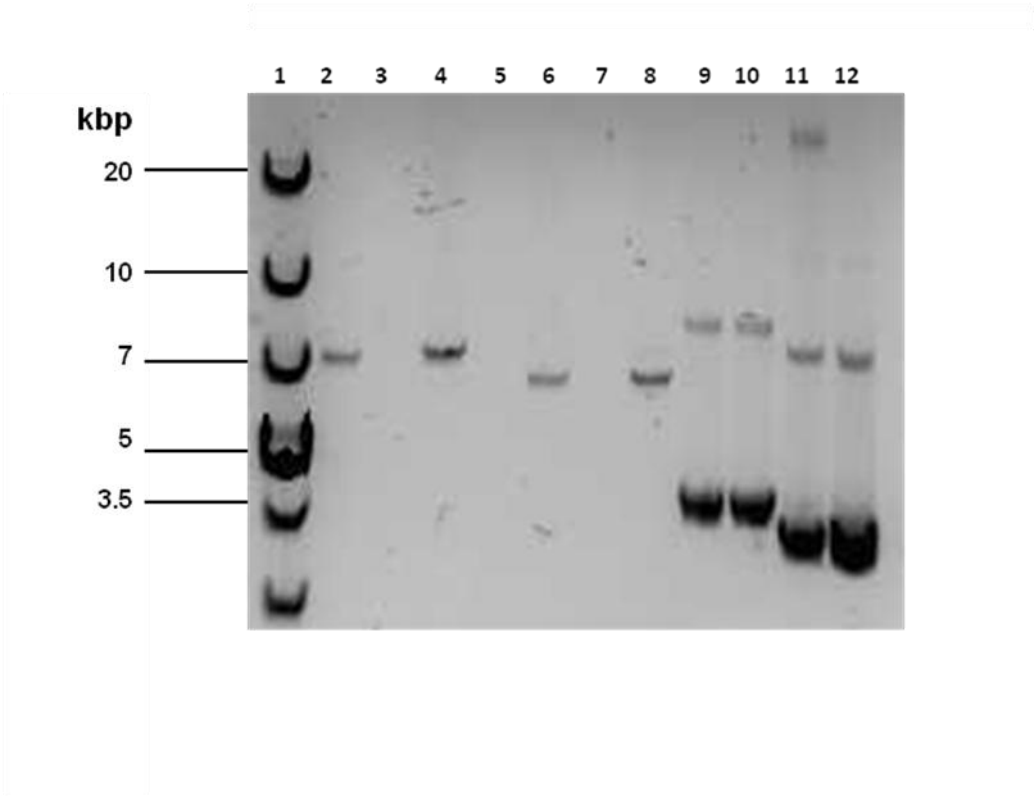

Figure 3.3: Agarose gel electrophoresis analyses of *EcoRI* digested and undigested pKH^{wt}, pKH^{S60C}, pKL^{wt} and pKL^{S60C} constructs after purification. Lane 1: Molecular weight marker, lane 2: digested pKH^{wt}, lane 4: digested pKH^{S60C}, lane 6: digested pKL^{wt}, lane 8: digested pKL^{S60C}, lane 9: undigested pKH^{wt}, lane 10: undigested pKH^{S60C}, lane 11: undigested pKL^{wt} and lane 12: undigested pKL^{S60C}. Molecular weights are shown in kilobase pairs (kbp) on the left.

3.4.1 Optimized expression of kCD4-IgG2^{wt} LC in HEK293T cells using different DNA carriers

A comparison of the transient expression profiles of pKL^{wt} using the maximum amounts of plasmid DNA concentrations recommended for Polyfect transfection reagent (4 µg) and Lipofectamine™ (10 µg) in HEK293T cells is shown in Figure 3.4.

Overall, proteins were transiently expressed in 25 cm^3 dishes with 7 mL of culture supernatant, harvested at 48 hours post-transfection, concentrated to 500 µL, and used (30 µL) for SDS-PAGE and Western blot analyses. The amount of detected

kCD4-IgG2^{wt} LC protein expressed from 4 µg of pKL^{wt} using Polyfect transfection reagent was similar to the amount of detected kCD4-IgG2^{wt} LC protein expressed from 10 µg of pKL^{wt} using Lipofectamine™, thus Polyfect transfection reagent was used in all subsequent HEK293T transfection experiments due to the lower plasmid concentrations required for transfections and lower cost of reagent.

Protein expression levels at 24 hours post-transfection were much lower than at 48 hours post-transfection (results not shown). Supernatants and cells were harvested at 48 hours post-transfection in all subsequent single-transfection optimization experiments.

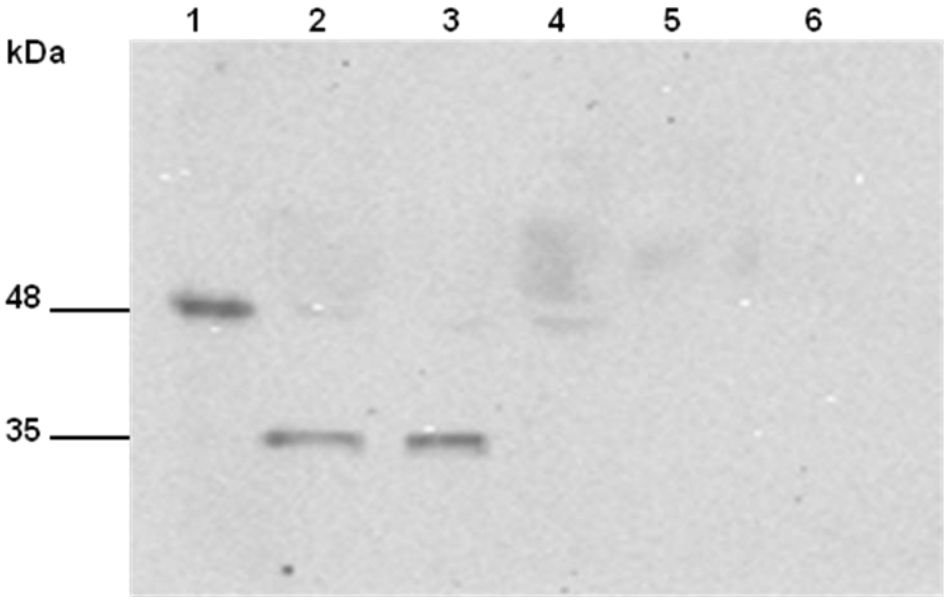

Figure 3.4: Western blot image showing the protein expression levels of 4 µg and 10 µg of kCD4-IgG2^{wt} LC using Polyfect transfection reagent and Lipofectamine™, respectively. Lane 1: 0.5 µg of positive control 4dsCD4^{S60C}, lane 2: kCD4-IgG2^{wt} LC expression from 10 µg of pKL^{wt} using Lipofectamine™, lane 3: kCD4-IgG2^{wt} LC expressed from 4 µg of pKL^{wt} using Polyfect transfection reagent, lane 6: negative control culture supernatant. Molecular weights in kilodaltons (kDa) are shown on the left.

3.4.2 Optimization of protein expression by varying concentrations of pKH^{wt}, pKH^{S60C}, pKL^{wt} and pKL^{S60C} with Polyfect transfection reagent

Levels of proteins expressed in HEK293T cells by transient transfection with 2 µg and 4 µg of pKH^{wt}, pKH^{S60C}, pKL^{wt} and pKL^{S60C} with appropriate amounts of Polyfect are shown in Figure 3.5.

The proteins were each expressed in 25 cm^3 flasks, 7 mL of culture supernatant, concentrated to 500 µL, and 30 µL thereof was analysed by SDS-PAGE and Western blot techniques. In addition, the transfected HEK293T cells were lysed with 500 µL of lysis buffer and 30 µL of the cell-lysate was analysed by SDS-PAGE and Western blot (results not shown).

The kCD4-IgG2^{wt} and kCD4-IgG2^{S60C} LC proteins were secreted into the culture supernatant, and similar expression levels of kCD4-IgG2^{S60C} LC protein were seen after transient transfections with 2 µg or 4 µg of pKL^{S60C} (Figure 3.5, lanes 6 and 8, respectively). The amount of kCD4-IgG2^{wt} LC protein expressed from 4 µg of pKL^{wt} was higher than the amount of protein expressed by 4 µg of pKL^{S60C}.

No expression of the kCD4-IgG2^{wt} or kCD4-IgG2^{S60C} HC proteins in the culture supernatant was detected at the two concentrations of pKH^{wt} or pKH^{S60C} tested. Interestingly, the kCD4-IgG2^{wt} and kCD4-IgG2^{S60C} HC and LC proteins were all detected in the cell-lysate in small quantities (data not shown).

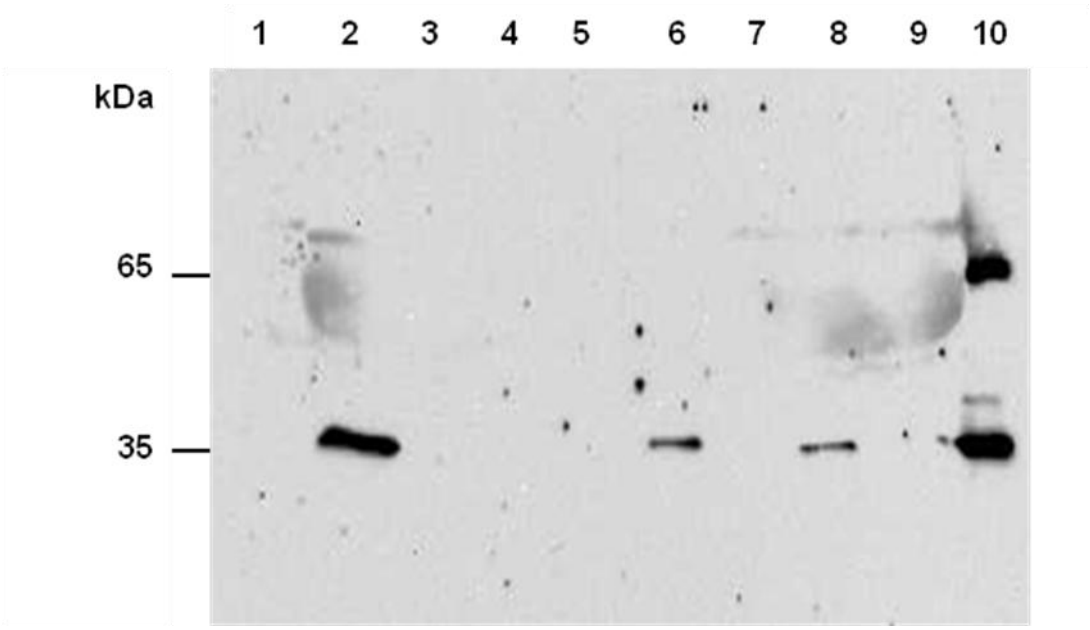

Figure 3.5: Western blot image showing the protein expression levels of 2 µg and 4 µg of pKL^{wt}, pKL^{S60C}, pKH^{wt} and pKH^{S60C} transfected with Polyfect transfection reagent into HEK293T cells in 25 cm^3 flasks. Lane 2: kCD4-IgG2^{wt} LC expression from 4 µg of pKL^{wt}, lane 3: kCD4-IgG2^{wt} HC expression from 2 µg of pKH^{wt}, lane 4: supernatant from untransfected cells, lane 5: kCD4-IgG2^{wt} HC expression from 4 µg of pKH^{wt}, lane 6: kCD4-IgG2^{S60C} LC expression from 2 µg of pKL^{S60C}, lane 7: kCD4-IgG2^{S60C} HC expression from 2 µg of pKH^{S60C}, lane 8: kCD4-IgG2^{S60C} LC expressed from 4 µg of pKL^{S60C}, lane 9: kCD4-IgG2^{S60C} HC expressed from 4 µg of pKH^{S60C} and lane 10: 0.5 µg of positive control NIH PRO 542.

Overall, transient transfection of HEK293T cells in 25cm^3 flasks, using 4 µg recombinant plasmid and 40 µL Polyfect transfection reagent, 7 mL culture supernatant and proteins being harvested at 48 hours post-transfection were considered optimal conditions.

3.5 Co-transfections for transient expression of kCD4-IgG2^{wt} and kCD4-IgG2^{S60C} heterotetrameric proteins

The ability of HEK293T cells to produce fully assembled kCD4-IgG2^{wt} and kCD4-IgG2^{S60C} protein is shown in Figures 3.6 and 3.7, respectively. A total of 400 mL of

culture supernatant containing heterotetrameric kCD4-IgG2^{wt} (or kCD4-IgG2^{S60C}) was concentrated to 500 µL (or 300 µL), and 60 µL was analysed by SDS-PAGE and Western blot analyses under non-reducing (Figure 3.6 A and 3.7) and reducing conditions (Figures 3.6 B).

Co-transfection of HEK293T cells with pKH^{wt} and pKL^{wt} allowed for the expression of a heterotetrameric kCD4-IgG2^{wt} molecule of the expected 200 kDa size under non-reducing conditions (Figure 3.6 A, lane 6), with individual heavy chains (65 kDa) and light chains (35 kDa) seen under reducing conditions (Figure 3.6B, lane 6). CD4 containing proteins of 130 kDa size were observed and presumed to be HC homodimers of kCD4-IgG2^{wt} (Figure 3.6 A, lane 6). The amount of assembled kCD4-IgG2^{wt} protein in the sample is approximately 0.6 µg, as determined by densitometry analysis (Figure 3.6 A, lane 6). Molecules smaller than 35 kDa size were excluded after the concentration step. The decreasing concentrations of the NIH PRO 542 positive control were used to quantify the amount of heterotetrameric kCD4-IgG2^{wt} present in the samples to greater than 500 ng. The heavy chains of NIH PRO 542 were not observed under reducing conditions, however. The amounts of detectable heavy chains of PRO 542 may be greater than 500 ng for this Western blotting analysis.

Under non-reducing conditions, supernatant analysis of co-transfections of HEK293T cells with pKH^{S60C} and pKL^{S60C} did not show high levels of the expected 200 kDa sized heterotetrameric kCD4-IgG2^{S60C} molecule, but the individual heavy and light chains are visible in relatively high amounts (Figure 3.7, lane 1). Considering that molecules smaller than 35 kDa were excluded during the concentration step, the 35 kDa size kCD4-IgG2^{S60C} LC proteins were not expected to be detected. Heterotetrameric kCD4-IgG2^{S60C} protein is likely to be more unstable than the heterotetrameric kCD4-IgG2^{wt} protein as more unassembled product is observed for the former compared to the latter. According to the NIH PRO 542 standard, the amount of heterotetrameric kCD4-IgG2^{S60C} expressed was considerably lower than 500 ng (approximately 25 ng) as determined by Western blot and densitometry analysis.

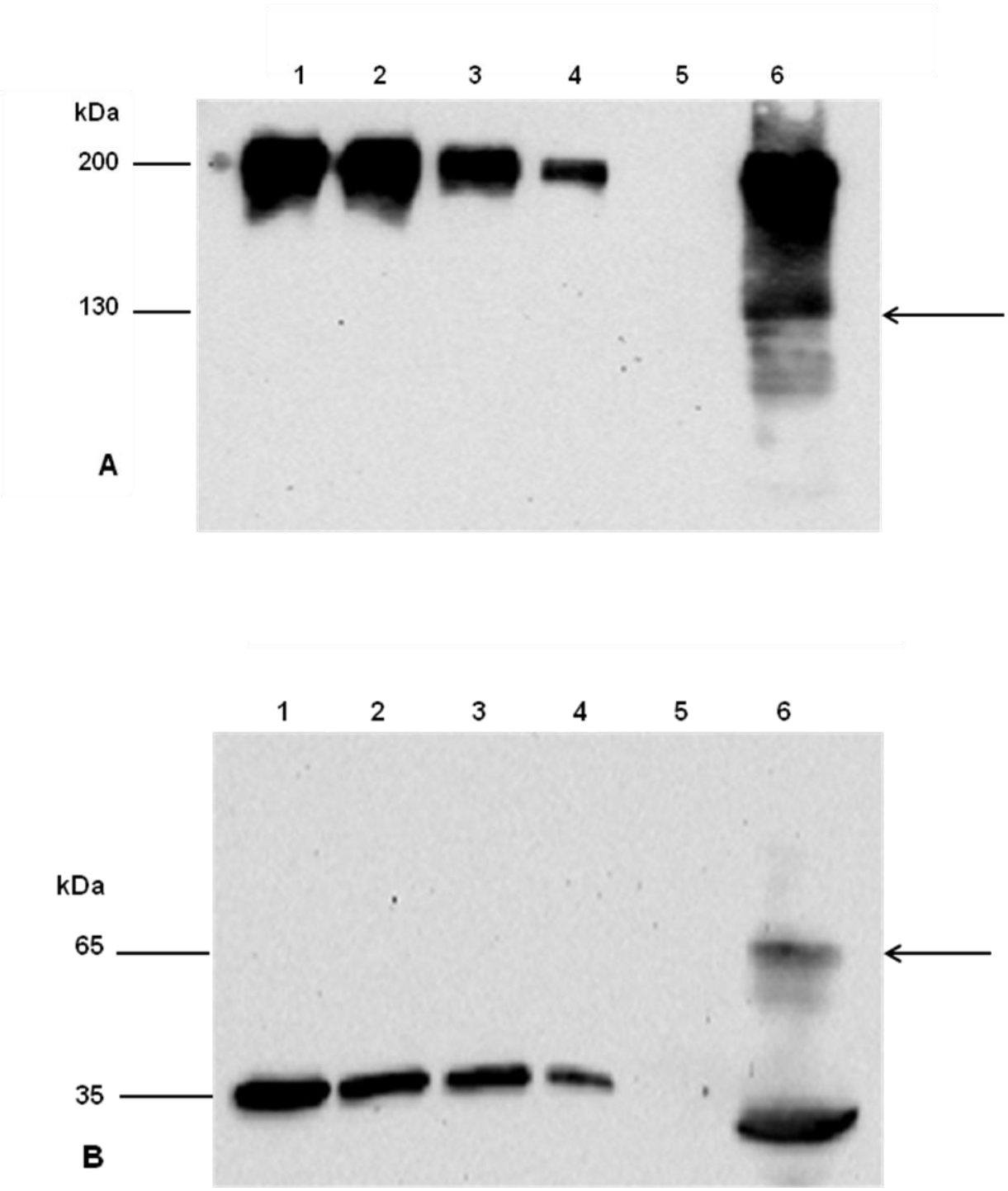

Figure 3.6: Western blot image showing expressed amounts of kCD4-IgG2^{wt}, NIH PRO 542 standards and control expression culture supernatant, under non-reducing (A) and reducing conditions (B). Lane 1: 500 ng of NIH PRO 542, lane 2: 250 ng of NIH PRO 542, lane 3: 100 ng of NIH PRO 542, lane 4: 50 ng of NIH PRO 542, lane 5: concentrated negative control

culture supernatant and lane 6: concentrated kCD4-IgG2^{wt} containing culture supernatant. The arrow indicates kCD4-IgG2^{wt} HC expressed.

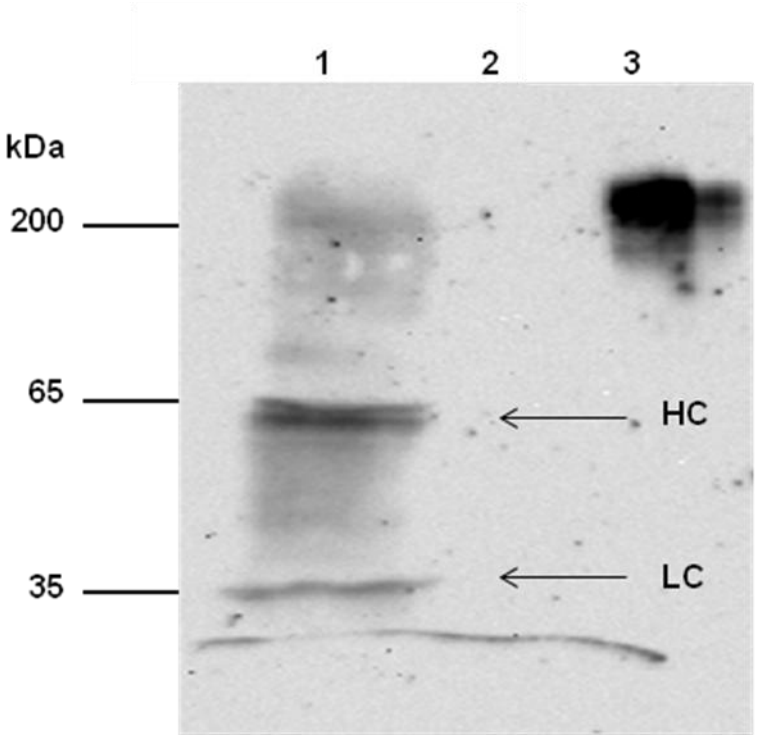

Figure 3.7: Western blot image showing expressed amounts of kCD4-IgG2^{S60C} with an NIH PRO 542 standard and control expression culture supernatant under non-reducing conditions. Lane 1: concentrated kCD4-IgG2^{S60C} containing culture supernatant, lane 2: concentrated negative control culture supernatant and lane 3: 500 ng of NIH PRO 542.

Overall, transient transfections were repeated under the optimal conditions described above, where culture supernatant containing heterotetrameric proteins was harvested, concentrated (where required), and used to establish purification protocols.

3.6 Purification of heterotetrameric kCD4-IgG2^{wt} and heterotetrameric kCD4-IgG2^{S60C}

Several protocols for the purification of heterotetrameric kCD4-IgG2^{wt} and kCD4-IgG2^{S60C} were evaluated using Protein-A resin from a column and beads. Expression of the relevant constructs was confirmed by SDS-PAGE and Western blot analysis prior to using the supernatant for purification.

3.6.1 Purification of heterotetrameric kCD4-IgG2^{wt} from serum-free conditioned medium using the Äkta FPLC system

Attempts to purify kCD4-IgG2^{wt} from culture supernatant loaded onto a Protein-A column was of limited success (results not shown). Overall, while monitoring the absorbance (A_{280}) of the sample during the purification process, a negligible amount (< 100 milliamps units) of protein was detected in the wash step, elution step and regeneration step. SDS-PAGE and Western blot analysis of concentrated flow-through, washes, eluate, regeneration solutions, and Protein-A resin from the column confirmed the absence of heterotetrameric kCD4-IgG2^{wt}.

Based on the volumes used, low concentrations of proteins expressed, and low binding capacity of the Protein-A resin used above, further purification protocols using Protein-A agarose beads from manufacturers other than GE Healthcare were investigated.

3.6.2 Purification of heterotetrameric kCD4-IgG2^{wt} and heterotetrameric kCD4-IgG2^{S60C} using Protein-A agarose beads

An affinity purification protocol of heterotetrameric kCD4-IgG2^{wt} and kCD4-IgG2^{S60C} using Protein-A agarose beads purchased from Bio-Rad (Hercules, USA) confirmed that the recombinant proteins could bind to the beads, but could not be effectively eluted.

Volumes of 65-70 mL of heterotetrameric kCD-IgG2^{wt} containing culture supernatant were routinely incubated with 1 mL of Protein-A agarose beads,

and 35 mL of kCD4-IgG2^{S60C} containing culture supernatant was then incubated with 0.5 mL of Protein-A agarose beads. Subsequently, 30 µL of the initial unbound material, bound material adsorbed to beads, concentrated washes, concentrated eluate and concentrated regenerate were analysed by SDS-PAGE and Western blot techniques (Figure 3.8). The kCD4-IgG2^{wt} heterotetramer was expressed (Figure 3.8 A, lane 9) and observed to bind Protein-A agarose beads (Figure 3.8 A, lane 10). Inability to detect kCD4-IgG2^{wt} in the eluate suggested that the recombinant proteins could not effectively dissociate from the beads. It was likely that small amounts of undetected kCD4-IgG2^{wt} were eluted, but were undetectable.

Similar results were seen of the kCD4-IgG2^{S60C} protein binding to the Protein-A beads, but with much lower amounts of proteins detected on the beads (Figure 3.8 B, lane 1).

To confirm that the kCD4-IgG2^{wt} and kCD4-IgG2^{S60C} proteins were still bound to the beads, a different elution buffer (0.1 M sodium acetate buffer at pH 3.5) was employed to elute the proteins. Elution of detectable amounts of kCD4-IgG2^{wt} and kCD4-IgG2^{S60C} with the sodium acetate buffer proved unsuccessful as well (data not shown).

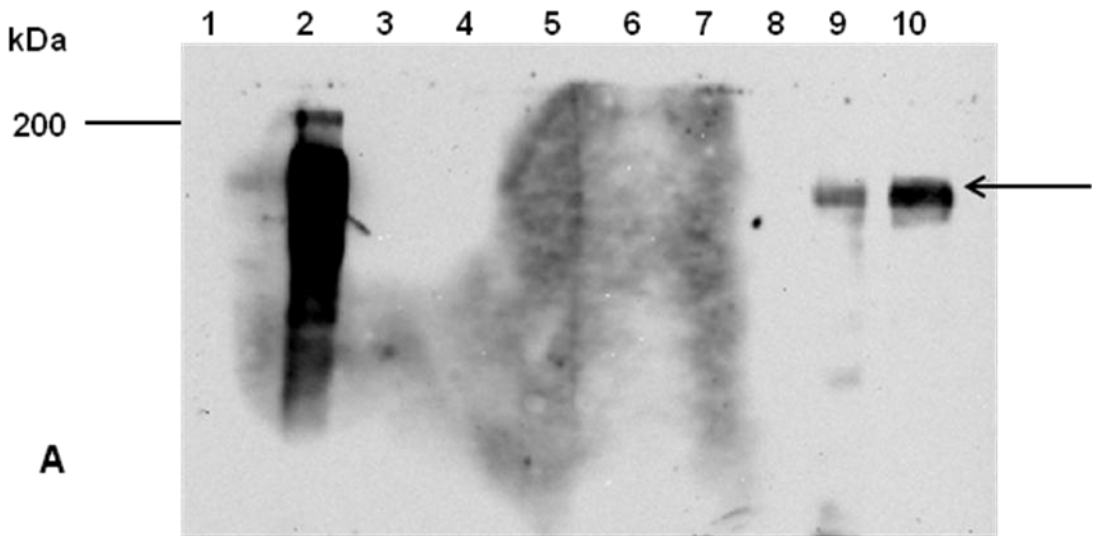

Figure 3.8 A: Western blot image showing samples of the steps during the purification process of kCD4-IgG2^{wt}. Lane 2: 1 µg of NIH PRO 542, lane 5: regenerate, lane 6: eluate, lane 7: washes, lane 9: concentrated supernatant sample before purification and lane 10: 30 µL of Protein-A beads with adsorbed heterotetrameric kCD4-IgG2^{wt} after 72 hours incubation of beads with kCD4-IgG2^{wt} containing culture supernatant. The arrow indicates kCD4-IgG2^{wt} bound to beads.

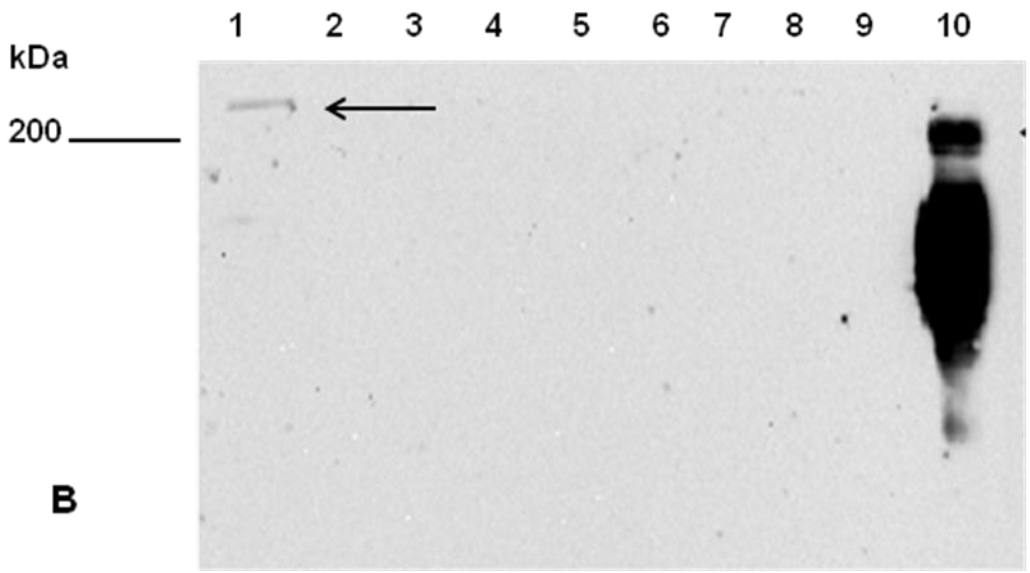

Figure 3.8 B: Western blot image showing the analysis of the samples collected during the purification of kCD4-IgG2^{S60C}. Lane 1: 30 µL of Protein-A beads with adsorbed heterotetrameric kCD4-IgG2^{S60C} after 72 hour incubation of beads with kCD4-IgG2^{S60C} containing culture supernatant, Lane 2: concentrated supernatant before purification, lane 3: washes, lane 4: eluate, lane 5: regenerate, lane 10: 1 µg of NIH PRO 542. The arrow indicates kCD4-IgG2^{S60C} bound to beads.

3.7 Immunoprecipitation of HIV gp120 by heterotetrameric kCD4-IgG2^{wt} bound to Protein-A agarose beads

3.7.1 Optimal binding of kCD4-IgG2^{wt} to Protein-A agarose beads

In preparation of the immunoprecipitation of gp120 using NIH PRO 542 and kCD4-IgG2^{wt} (both adsorbed to Protein-A agarose beads), the binding capacity of the Protein-A beads was measured. Concurrently, the ability of gp120 Bal and 93TH975 to bind to the anti-gp120 antibody cocktail (composed of Chessie 13-39.1 supernatant, ID6 and NEA-9301) was assessed.

Figure 3.9 A shows that equivalent amounts of kCD4-IgG2^{wt} and NIH PRO542 positive control bind to the same amount of Protein-A agarose beads. Also detected binding to the Protein-A agarose beads were the HC homodimers of PRO 542 and

kCD4-IgG2^{wt} (130 kDa size) (Fig 3.9 A lanes 3 and 5, respectively) which migrated similar distances as gp120 Bal (Fig 3.9 B, lane 8).

Interestingly, the anti-gp120 antibody cocktail detected gp120 Bal, but not gp120 93TH975 (Figure 3.9 B).

Immunoprecipitation assays were conducted using gp120 Bal, with the same amounts of PRO 542 (as a control) and kCD4-IgG2^{wt}.

3.7.2 Immunoprecipitation of HIV gp120 by heterotetrameric kCD4-IgG2^{wt} bound to Protein-A agarose beads

The gp120 Bal protein bound to heterotetrameric NIH PRO 542 and kCD4-IgG2^{wt} (pre-incubated with Protein-A agarose beads) implying that the CD4 containing proteins were fully folded and had functional CD4 and Fc portions (Figure 3.10, lanes 3 and 7, respectively). Based on the ability of fully folded kCD4-IgG2^{wt} and kCD4-IgG2^{S60C} to bind Protein-A agarose beads and the ability of heterotetrameric kCD4-IgG2^{wt} to bind gp120 Bal, surface plasmon resonance (SPR) experiments were conducted to confirm the specificity of kCD4-IgG2^{wt} and kCD4-IgG2^{S60C} for various gp120s.

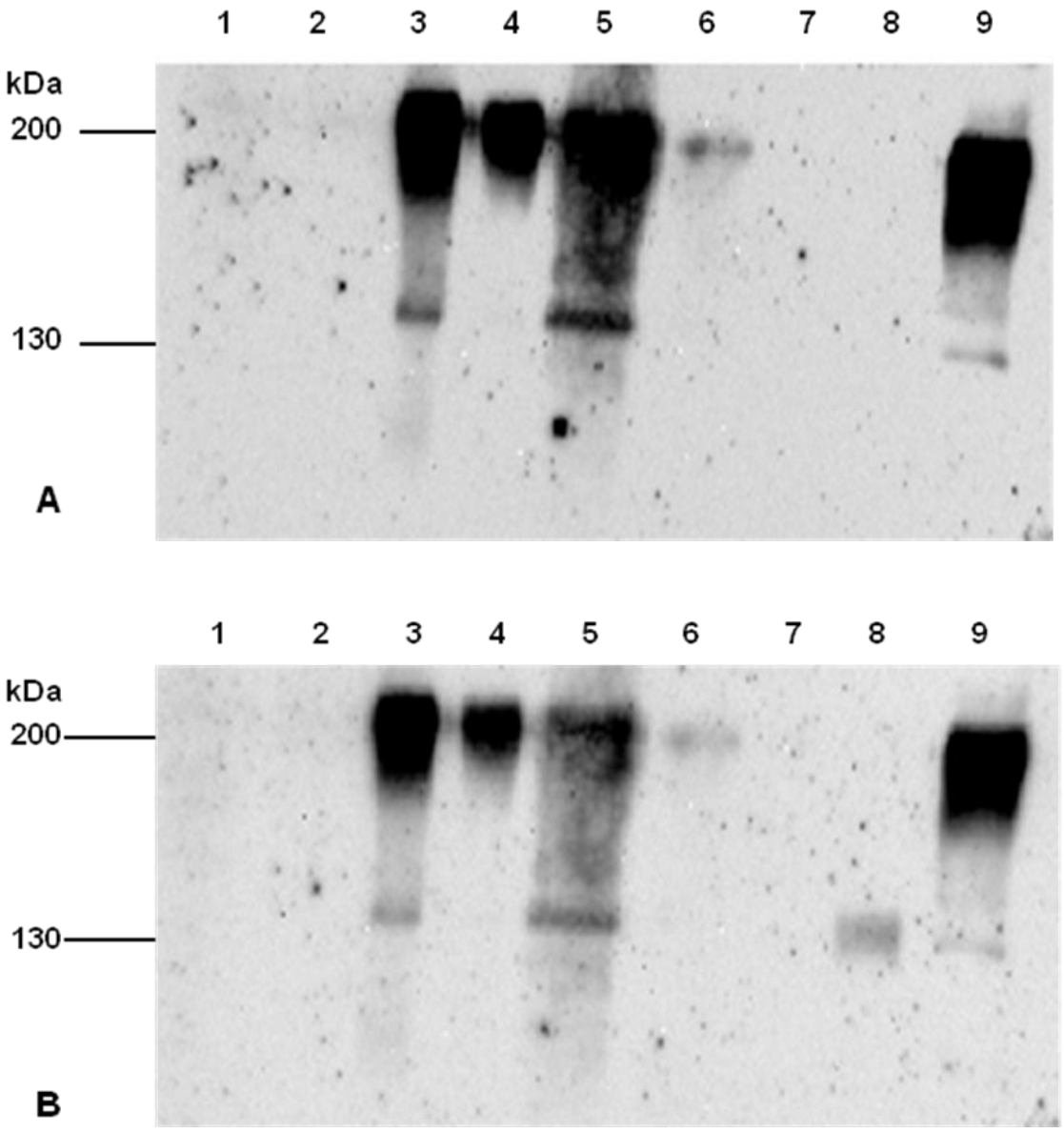

Figure 3.9: Western blot image showing the binding capacity of Protein-A agarose beads to kCD4-IgG2^{wt} using anti-CD4 antibodies (A) and detection of gp120 using anti-gp120 antibodies (B). Lane 1: Protein-A beads incubated with negative control expression culture supernatant, lane 2: Unbound materials to Protein-A beads from control expression culture supernatant, lane 3: Protein-A beads incubated with NIH PRO 542, lane 4: Unbound NIH PRO 542 to Protein-A beads, lane 5: kCD4-IgG2^{wt} containing culture supernatant incubated with Protein-A beads, lane 6: Unbound kCD4-IgG2^{wt} to Protein-A beads, lane 7: 0.5 µg of HIV gp120 93TH975, lane 8: 0.5 µg of HIV gp120 Bal and lane 9: 1 µg of NIH PRO 542.

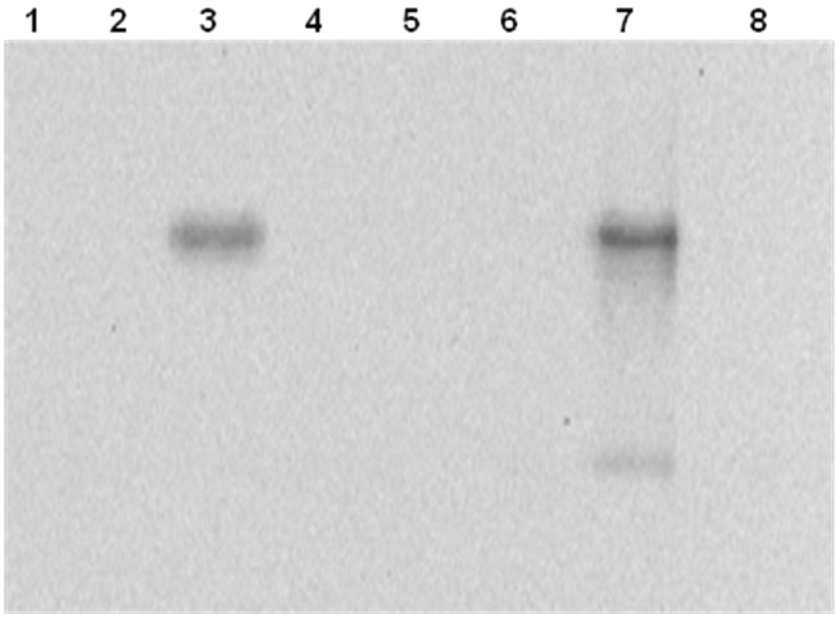

Figure 3.10: Western blot image of the immunoprecipitation of HIV-1 gp120 Bal by kCD4-IgG2^{wt} adsorbed to Protein-A agarose beads. Lane 1: Protein-A beads incubated with control culture supernatant only, lane 2: gp120 Bal bound to Protein-A beads treated with control culture supernatant, lane 3: gp120 Bal bound to Protein-A beads with adsorbed NIH PRO 542, lane 4: unbound gp120 from Protein-A beads with adsorbed NIH PRO 542, lane 5: Protein-A beads only, lane 6: unbound gp120 to Protein-A beads, lane 7: gp120 Bal bound to Protein-A beads with adsorbed kCD4-IgG2^{wt}, lane 8: unbound gp120 from Protein-A beads with adsorbed kCD4-IgG2^{wt}.

3.8 SPR analysis of gp120 binding to heterotetrameric kCD4-IgG2^{wt} and heterotetrameric kCD4-IgG2^{S60C}

The ability of kCD4-IgG2^{wt} and kCD4-IgG2^{S60C} (in supernatant) to bind gp120 from different HIV-1 subtype B and C isolates, as compared to NIH PRO 542, 2dsCD4^{wt} and 2dsCD4^{S60C}, was successfully determined by SPR (Figure 3.11).

The sensorgrams (Figure 3.11) show the intensity of interaction of the various analytes interacting with different gp120 ligands over time and are measured in response units (RU). Figures 3.11 A to 3.11 F show six different analytes binding to six gp120s, whereas Figures 3.11 G to 3.11 L show the level of binding of MAb 17b to the gp120s CD4i after analyte binding.

Overall, the kCD4-IgG2^{wt} protein in supernatant was capable of binding the panel of six gp120s (Figure 3.11 A-F). Only two gp120s did not have their CD4 induced epitopes (CD4i) exposed by kCD4-IgG2^{wt} for MAb 17b binding (Figure 3.11 G and K). The kCD4-IgG2^{S60C} protein in supernatant was not detected to bind any of the gp120s. Surprisingly the CoRbs of four out of six gp120s was minimally exposed for MAb 17b binding by kCD4-IgG2^{S60C} (Figure 3.11 G, H, K and L).

PRO 542 from the NIH was observed to bind all gp120s with RU levels greater than 1000 except for gp120 ZM (RU of approximately 620, Figure 3.11 E). All the sensorgrams displaying NIH PRO 542 binding to gp120 showed an association phase, equilibrium and dissociation phase. Although NIH PRO 542 was able to bind all the gp120s, it was unable to elicit the CD4i of gp120 CN54 and ZM (Figure 3.11 G and K) for MAb 17b binding. The gp120s which had their CD4i exposed by NIH PRO 542 (gp120 SF162, IN, ZA and Bal) could bind minimally to MAb 17b with RU levels between 20 and 50 (Figure 3.11 H, I, J and L).

The 2dsCD4^{wt} protein was observed to bind the six gp120s with RU levels greater than 600 except for gp120 ZM and Bal (RU levels of 300 and 400, respectively; Figure 3.11 E and F). As with NIH PRO 542, an association, equilibrium and dissociation phase was observed with all 2dsCD4^{wt}-gp120 interactions. The 2dsCD4^{wt} protein was capable of exposing the CD4i of five gp120s with RU levels ranging from 40 to 135 (Figure 3.11 G, H, I, J, and L). The sensorgrams showing MAb 17b binding gp120s also have distinct association, equilibrium and dissociation phases.

The 2dsCD4^{S60C} protein was found to bind gp120 CN54, SF162, IN, ZA and Bal (Figure 3.11 A to F) in similar amounts to NIH PRO 542. Notably, 2dsCD4^{S60C} showed significantly higher binding to gp120 ZM than NIH PRO 542 (Figure 3.11 E). The sensorgrams of 2dsCD4^{S60C} interacting with gp120 all have distortions in the association phase due to air bubbles that were introduced onto the chip surface, because the sample volume was slightly low upon injection, but did not affect the subsequent interaction of 2dsCD4^{S60C} with gp120 significantly. All of the 2dsCD4^{S60C}-gp120 interactions were observed to have association, equilibrium and dissociation phases as the NIH PRO 542-gp120 interactions. The 2dsCD4^{S60C} protein, as NIH PRO 542, was unable to expose the CD4i of gp120 CN54 and ZM (Figure 3.11 G and K). The gp120s which had their CD4i exposed (gp120 SF162, IN, ZA and Bal) bound MAb 17b in highly similar levels to those observed when NIH PRO 542 elicited the CD4i (Figure 3.11 H, I, J and L).

The kCD4-IgG2^{wt} protein in supernatant bound all six gp120s with RU levels greater than 180 (Figure 3.11 A to F). The interactions with gp120 all involved an association, equilibrium and dissociation phase. Interestingly, little amount of dissociation from gp120 was observed by kCD4-IgG2^{wt} except in the cases of gp120 IN and ZA, where a relatively large amount of kCD4-IgG2^{wt} dissociated from the gp120s (Figure 3.11, C and D). Notably, the concentration of kCD4-IgG2^{wt} in supernatant interacting with the gp120s was approximately half that of NIH PRO 542, however NIH PRO 542 bound the same gp120s with 5 fold higher RU levels. The kCD4-IgG2^{wt} protein was observed to expose the CD4i of gp120 SF162 and ZA in similar amounts to NIH PRO 542 and 2dsCD4^{S60C}. Overall, kCD4-IgG2^{wt} could not elicit the CD4i of gp120 CN54 and gp120 ZM (Figure 3.11 G and K), but registered MAb 17b binding RU levels greater than 20 where elicitation occurred, except in the case of gp120 Bal (RU level of approximately 10; Figure 3.11 L).

The kCD4-IgG2^{S60C} protein in supernatant could not register binding to any gp120; however this is attributed to low amounts of the heterotetramer present in the supernatant sample (approximately 25 ng). Even though no protein was observed to bind gp120 from the kCD4-IgG2^{S60C} supernatant, elicitation of the gp120 CN54, SF162, ZM and Bal CD4i were observed (Figure 3.11 G, H, K and L).

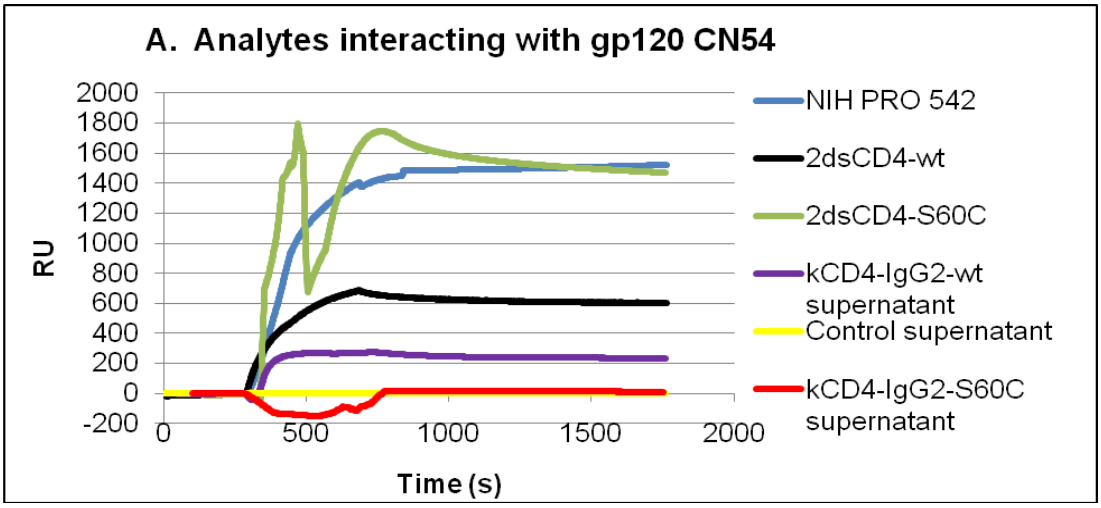
A. Analytes interacting with gp120 CN54
RU
Time (s)
NIH PRO 542
2dsCD4-wt
2dsCD4-S60C
kCD4-IgG2-wt supernatant
Control supernatant
kCD4-IgG2-S60C supernatant

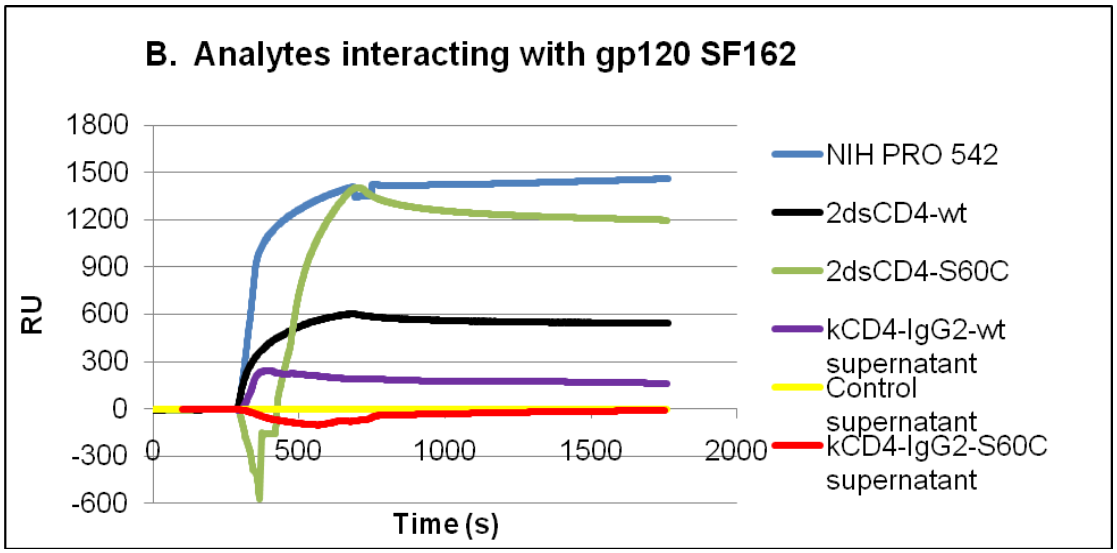
B. Analytes interacting with gp120 SF162
RU
Time (s)
NIH PRO 542
2dsCD4-wt
2dsCD4-S60C
kCD4-IgG2-wt supernatant
Control supernatant
kCD4-IgG2-S60C supernatant

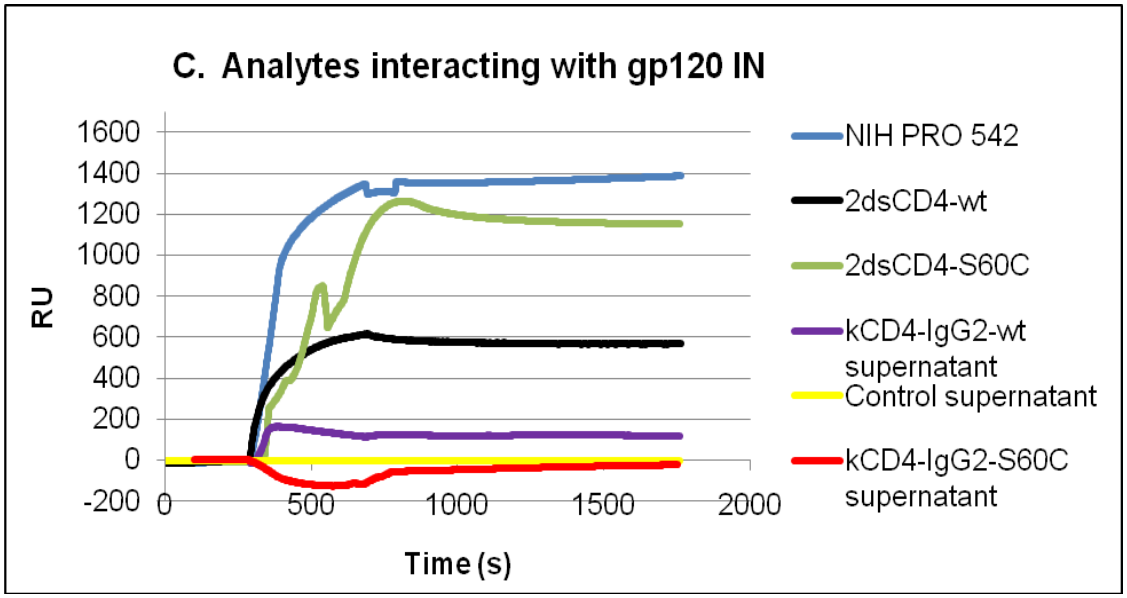
C. Analytes interacting with gp120 IN
RU
Time (s)
NIH PRO 542
2dsCD4-wt
2dsCD4-S60C
kCD4-IgG2-wt supernatant
Control supernatant
kCD4-IgG2-S60C supernatant

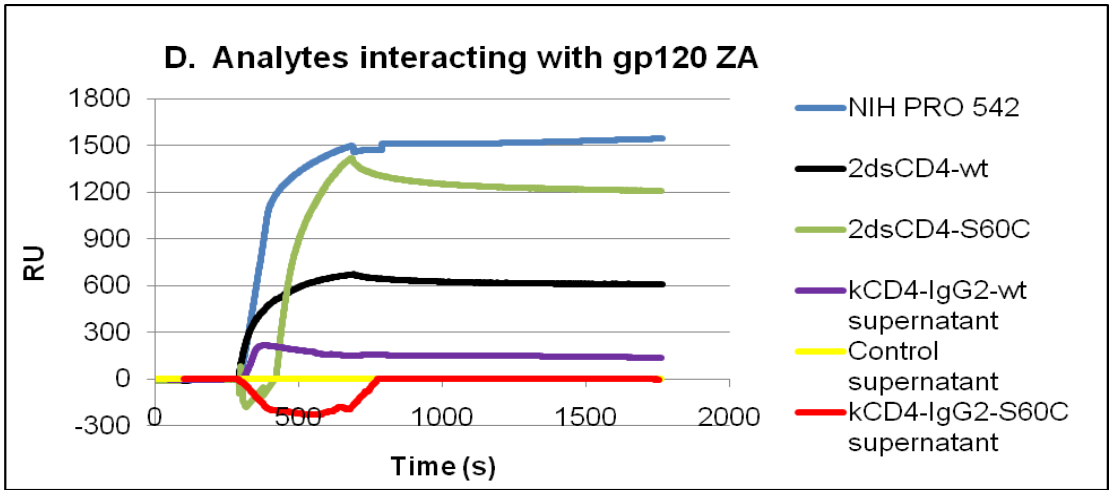
D. Analytes interacting with gp120 ZA
RU
1800
1500
1200
900
600
300
0
-300
0
500
1000
1500
2000
Time (s)
NIH PRO 542
2dsCD4-wt
2dsCD4-S60C
kCD4-IgG2-wt supernatant
Control supernatant
kCD4-IgG2-S60C supernatant

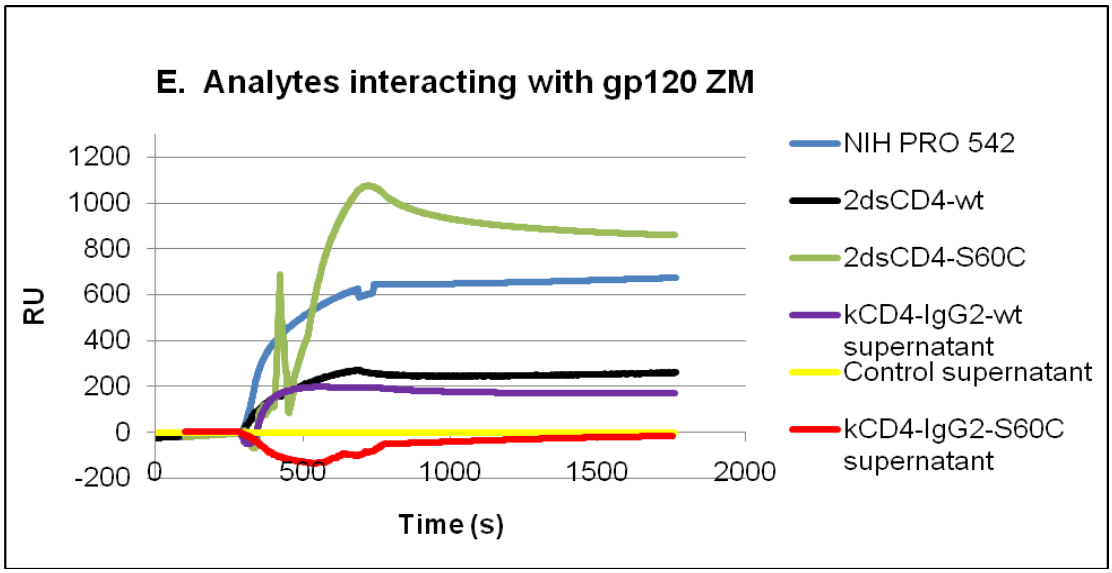
E. Analytes interacting with gp120 ZM
RU
1200
1000
800
600
400
200
0
-200
0
500
1000
1500
2000
Time (s)
NIH PRO 542
2dsCD4-wt
2dsCD4-S60C
kCD4-IgG2-wt supernatant
Control supernatant
kCD4-IgG2-S60C supernatant

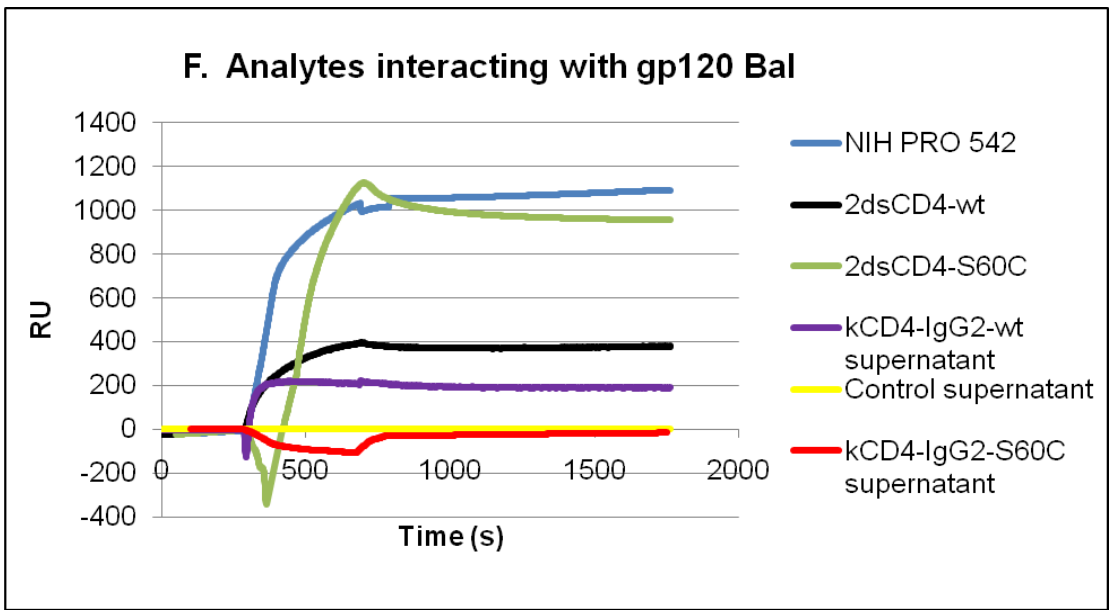
F. Analytes interacting with gp120 Bal
RU
1400
1200
1000
800
600
400
200
0
-200
-400
0
500
1000
1500
2000
Time (s)
NIH PRO 542
2dsCD4-wt
2dsCD4-S60C
kCD4-IgG2-wt supernatant
Control supernatant
kCD4-IgG2-S60C supernatant

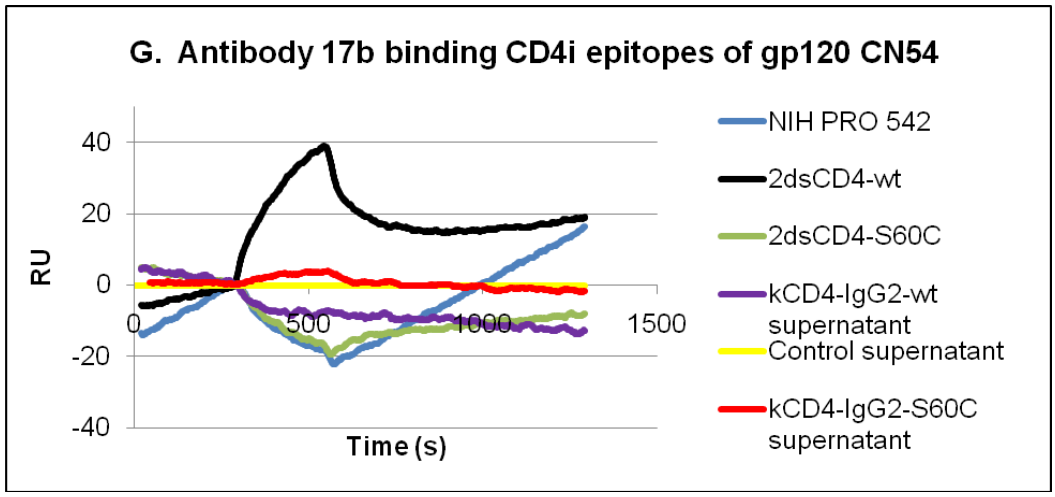
G. Antibody 17b binding CD4i epitopes of gp120 CN54
RU
40
20
0
-20
-40
0
500
1000
1500
Time (s)
NIH PRO 542
2dsCD4-wt
2dsCD4-S60C
kCD4-IgG2-wt supernatant
Control supernatant
kCD4-IgG2-S60C supernatant

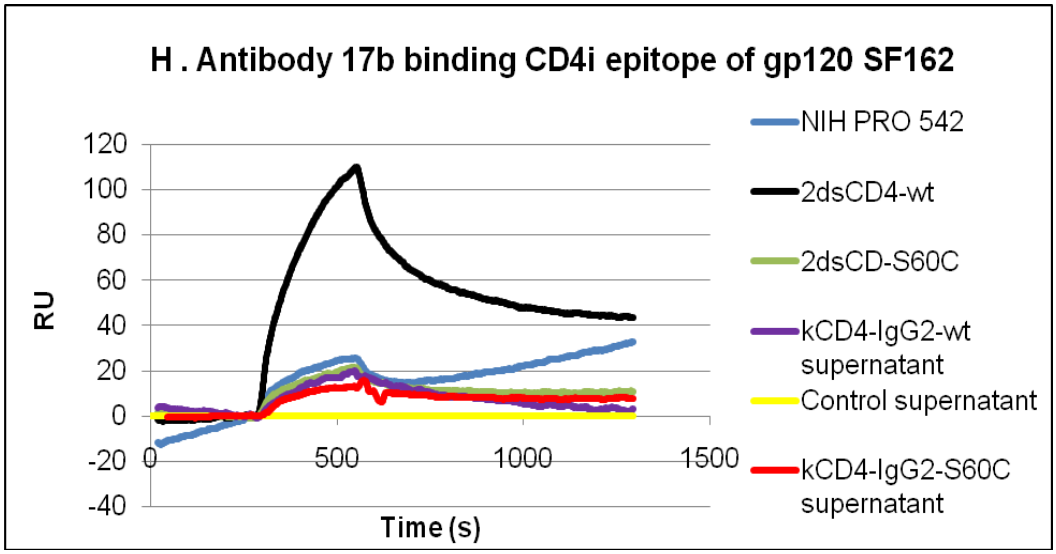
H . Antibody 17b binding CD4i epitope of gp120 SF162
RU
120
100
80
60
40
20
0
-20
-40
0
500
1000
1500
Time (s)
NIH PRO 542
2dsCD4-wt
2dsCD-S60C
kCD4-IgG2-wt supernatant
Control supernatant
kCD4-IgG2-S60C supernatant

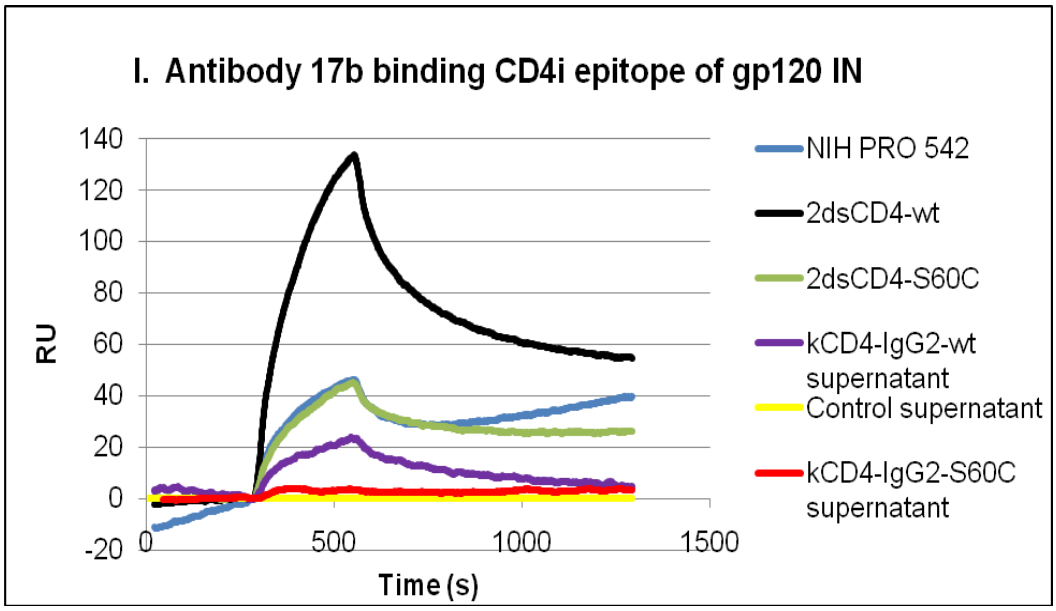
I. Antibody 17b binding CD4i epitope of gp120 IN
RU
140
120
100
80
60
40
20
0
-20
0
500
1000
1500
Time (s)
NIH PRO 542
2dsCD4-wt
2dsCD4-S60C
kCD4-IgG2-wt supernatant
Control supernatant
kCD4-IgG2-S60C supernatant

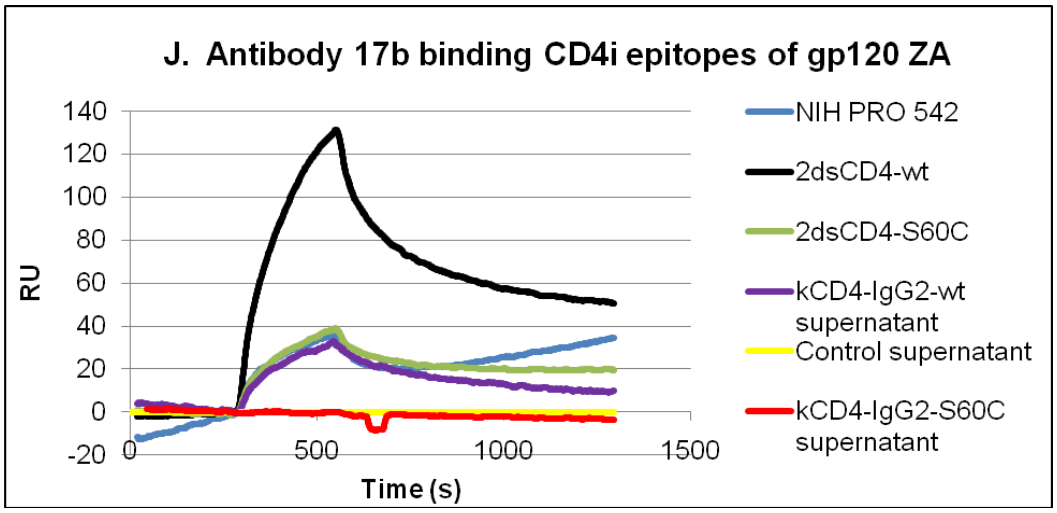

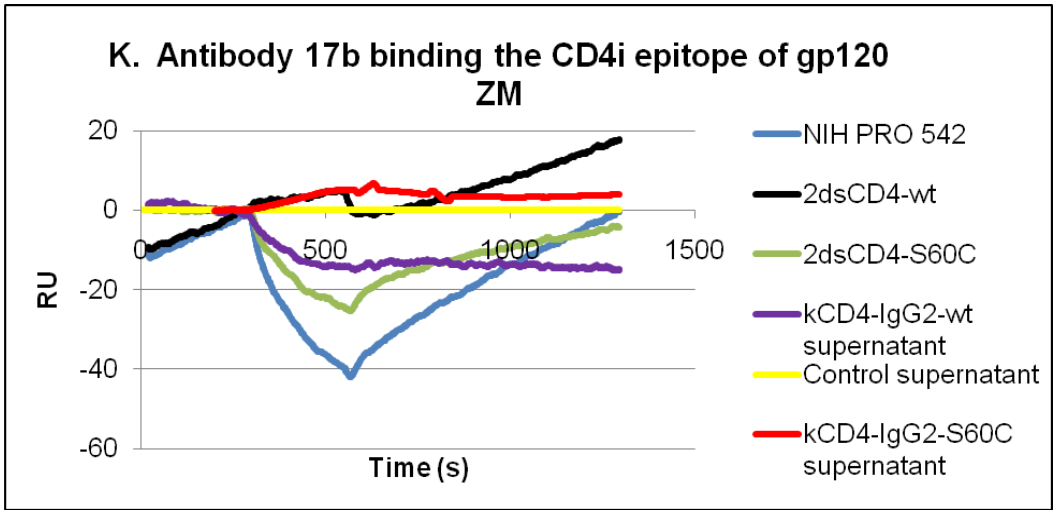

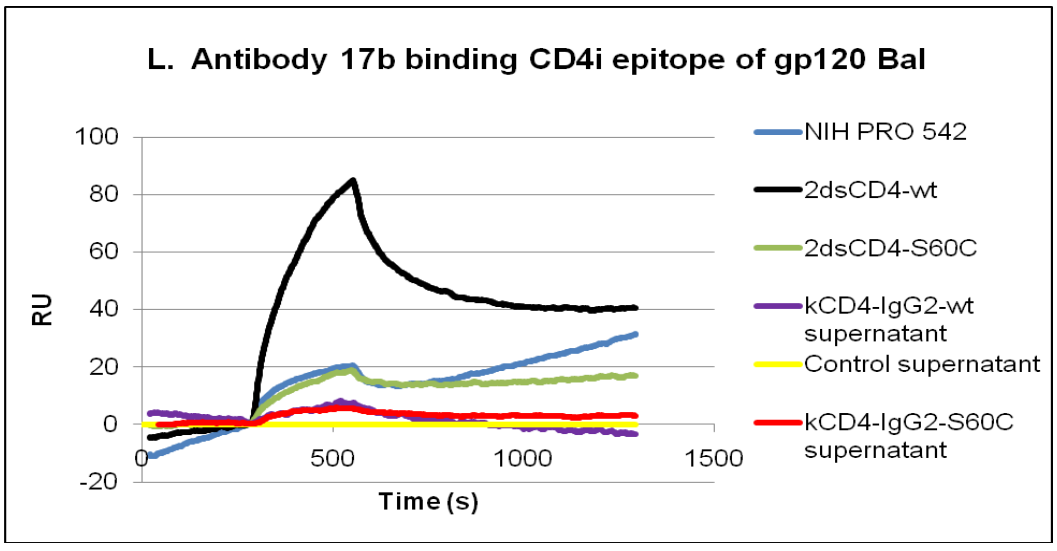

Figure 3.11: The interactions of selected analytes with various immobilised gp120 from HIV clades B and C (A-F), as well as the binding of MAb 17b to the

CD4i of various gp120s exposed by the selected analytes (G-L). The sensorgrams coloured blue are relevant to NIH PRO 542, green sensorgrams are relevant to 2dsCD4^{S60C}, black sensorgrams are relevant to 2dsCD4^{wt}, red sensorgrams are relevant to kCD4-IgG2^{S60C} in supernatant, purple sensorgrams are relevant to kCD4-IgG2^{wt} in supernatant and yellow sensorgrams are relevant to the control supernatant.

Chapter 4: Discussion

The overall aim of this study was to design and produce a novel form of CD4-IgG2 (kCD4-IgG2^{wt}) which would be structurally and functionally identical to PRO 542, composed of CD4 domains one and two (D1D2) replacing the variable heavy and light chain regions of IgG2. A mutant version of the CD4-IgG2 protein (kCD4-IgG2^{S60C}) was also generated, which had an S60C mutation in the CD4 portions, intended to increase the affinity of kCD4-IgG2^{wt} for HIV-1 gp120. Overall, the structural integrity of heterotetrameric kCD4-IgG2^{wt} and kCD4-IgG2^{S60C} proteins was determined by incubating the proteins with an anti-CD4 antibody (MT310) and or the binding of the proteins to Protein-A agarose beads. For comparison, PRO 542 (donated by the NIH) was used as a positive control. Protein-A affinity chromatography protocols were then employed to purify kCD4-IgG2^{wt} and kCD4-IgG2^{S60C}, albeit with limited success. Ultimately, the functional specificity of kCD4-IgG2^{wt} and kCD4-IgG2^{S60C} was evaluated using SPR. The kCD4-IgG2^{wt} and kCD4-IgG2^{S60C} proteins abilities to bind various gp120 molecules from HIV clades B and C were tested; using NIH PRO 542, 2dsCD4^{wt} and 2dsCD4^{S60C} as positive controls. Following is a discussion of the results obtained.

4.1 The design and synthesis of the kCD4-IgG2^{wt} and kCD4-IgG2^{S60C} encoding expression vectors

HIV (which causes AIDS) binds to cell-surface CD4 protein expressed on CD4+ T cells, monocytes and macrophages using the viral gp120 envelope glycoprotein receptor as the initial step in the infection process [22, 213, 214]. In light of this, therapeutic molecules that incorporate the gp120 binding site of CD4 neutralise HIV potently [153, 164, 165, 167-169, 174, 176, 177, 181, 190, 191, 194, 195, 215-218]. Soluble CD4 and CD4-immunoglobulin fusions have been formulated to mimic cell-surface CD4 structurally and functionally [164, 169-171, 174, 175, 179, 183, 185, 190, 191, 217, 219]. The CD4-based agents are capable of uncoating HIV of its gp120 protein, competitively inhibiting HIV binding to cell-surface CD4 and reducing cell-to cell spread of HIV by syncytium formation [169, 177, 179, 220].

One polyvalent CD4-based agent showing great activity against HIV is PRO 542, produced by Progenics Pharmaceuticals, Inc of Tarrytown, New York. PRO 542 is a heterotetrameric protein comprised of the CD4 D1D2 regions fused to the CH1

region of IgG2 and the constant domain of human kappa light chains. By virtue of incorporating an IgG2 Fc portion in the design of PRO 542, the heterotetramer displays increased serum life-time compared to soluble CD4. In addition, PRO 542 has higher avidity for HIV than the monovalent soluble CD4 or divalent CD4-Ig [153, 220-222].

In this study, the unique design and production of a PRO 542-like molecule is described. In addition, a mutant form of PRO 542 was uniquely generated in this study, to bind gp120 with higher affinity. The mutant forms of PRO 542 have not been characterised.

To produce PRO 542, Beaudry *et al* (1992) designed and synthesised the CD4-IgG2HC-pRcCMV (ATCC no. 75193) and CD4-kLC-pRcCMV (ATCC no. 75194) expression vectors which encode the heavy chains (HC) and light chains (LC) of PRO 542, respectively. The sequence encoding the LC of PRO 542 was subsequently sub-cloned from CD4-kLC-pRcCMV into pPPI-2, which contains the β-globin promoter that directs the transcription of the dihydrofolate reductase gene (DHFR). The sequence encoding the HC of PRO 542 was constructed using genomic DNA (containing introns) whereas the light chain encoding sequence did not contain introns. Both the HC and LC encoding sequences of PRO 542 were inserted in separate expression vectors, containing, among other elements, the Human cytomegalovirus immediate-early (CMV) promoter [153, 206, 207, 220].

In contrast, the sequence used to encode the HC of kCD4-IgG2^{wt} in this study was exclusively cDNA in nature. The cDNA sequence encoding D1D2 domains of CD4 was fused to the first codon encoding the CH1 region of an IgG2 Fc portion. The kCD4-IgG2^{wt} HC encoding sequence was then synthesized and inserted in a pcDNA 3.1 (+) plasmid by GeneArt (Regensburg, Germany) and the whole construct was called pKH^{wt}.

The LC encoding sequence of kCD4-IgG2^{wt}, however, was designed identically to the sequences encoding the LC of PRO 542 described by Beaudry *et al* (1992) [220]. The cDNA sequence encoding the D1D2 region of CD4 was fused to the first codon encoding the human constant kappa light chain portion. The complete kCD4-

IgG2^{wt} LC encoding sequence was synthesized and inserted in a pcDNA 3.1 (+) plasmid by GeneArt, and the whole construct was referred to as pKL^{wt}.

The HC and LC encoding cDNA sequences of kCD4-IgG2^{S60C} were identical to the HC and LC cDNA sequences of kCD4-IgG2^{wt}, respectively, except at the codons coding for residue 60 in the CD4 portions. The HC and LC cDNA sequences of kCD4-IgG2^{S60C} contain a codon coding for a cysteine residue at position 60 in the CD4 portions. The HC and LC cDNA sequences of kCD4-IgG2^{wt}, however, contain a codon coding for a serine 60 residue in the CD4 portions. The kCD4-IgG2^{S60C} LC encoding cDNA sequence was synthesized and inserted in a pcDNA 3.1 (+) plasmid by GeneArt and the whole construct was referred to as pKL^{S60C}. In addition, the kCD4-IgG2^{S60C} HC encoding cDNA sequence was also inserted in a separate pcDNA 3.1 (+) plasmid and referred to as pKH^{S60C}. The pKH^{S60C} construct was also synthesized by GeneArt.

To express the individual chains of the kCD4-IgG^{wt} and kCD4-IgG2^{S60C}, the pcDNA 3.1 (+) expression vector was selected as it contains the Human cytomegalovirus immediate-early (CMV) promoter (as constructs used to express PRO 542 HC and LC) which permits high protein expression levels in a wide variety of mammalian cells [153, 220, 222]. In addition, the cDNA sequences coding for the individual chains of kCD4-IgG2^{wt} and kCD4-IgG2^{S60C} were codon-optimized for expression in mammalian cells.

4.2 Single-expression studies of pKH^{wt}, pKH^{S60C}, pKL^{wt} and pKL^{S60C}

Two and four micrograms of pKH^{wt}, pKH^{S60C}, pKL^{wt} and pKL^{S60C} constructs were transfected into HEK293T cells in 25 cm^3 flasks using Polyfect transfect transfection reagent. After 48 hours, the recombinant protein expression levels of the individual constructs were measured.

The secretion of kCD4-IgG2^{wt} and kCD4-IgG2^{S60C} HC protein was not observed in the culture supernatant after 2 or 4 µg of pKH^{wt} and pKH^{S60C} was transfected into HEK293T cells. This observation was unsurprising as previous studies have shown that individual HC or HC homodimers are not secreted into the supernatant, but are retained intracellularly [223]. Newly synthesized HC proteins are not secreted, but

are bound to heavy chain binding protein (BiP) in the endoplasmic reticulum until they are matched with LC proteins [224, 225]. Analysis of the cell-lysates from cells producing kCD4-IgG2^{wt} and kCD4-IgG2^{S60C} HC revealed the presence of HC protein (65 kDa in size), however we did not quantify the amounts of intracellularly retained HC.

Four micrograms of the pKL^{wt} construct was able to express kCD4-IgG2^{wt} LC protein with a size of 35 kDa, observed in Western blot analysis (Figure 3.5). Expectedly, HEK293T cells were capable of producing and secreting LC protein into the culture supernatant. In contrast, 2 and 4 µg of pKL^{S60C} construct transfected into HEK293T cells both produced approximately one fifth the amount of LC protein that pKL^{wt} produced (Figure 3.5), according to Western blot and densitometry analysis. It is unclear why the amounts of secreted kCD4-IgG2^{S60C} LC were lower compared to secreted kCD4-IgG2^{wt}; however the S60C mutation may have reduced the amount of secreted protein or the stability of the protein. It is suspected that the S60C mutation may have delayed the maturation of fully folded LC proteins, causing the protein to be retained intracellularly.

4.3 Co-transfection of pKH^{wt} with pKL^{wt} to produce heterotetrameric kCD4-IgG2^{wt}, as well as the co-transfection of pKH^{S60C} with pKL^{S60C} for the production of heterotetrameric kCD4-IgG2^{S60C}

To confirm the ability of HEK293T cells to produce heterotetrameric kCD4-IgG2^{wt} protein identical to PRO 542, described by Beaudry *et al* (1992), the pKH^{wt} and pKL^{wt} were co-transfected in HEK293T cells. Concurrently, the pKH^{S60C} and pKL^{S60C} constructs were also co-transfected to evaluate the ability of HEK293T cells to produce heterotetrameric KCD4-IgG2^{S60C}.

The co-transfection of pKH^{wt} with pKL^{wt} in HEK293T cells allowed for the production of individual kCD4-IgG2^{wt} HC and LC proteins, which assembled together to form heterotetrameric kCD4-IgG2^{wt} protein (200 kDa in size) that was secreted into the culture supernatant (Figure 3.6 A, lane 6). According to the NIH PRO 542 standards used in the Western blot analysis and densitometry, approximately 0.6 µg of heterotetrameric kCD4-IgG2^{wt} protein was present in the analysed sample obtained

from the culture supernatant containing heterotetrameric kCD4-IgG2^{wt} protein. Overall, this implied that a total of approximately 10 µg of heterotetrameric kCD4-IgG2^{wt} protein was expressed in 400 mL of culture supernatant.

Co-transfection of pKH^{S60C} with pKL^{S60C} in HEK293T cells permitted the expression of individual kCD4-IgG2^{S60C} HC and LC proteins which assembled together to produce a heterotetramer (of 200 kDa size) which was secreted into the culture supernatant (Figure 3.7, lane 1) as well. The amounts of heterotetrameric kCD4-IgG2^{S60C} secreted were exceedingly low compared to amounts of secreted heterotetrameric kCD4-IgG2^{wt}. In fact, it is estimated that approximately 25 ng of heterotetrameric kCD4-IgG2^{S60C} was observed in the sample analysed using Western blot and densitometry. Also observed in the same sample, were relatively large amounts of HC and LC of kCD4-IgG2^{S60C} (65 kDa and 35 kDa in size, respectively) compared to amounts of heterotetramer. Considering that proteins having a size less than 50 kDa were excluded from the sample after the concentrating process, no uncoupled LC proteins were expected to be seen in the sample. Also, no uncoupled HC proteins are secreted [224, 225], suggesting that large amounts of heterotetrameric kCD4-IgG2^{S60C} were unstable and had disassembled into component protein chains after secretion. In total, it estimated that 0.4 µg of assembled heterotetrameric kCD4-IgG2^{S60C} were produced in 400 mL of culture supernatant. This result highlights the fact that the S60C mutation affects the assembly and secretion of heterotetrameric kCD4-IgG2^{S60C} adversely. To improve the yield of stable heterotetramers, alternative strategies ought to be investigated.

A variety of methods to produce PRO 542 are described, which may be employed to improve the yield of heterotetrameric kCD4-IgG2^{wt} and kCD4-IgG2^{S60C} [153, 220, 222]. Beaudry *et al* (1992) produced PRO 542 by transiently co-transfecting equimolar amounts of CsCl-purified CD4-IgG2HC-pRcCMV and CD4-kLC-pPPI-2 expression vectors, in African green monkey kidney (CosM5) cells using the calcium-phosphate precipitation technique [220, 222]. Thereafter, Beaudry *et al* (1995) produced PRO 542 by stably expressing the heterotetramer in DXB-11 Chinese hamster ovary (CHO) cells deficient of DHFR. This was achieved by transfecting 20 µg of CD4-IgG2HC-pRcCMV, 20 µg of CD4-kLC-pPPI-2 and 20 ng of p410 (encoding DHRF) into the DXB-11 CHO cells and selecting for transfectants

producing PRO 542 using step-wise increases of methotrexate. The amounts of PRO 542 generated by transient and stable expression are not documented however [153, 220, 222]. By employing some of these strategies, the yield of kCD4-IgG2^{wt} and kCD4-IgG2^{S60C} may be improved.

In order to increase the yield of fully folded and assembled heterotetrameric kCD4-IgG2^{wt} or kCD4-IgG2^{S60C}, one may attempt producing them in bacterial systems. One may effectively use *Escherichia coli* (*E. coli*) BL21(DE3) or HB2151 cells, which are deficient in cellular proteases, to produce the heterotetrameric IgG and extract the protein from the bacterial periplasmic space [226]. Alternatively, the individual chains of the heterotetramers may be produced separately in bacterial cells and refolded *in vitro* [227-230].

4.4 Purification of heterotetrameric kCD4-IgG2^{wt} and heterotetrameric kCD4-IgG2^{S60C}

The heterotetrameric kCD4-IgG2^{wt} and kCD4-IgG2^{S60C} proteins were purified using Protein-A affinity chromatography with limited success. Both of the heterotetramers were observed to bind Protein-A agarose beads, but not a HiTrap Protein-A HP column (from GE Healthcare).

Protein-A is an antigen derived from the cell wall of *Staphylococcus Aureaus* (*S. aureus*) which reacts with human gamma globulins [231]. Protein-A is a 42 kDa protein which has four binding sites specific for the Fc portions of IgG. The interaction between Protein-A and the IgG Fc is relatively strong and specific (K_a is approximately 1 x 10^8 M). It is therefore highly effective to use immobilised Protein-A for the purpose of precipitating or purifying IgG Fc containing molecules, as the interaction occurs readily at physiologic conditions (pH 7 to 7.2).

To purify kCD4-IgG2^{wt}, supernatant containing kCD4-IgG2^{wt} was loaded in a HiTrap Protein-A HP column (from GE Healthcare) (pre-equilibrated with PBS). The unbound proteins were washed off the column and the bound proteins were then eluted with a sodium acetate buffer at pH 3.5 into aliquots of 1M tris/HCl at pH 9. The heterotetrameric kCD4-IgG2^{wt} protein was not detected in the eluate, washes and regenerate. It is likely that some kCD4-IgG2^{wt} protein was removed from the column

in the wash step, reducing the amount of protein remaining on the column for elution. Therefore, the amounts of kCD4-IgG2^{wt} protein which were eluted may have been below the detection limits of the Western blot analysis and densitometry.

In comparison, Beaudry *et al* (1992) and Beaudry *et al* (1995) passed supernatant containing PRO 542 through a Protein-A Sepharose fast flow column (pre-equilibrated with PBS) at a flow rate of 60 mL/hour. After extensive washing, PRO 542 was eluted with 100 mM glycine/HCl buffer at pH 3.5, directly into aliquots of 1 M tris/HCl at pH 8, to neutralise the fractions. Beaudry *et al* (1992) purified PRO 542 successfully in this manner [153, 220, 222].

An alternative method of purifying kCD4-IgG2^{wt} and kCD4-IgG2^{S60C} was therefore employed, using Protein-A agarose beads from Bio-Rad, in a batch-type process instead of the HiTrap Protein-A HP column. The supernatants containing heterotetrameric kCD4-IgG2^{wt} and kCD4-IgG2^{S60C} proteins were incubated with Protein-A agarose beads (pre-equilibrated with sodium phosphate buffer pH 6.5-7). The beads were then washed thoroughly to remove unbound proteins, before the bound proteins were eluted in acidic conditions (citric acid buffer pH 3.5/sodium acetate buffer pH 3.5) into aliquots of 1 M tris/HCl at pH 9. Following the elution step, the Protein-A beads were regenerated. It was observed that both heterotetrameric kCD4-IgG2^{wt} and kCD4-IgG2^{S60C} proteins were capable of binding Protein-A beads, but could not be detected in the eluate. No heterotetrameric kCD4-IgG2^{wt} and kCD4-IgG2^{S60C} proteins were observed in the eluate, wash or regenerate for that matter. The washing of the kCD4-IgG2^{wt} and kCD4-IgG2^{S60C} proteins may have reduced the amounts of protein remaining on the column for elution. The eluted proteins may have been at amounts too low to detect in the Western blot analysis and densitometry.

The amounts of heterotetrameric kCD4-IgG2^{wt} observed to bind the Protein-A agarose beads were considerably larger than those of kCD4-IgG2^{S60C} proteins bound to beads, however. Due to the exceedingly low expression and secretion of kCD4-IgG2^{S60C}; coupled with low precipitation by Protein-A, it became clear that interventions to improve expression efficiency of kCD4-IgG2^{S60C} are required.

Further functional characterisation of kCD4-IgG2^{S60C} was limited, in view of the low amounts of the heterotetramer produced.

4.5 The immunoprecipitation of gp120 by heterotetrameric kCD4-IgG2^{wt} adsorbed to Protein-A agarose beads

The structural integrity of heterotetrameric kCD4-IgG2^{wt} was assessed successfully, in spite of the inability to elute the heterotetramer from a Protein-A column and beads. Heterotetrameric kCD4-IgG2^{wt}, adsorbed to Protein-A agarose beads, was capable of binding gp120 Bal.

HIV gp120 binds specifically and stably to the D1D2 regions of soluble CD4 derivatives with similar affinity to cell-surface CD4 (K_D of approximately 1 x 10^{-9} M) [166, 180, 232].

Fully assembled and folded heterotetrameric kCD4-IgG2^{wt} was expected to bind gp120 like NIH PRO 542. The heterotetrameric kCD4-IgG2^{wt} containing supernatant and NIH PRO 542 in PBS were incubated with Protein-A agarose beads from Bio-Rad. It was observed that similar amounts of heterotetrameric kCD4-IgG2^{wt} and NIH PRO 542 remained adsorbed to the beads after thorough washing. The gp120 Bal protein was then incubated with kCD4-IgG2^{wt}-Protein-A complexes and NIH PRO 542-Protein-A complexes. It was observed that gp120 Bal binds to kCD4-IgG2^{wt}-Protein-A complexes in similar amounts to NIH PRO 542-Protein-A complexes. The results showed that the heterotetrameric kCD4-IgG2^{wt} protein expressed in this study was not only fully folded and assembled, but functional by virtue of binding Protein-A and gp120, concurrently, as NIH PRO 542.

NIH PRO 542 binds to gp120 from genetically diverse strains of HIV-1 [6, 82, 200, 202, 203, 233]. To confirm that heterotetrameric kCD4-IgG2^{wt} and kCD4-IgG2^{S60C} expressed in this study had similar activity against various gp120s as NIH PRO 542, SPR studies were conducted.

4.6 SPR studies

SPR is a technique used to measure interactions between unlabelled molecules, in real-time and with high sensitivity. Information obtained from SPR is the change in mass on a gold-plated sensor surface, induced by an immobilised ligand binding to its cognate receptor. The changes in refractive index at the site of the ligand-analyte interaction are plotted against time to generate a sensorgram. If no changes in refractive index (response units (RU)) are observed over time, it is assumed that the ligand and analyte do not bind each other. If the change in refractive index increases over time, it is suggestive that ligand and analyte bind to each other. Due to the low amounts of ligands and analyte required and the sensitivity of the technique, SPR is a popular choice for binding studies [234-242].

The gp120-2dsCD4 interaction has been characterised by Zhou *et al* (2007), as well as Cerutti *et al*. (2010) using SPR [180, 232]. In addition, the interaction of $2dsCD4^{S60C}$ (refer to 1.7.4.3) with gp120 was also characterised by Cerutti *et al* (2010). The affinity calculated for the gp120-$2dsCD4^{wt}$ interaction was 53 nM, whereas the affinity calculated for the gp120-$2dsCD4^{S60C}$ interaction was 6 nM. Both the $2dsCD4^{wt}$ and $2dsCD4^{S60C}$ proteins were observed to associate with gp120 in similar amounts, however the $2dsCD4^{S60C}$ protein was found to dissociate from gp120 less rapidly than $2dsCD4^{wt}$ [180].

In this study, SPR was used to determine the functional specificity of heterotetrameric kCD4-$IgG2^{wt}$ and kCD4-$IgG2^{S60C}$ (both in supernatant) (analytes) by passing the heterotetramers over six different gp120s (ligands) from HIV-1 clade B and C, and measuring the levels of the interactions (Figure 3.11). Fully folded and assembled kCD4-$IgG2^{wt}$ and kCD4-$IgG2^{S60C}$ heterotetramers were expected to bind immobilised gp120. As positive controls, NIH PRO 542, $2dsCD4^{wt}$ and $2dsCD4^{S60C}$ were also passed over the same panel of immobilised gp120s (Figure 3.11). The negative control used in the study was culture supernatant obtained from mock transfections (Figure 3.11).

After passing the analytes over the six immobilised gp120s, MAb 17b was also passed over the flow cells to assess if it would bind the CoRbs of gp120, exposed by the analytes.

The engagement of gp120 by CD4 induces conformational changes in gp120 which expose the gp120 co-receptor binding site (CoRbs), allowing MAb 17b to bind the CD4 induced epitope (CD4i) [106, 110, 154, 172, 243-246]. Previous studies by Sullivan *et al* (1998) showed that the binding of MAb 17b to monomeric gp120 is minimal to none, without the prior engagement of gp120 by a CD4 moiety. If MAb 17b binds to gp120 minimally without the prior engagement of CD4, amounts of MAb 17b observed to bind gp120 increase as increasing amounts of CD4 are added to the reaction [110].

SPR data showed that kCD4-IgG2^{wt}, NIH PRO 542, 2dsCD4^{wt} and 2dsCD4^{S60C} were all capable of binding the panel of six gp120s, but kCD4-IgG2^{S60C} was not detected to bind any of the gp120s (Figure 3.11 A to F). For the analytes that bound gp120, three phases in the sensorgrams were observed: an association, equilibrium and dissociation phase.

In view of the low amounts of heterotetrameric kCD4-IgG2^{S60C} protein (approximately 12 ng) present in the supernatant passed over the gp120s, it was not surprising that no binding was observed. The RU levels for all the kCD4-IgG2^{S60C}-gp120 interactions were similar to those registered by the negative control with gp120s (Figure 3.11 A to F). The supernatant containing minimal amounts of heterotetrameric kCD4-IgG2^{S60C} was observed to expose the CoRbs of gp120 CN54, SF162, gp120 ZM and Bal (Figure 3.11 G, H, K and L). This result was unexpected since MAb 17b was observed to bind to these gp120s minimally without the prior, detectable engagement of kCD4-IgG2^{S60C} or components thereof.

The abilities of kCD4-IgG2^{wt}, NIH PRO 542, 2dsCD4^{wt} and 2dsCD4^{S60C} to induce the exposure of the gp120s CoRbs were different, except in the case of gp120 ZM where none of the analytes were capable of exposing the CoRbs for MAb 17b binding (Figure 3.11 K). Notably, 2dsCD4^{wt} was the only protein capable of eliciting the exposure of the CoRbs of five gp120s (Figure 3.11 G to J and L). Remarkably, kCD-IgG2^{wt} was capable of eliciting the exposure of gp120 SF162, IN, ZA and Bal CoRbs (Figure 3.11 H, I, J and L) as NIH PRO 542 and 2dsCD4^{S60C} and 2dsCD4^{wt}. Although kCD4-IgG2^{wt}, NIH PRO 542 and 2dsCD4^{S60C} bound to gp120 CN54, they

could not elicit the exposure of the gp120 CN54 CoRbs (Figure 3.11 A and G, respectively).

Overall, these results pointed to the fact that kCD4-IgG2^{wt} was fully assembled and folded, but also bound various gp120s like NIH PRO 542, 2dsCD4^{wt} and 2dsCD4^{S60C}.

Chapter 5: Conclusion

The objective of this study was to generate the kCD4-IgG2^{wt} protein which was structurally and functionally identical to PRO 542. An additional objective was to produce a mutant form of kCD4-IgG2^{wt} containing an S60C mutation (kCD4-IgG2^{S60C}) in the CD4 portion.

The S60C mutation in 2dsCD4 was previously shown to increase the affinity of CD4 for gp120 [180], therefore, kCD4-IgG2^{S60C} was intended to have enhanced binding activity against gp120, relative to kCD4-IgG2^{wt} and PRO 542 obtained from the NIH.

The pKH^{wt} and pKL^{wt} constructs designed in this study were capable of successfully producing the kCD4-IgG2^{wt} HC and LC proteins in HEK293T cells, respectively. Concurrently, the pKH^{S60C} and pKL^{S60C} constructs designed in this study were capable of producing the kCD4-IgG2^{S60C} HC and LC proteins, respectively. The production of assembled and secreted heterotetrameric kCD4-IgG2^{wt} was attained by the co-transfection of pKH^{wt} and pKL^{wt} constructs in HEK293T cells. The HEK293T cells also achieved assembly of heterotetrameric kCD4-IgG2^{S60C}, by the co-transfection of pKH^{S60C} and pKL^{S60C}, but the amounts of secreted kCD4-IgG2^{S60C} heterotetramer were far lower compared to secreted heterotetrameric kCD4-IgG2^{wt}. It was suspected, however, that the S60C mutation may have affected the proper folding of the heterotetramer, thus delaying or reducing the secretion of the heterotetramer into the culture supernatant. In addition, relatively large amounts of uncoupled kCD4-IgG2^{S60C} HC and LC were present in the supernatant suggesting that heterotetrameric kCD4-IgG2^{S60C} may be unstable in the culture supernatant.

Although the heterotetrameric kCD4-IgG2^{wt} and kCD4-IgG2^{S60C} proteins were purified with limited success using different Protein-A affinity chromatography protocols, both proteins were observed to bind Protein-A agarose beads as NIH PRO 542, indicating that the Fc portions of both proteins were fully folded. The structural integrity of the kCD4-IgG2^{S60C} CD4 portion could not be determined; however the kCD4-IgG2^{wt} CD4 portions were fully folded as they could bind gp120 Bal like NIH PRO 542.

According to SPR data generated in this study, kCD4-IgG2^{wt} was capable of binding to six different gp120 from HIV-1 clades B and C, and inducing their CoRbs like NIH

PRO 542, 2dsCD4^{wt} and 2dsCD4^{S60C}. The low amounts of expressed heterotetrameric kCD4-IgG2^{S60C} prevented the determination of its structural integrity and functional specificity in SPR studies.

Overall, the design and production of kCD4-IgG2^{wt} which was structurally and functionally identical to NIH PRO 542, was successful and showed that our strategies in generating functional CD4-Immunoglobulin fusion proteins were comparable in efficacy to strategies employed by other groups. This study showed that functional CD4-based fusion proteins with activity against gp120 can be generated according to our strategies.

Future studies are aimed at improving the yields of kCD4-IgG2^{wt} and kCD4-IgG2^{S60C} by modifying the expression vectors for enhance protein production in mammalian cells or optimizing production of the proteins in bacterial systems. We aim to also characterise the kinetics of the kCD4-IgG2^{wt}-gp120 and kCD4-IgG2^{S60C}-gp120 interactions to see if our proteins have more potent activity than other CD4-based agents described by other groups.

Chapter 6: References

1. Gottlieb, M.S., et al., *Pneumocystis carinii pneumonia and mucosal candidiasis in previously healthy homosexual men: evidence of a new acquired cellular immunodeficiency.* N Engl J Med, 1981. **305**(24): p. 1425-31.
2. Durack, D.T., *Opportunistic infections and Kaposi's sarcoma in homosexual men.* N Engl J Med, 1981. **305**(24): p. 1465-7.
3. Kuiken, C., et al., *HIV sequence compendium.* Theoretical biology and biophysics group, Los Alamos Nation Laboratory, NM, LA-UR 10-03684, 2010.
4. *Aids epidemic update.* Available from: http://www.unaids.org/en/media/unaids/contentassets/dataimport/pub/report/2009/jc1700_epi_update_2009_en.pdf, 2009.
5. Gallo, R.C., et al., *Frequent detection and isolation of cytopathic retroviruses (HTLV-III) from patients with AIDS and at risk for AIDS.* Science, 1984. **224**(4648): p. 500-3.
6. Zhu, P., W.C. Olson, and K.H. Roux, *Structural flexibility and functional valence of CD4-IgG2 (PRO 542): potential for cross-linking human immunodeficiency virus type 1 envelope spikes.* J Virol, 2001. **75**(14): p. 6682-6.
7. Gelderblom, H.R., et al., *Fine structure of human immunodeficiency virus (HIV) and immunolocalization of structural proteins.* Virology, 1987. **156**(1): p. 171-6.
8. Gelderblom, H.R., M. Ozel, and G. Pauli, *Morphogenesis and morphology of HIV. Structure-function relations.* Arch Virol, 1989. **106**(1-2): p. 1-13.
9. Ozel, M., G. Pauli, and H.R. Gelderblom, *The organization of the envelope projections on the surface of HIV.* Arch Virol, 1988. **100**(3-4): p. 255-66.
10. Stevens, W. and M. Papathanasopoulos, A, eds. *Molecular Medicine for Clinicians, Chapter 26: Introduction to HIV*. Molecular Medicine for Clinicians. 2009, University of the Witwatersrand Press. 311-324.
11. Gelderblom, H.R., *Assembly and morphology of HIV: potential effect of structure on viral function.* AIDS, 1991. **5**(6): p. 617-37.
12. Brenchley, J.M., et al., *CD4+ T cell depletion during all stages of HIV disease occurs predominantly in the gastrointestinal tract.* J Exp Med, 2004. **200**(6): p. 749-59.

13. Wyatt, R., et al., *The antigenic structure of the HIV gp120 envelope glycoprotein.* Nature, 1998. **393**(6686): p. 705-11.
14. Chen, L., et al., *Structural basis of immune evasion at the site of CD4 attachment on HIV-1 gp120.* Science, 2009. **326**(5956): p. 1123-7.
15. Du, S.X., et al., *Effect of trimerization motifs on quaternary structure, antigenicity, and immunogenicity of a noncleavable HIV-1 gp140 envelope glycoprotein.* Virology, 2009. **395**(1): p. 33-44.
16. Weissenhorn, W., et al., *Atomic structure of the ectodomain from HIV-1 gp41.* Nature, 1997. **387**(6631): p. 426-30.
17. Liu, J., et al., *Molecular architecture of native HIV-1 gp120 trimers.* Nature, 2008. **455**(7209): p. 109-13.
18. Buonaguro, L., et al., *Can HIV p24 be a suitable scaffold for presenting Env antigens?* Clin Vaccine Immunol. **18**(11): p. 2003-4.
19. Binley, J.M., et al., *Analysis of the interaction of antibodies with a conserved enzymatically deglycosylated core of the HIV type 1 envelope glycoprotein 120.* AIDS Res Hum Retroviruses, 1998. **14**(3): p. 191-8.
20. Grundner, C., et al., *Factors limiting the immunogenicity of HIV-1 gp120 envelope glycoproteins.* Virology, 2004. **330**(1): p. 233-48.
21. Liu, J., E.R. Wright, and H. Winkler, *3D visualization of HIV virions by cryoelectron tomography.* Methods Enzymol. **483**: p. 267-90.
22. Wyatt, R. and J. Sodroski, *The HIV-1 envelope glycoproteins: fusogens, antigens, and immunogens.* Science, 1998. **280**(5371): p. 1884-8.
23. Mariani, S.A., E. Vicenzi, and G. Poli, *Asymmetric HIV-1 co-receptor use and replication in CD4(+) T lymphocytes.* J Transl Med. **9 Suppl 1**: p. S8.
24. Hufert, F.T., et al., *Germinal centre CD4+ T cells are an important site of HIV replication in vivo.* AIDS, 1997. **11**(7): p. 849-57.
25. Walker, C.M., *How do CD8+ T lymphocytes control HIV replication in vivo?* Res Immunol, 1989. **140**(1): p. 115-8; discussion 122-3.
26. Su, L., et al., *Identification of HIV-1 determinants for replication in vivo.* Virology, 1997. **227**(1): p. 45-52.
27. Chun, T.W., et al., *Suppression of HIV replication in the resting CD4+ T cell reservoir by autologous CD8+ T cells: implications for the development of therapeutic strategies.* Proc Natl Acad Sci U S A, 2001. **98**(1): p. 253-8.

28. Baker, J.V., et al., *HIV Replication, Inflammation, and the Effect of Starting Antiretroviral Therapy on Plasma Asymmetric Dimethylarginine, a Novel Marker of Endothelial Dysfunction.* J Acquir Immune Defic Syndr.
29. Plantier, J.C., et al., *A new human immunodeficiency virus derived from gorillas.* Nat Med, 2009. **15**(8): p. 871-2.
30. Lynch, R.M., et al., *Appreciating HIV type 1 diversity: subtype differences in Env.* AIDS Res Hum Retroviruses, 2009. **25**(3): p. 237-48.
31. Walker, P.R., et al., *Comparative population dynamics of HIV-1 subtypes B and C: subtype-specific differences in patterns of epidemic growth.* Infect Genet Evol, 2005. **5**(3): p. 199-208.
32. Carobene, M.G., et al., *Differences in frequencies of drug resistance-associated mutations in the HIV-1 pol gene of B subtype and BF intersubtype recombinant samples.* J Acquir Immune Defic Syndr, 2004. **35**(2): p. 207-9.
33. Gao, F., et al., *Evidence of two distinct subsubtypes within the HIV-1 subtype A radiation.* AIDS Res Hum Retroviruses, 2001. **17**(8): p. 675-88.
34. Puchhammer-Stockl, E., et al., *Introduction of HIV-1 subtypes C, E and A into Austria.* Clin Diagn Virol, 1998. **9**(1): p. 25-8.
35. von Briesen, H., et al., *Isolation frequency and growth properties of HIV-variants: multiple simultaneous variants in a patient demonstrated by molecular cloning.* J Med Virol, 1987. **23**(1): p. 51-66.
36. Iordanskiy, S., et al., *Subtype-associated differences in HIV-1 reverse transcription affect the viral replication.* Retrovirology. **7**: p. 85.
37. Buonaguro, L., M.L. Tornesello, and F.M. Buonaguro, *Human immunodeficiency virus type 1 subtype distribution in the worldwide epidemic: pathogenetic and therapeutic implications.* J Virol, 2007. **81**(19): p. 10209-19.
38. Roques, P., et al., *Phylogenetic characteristics of three new HIV-1 N strains and implications for the origin of group N.* AIDS, 2004. **18**(10): p. 1371-81.
39. Peeters, M., C. Toure-Kane, and J.N. Nkengasong, *Genetic diversity of HIV in Africa: impact on diagnosis, treatment, vaccine development and trials.* AIDS, 2003. **17**(18): p. 2547-60.
40. Buonaguro, L., et al., *Genetic and phylogenetic evolution of HIV-1 in a low subtype heterogeneity epidemic: the Italian example.* Retrovirology, 2007. **4**: p. 34.

41. Tscherning-Casper, C., et al., *Evidence of the existence of a new circulating recombinant form of HIV type 1 subtype A/J in Cameroon. The European Network on the Study of In Utero Transmission of HIV-1.* AIDS Res Hum Retroviruses, 2000. **16**(13): p. 1313-8.
42. Wilbe, K., et al., *Identification of two CRF11-cpx genomes and two preliminary representatives of a new circulating recombinant form (CRF13-cpx) of HIV type 1 in Cameroon.* AIDS Res Hum Retroviruses, 2002. **18**(12): p. 849-56.
43. Fauci, A.S., *Multifactorial nature of human immunodeficiency virus disease: implications for therapy.* Science, 1993. **262**(5136): p. 1011-8.
44. Kahn, J.O. and B.D. Walker, *Acute human immunodeficiency virus type 1 infection.* N Engl J Med, 1998. **339**(1): p. 33-9.
45. Chun, T.W., et al., *Early establishment of a pool of latently infected, resting CD4(+) T cells during primary HIV-1 infection.* Proc Natl Acad Sci U S A, 1998. **95**(15): p. 8869-73.
46. De Maria, A., et al., *Infection of CD8+ T lymphocytes with HIV. Requirement for interaction with infected CD4+ cells and induction of infectious virus from chronically infected CD8+ cells.* J Immunol, 1991. **146**(7): p. 2220-6.
47. Wallis, C.L., et al., *Affordable in-house antiretroviral drug resistance assay with good performance in non-subtype B HIV-1.* J Virol Methods. **163**(2): p. 505-8.
48. Schnittman, S.M., et al., *The reservoir for HIV-1 in human peripheral blood is a T cell that maintains expression of CD4.* Science, 1989. **245**(4915): p. 305-8.
49. Faal, M., et al., *Providing immediate CD4 count results at HIV testing improves ART initiation.* J Acquir Immune Defic Syndr. **58**(3): p. e54-9.
50. Connell, B.J., et al., *Emergence of X4 usage among HIV-1 subtype C: evidence for an evolving epidemic in South Africa.* AIDS, 2008. **22**(7): p. 896-9.
51. Castor, D., et al., *The relationship between genotypic sensitivity score and treatment outcomes in late stage HIV disease after supervised HAART.* J Med Virol, 2009. **81**(8): p. 1323-35.
52. Grant, R.M., et al., *AIDS. Promote HIV chemoprophylaxis research, don't prevent it.* Science, 2005. **309**(5744): p. 2170-1.

53. Chun, T.W., et al., *Effect of interleukin-2 on the pool of latently infected, resting CD4+ T cells in HIV-1-infected patients receiving highly active anti-retroviral therapy.* Nat Med, 1999. **5**(6): p. 651-5.
54. De Clercq, E., *Anti-HIV drugs: 25 compounds approved within 25 years after the discovery of HIV.* Int J Antimicrob Agents, 2009. **33**(4): p. 307-20.
55. Abeyakirthi, S., et al., *Arginase is overactive in psoriatic skin.* Br J Dermatol. **163**(1): p. 193-6.
56. De Clercq, E., *Anti-HIV drugs.* Verh K Acad Geneeskd Belg, 2007. **69**(2): p. 81-104.
57. De Clercq, E., *Emerging anti-HIV drugs.* Expert Opin Emerg Drugs, 2005. **10**(2): p. 241-73.
58. De Clercq, E., *Looking back in 2009 at the dawning of antiviral therapy now 50 years ago an historical perspective.* Adv Virus Res, 2009. **73**: p. 1-53.
59. Sax, P.E., *FDA approval: maraviroc.* AIDS Clin Care, 2007. **19**(9): p. 75.
60. *FDA approves maraviroc tablets.* AIDS Patient Care STDS, 2007. **21**(9): p. 702.
61. *FDA notifications. Maraviroc approved as a CCR5 co-receptor antagonist.* AIDS Alert, 2007. **22**(9): p. 103.
62. Administration, U.S.F.a.D., *Generic drugs used in the treatment of HIV infection,* *http://www.fda.gov/ForConsumers/byAudience/ForPatientAdvocates/HIVandAIDSActivities/ucm118915.htm*. Aug 2011.
63. Lalezari, J.P. and A.D. Luber, *Enfuvirtide.* Drugs Today (Barc), 2004. **40**(3): p. 259-69.
64. Matthews, T., et al., *Enfuvirtide: the first therapy to inhibit the entry of HIV-1 into host CD4 lymphocytes.* Nat Rev Drug Discov, 2004. **3**(3): p. 215-25.
65. Dorr, P., et al., *Maraviroc (UK-427,857), a potent, orally bioavailable, and selective small-molecule inhibitor of chemokine receptor CCR5 with broad-spectrum anti-human immunodeficiency virus type 1 activity.* Antimicrob Agents Chemother, 2005. **49**(11): p. 4721-32.
66. Gulick , R.M., *Maraviroc for previously treated patients with R5 HIV - 1 infection.* New England Journal of Medicine (NEJM), 2008. **359**(14): p. 1429-1441.

67. Hunt, J.S. and F. Romanelli, *Maraviroc, a CCR5 coreceptor antagonist that blocks entry of human immunodeficiency virus type 1.* Pharmacotherapy, 2009. **29**(3): p. 295-304.
68. Fatkenheuer, G., et al., *Subgroup analyses of maraviroc in previously treated R5 HIV-1 infection.* N Engl J Med, 2008. **359**(14): p. 1442-55.
69. Lieberman-Blum, S.S., H.B. Fung, and J.C. Bandres, *Maraviroc: a CCR5-receptor antagonist for the treatment of HIV-1 infection.* Clin Ther, 2008. **30**(7): p. 1228-50.
70. *Anti-HIV agents. Maraviroc and resistance.* TreatmentUpdate, 2007. **19**(6): p. 4-5.
71. Martin, J., et al., *A liquid chromatography-tandem mass spectrometry assay for quantification of nevirapine, indinavir, atazanavir, amprenavir, saquinavir, ritonavir, lopinavir, efavirenz, tipranavir, darunavir and maraviroc in the plasma of patients infected with HIV.* J Chromatogr B Analyt Technol Biomed Life Sci, 2009. **877**(27): p. 3072-82.
72. Gulick, R.M., et al., *Maraviroc for previously treated patients with R5 HIV-1 infection.* N Engl J Med, 2008. **359**(14): p. 1429-41.
73. *Anti-HIV agents. Access to maraviroc.* TreatmentUpdate, 2007. **19**(3): p. 5-6.
74. Saracino, A., et al., *Are the proposed env mutations actually associated with resistance to maraviroc?* J Acquir Immune Defic Syndr. **53**(4): p. 550-2.
75. Peytavin, G., *[Clinical pharmacokinetic of maraviroc].* Med Mal Infect, 2008. **38 Suppl 1**: p. S12-6.
76. Alcami, J., *[Conclusions and perspectives. Maraviroc].* Enferm Infecc Microbiol Clin, 2008. **26 Suppl 11**: p. 49-54.
77. *Maraviroc approved for use in treatment-experienced CCR5-tropic HIV-1.* AIDS Alert, 2009. **24**(1): p. 10-2.
78. *Maraviroc reduces viral load in naive patients at 48 weeks.* AIDS Patient Care STDS, 2007. **21**(9): p. 703-4.
79. Liu, J., et al., *Structure of the HIV-1 gp41 membrane-proximal ectodomain region in a putative prefusion conformation.* Biochemistry, 2009. **48**(13): p. 2915-23.
80. Dey, A.K., et al., *Specific amino acids in the N-terminus of the gp41 ectodomain contribute to the stabilization of a soluble, cleaved gp140*

envelope glycoprotein from human immunodeficiency virus type 1. Virology, 2007. **360**(1): p. 199-208.

81. Gabuzda, D., et al., *Identification of membrane anchorage domains of the HIV-1 gp160 envelope glycoprotein precursor.* J Acquir Immune Defic Syndr, 1991. **4**(1): p. 34-40.
82. Nagashima, K.A., et al., *Human immunodeficiency virus type 1 entry inhibitors PRO 542 and T-20 are potently synergistic in blocking virus-cell and cell-cell fusion.* J Infect Dis, 2001. **183**(7): p. 1121-5.
83. Lalezari, J.P., et al., *Enfuvirtide, an HIV-1 fusion inhibitor, for drug-resistant HIV infection in North and South America.* N Engl J Med, 2003. **348**(22): p. 2175-85.
84. Trottier, B., et al., *Safety of enfuvirtide in combination with an optimized background of antiretrovirals in treatment-experienced HIV-1-infected adults over 48 weeks.* J Acquir Immune Defic Syndr, 2005. **40**(4): p. 413-21.
85. Lalezari, J.P., *Clinical safety and efficacy of enfuvirtide (T-20), a new fusion inhibitor. A review of the presentation at the satellite symposium "New hope: advancing care in HIV infection" at the 15th annual Association of Nurses in AIDS Care conference, November 2002.* AIDS Read, 2003. **13**(3 Suppl): p. S9-13.
86. Lalezari, J.P., et al., *A controlled Phase II trial assessing three doses of enfuvirtide (T-20) in combination with abacavir, amprenavir, ritonavir and efavirenz in non-nucleoside reverse transcriptase inhibitor-naive HIV-infected adults.* Antivir Ther, 2003. **8**(4): p. 279-87.
87. Nelson, M., et al., *Durable efficacy of enfuvirtide over 48 weeks in heavily treatment-experienced HIV-1-infected patients in the T-20 versus optimized background regimen only 1 and 2 clinical trials.* J Acquir Immune Defic Syndr, 2005. **40**(4): p. 404-12.
88. Ketas, T.J., et al., *Entry inhibitors SCH-C, RANTES, and T-20 block HIV type 1 replication in multiple cell types.* AIDS Res Hum Retroviruses, 2003. **19**(3): p. 177-86.
89. Lalezari, J.P., et al., *Influence of subcutaneous injection site on the steady-state pharmacokinetics of enfuvirtide (T-20) in HIV-1-infected patients.* J Clin Virol, 2003. **28**(2): p. 217-22.

90. Kilby, J.M., et al., *The safety, plasma pharmacokinetics, and antiviral activity of subcutaneous enfuvirtide (T-20), a peptide inhibitor of gp41-mediated virus fusion, in HIV-infected adults.* AIDS Res Hum Retroviruses, 2002. **18**(10): p. 685-93.
91. Wheeler, D.A., et al., *Safety, tolerability, and plasma pharmacokinetics of high-strength formulations of enfuvirtide (T-20) in treatment-experienced HIV-1-infected patients.* J Clin Virol, 2004. **30**(2): p. 183-90.
92. Reynes, J., et al., *TORO: ninety-six-week virologic and immunologic response and safety evaluation of enfuvirtide with an optimized background of antiretrovirals.* AIDS Patient Care STDS, 2007. **21**(8): p. 533-43.
93. Dwyer, J.J., et al., *Design of helical, oligomeric HIV-1 fusion inhibitor peptides with potent activity against enfuvirtide-resistant virus.* Proc Natl Acad Sci U S A, 2007. **104**(31): p. 12772-7.
94. Eron, J.J., et al., *Switch to a raltegravir-based regimen versus continuation of a lopinavir-ritonavir-based regimen in stable HIV-infected patients with suppressed viraemia (SWITCHMRK 1 and 2): two multicentre, double-blind, randomised controlled trials.* Lancet. **375**(9712): p. 396-407.
95. Liu, Y., et al., *CD4-independent infection of astrocytes by human immunodeficiency virus type 1: requirement for the human mannose receptor.* J Virol, 2004. **78**(8): p. 4120-33.
96. He, J., et al., *CCR3 and CCR5 are co-receptors for HIV-1 infection of microglia.* Nature, 1997. **385**(6617): p. 645-9.
97. Hesselgesser, J., et al., *CD4-independent association between HIV-1 gp120 and CXCR4: functional chemokine receptors are expressed in human neurons.* Curr Biol, 1997. **7**(2): p. 112-21.
98. Edinger, A.L., et al., *CD4-independent, CCR5-dependent infection of brain capillary endothelial cells by a neurovirulent simian immunodeficiency virus strain.* Proc Natl Acad Sci U S A, 1997. **94**(26): p. 14742-7.
99. Sattentau, Q.J. and R.A. Weiss, *The CD4 antigen: Physiological ligand and HIV receptor.* Cell, 1988. **52**(5): p. 631-633.
100. Maddon, P.J., et al., *The T4 gene encodes the AIDS virus receptor and is expressed in the immune system and the brain.* Cell, 1986. **47**(3): p. 333-348.

101. Maddon, P.J., et al., *The isolation and nucleotide sequence of a cDNA encoding the T cell surface protein T4: a new member of the immunoglobulin gene family.* Cell, 1985. **42**(1): p. 93-104.
102. Dalgleish, A.G., et al., *The CD4 (T4) antigen is an essential component of the receptor for the AIDS retrovirus.* Nature, 1984. **312**(5996): p. 763-7.
103. Klasse, P.J. and J.P. Moore, *Kinetics of the HIV-CD4 interactions and virus-cell fusion.* AIDS, 1992. **6**(3): p. 325-7.
104. Choe, H.R. and J. Sodroski, *Contribution of charged amino acids in the CDR2 region of CD4 to HIV-1 gp120 binding.* J Acquir Immune Defic Syndr, 1992. **5**(2): p. 204-10.
105. van Anken, E., et al., *Only five of 10 strictly conserved disulfide bonds are essential for folding and eight for function of the HIV-1 envelope glycoprotein.* Mol Biol Cell, 2008. **19**(10): p. 4298-309.
106. Kwong, P.D., et al., *Structure of an HIV gp120 envelope glycoprotein in complex with the CD4 receptor and a neutralizing human antibody.* Nature, 1998. **393**(6686): p. 648-59.
107. Sanders, R.W., et al., *Evolution rescues folding of human immunodeficiency virus-1 envelope glycoprotein GP120 lacking a conserved disulfide bond.* Mol Biol Cell, 2008. **19**(11): p. 4707-16.
108. Kwong, P.D., et al., *Structures of HIV-1 gp120 envelope glycoproteins from laboratory-adapted and primary isolates.* Structure, 2000. **8**(12): p. 1329-39.
109. Myszka, D.G., et al., *Energetics of the HIV gp120-CD4 binding reaction.* Proc Natl Acad Sci U S A, 2000. **97**(16): p. 9026-31.
110. Sullivan, N., et al., *CD4-Induced conformational changes in the human immunodeficiency virus type 1 gp120 glycoprotein: consequences for virus entry and neutralization.* J Virol, 1998. **72**(6): p. 4694-703.
111. Andrianov, A.M., *Spatial structure model of the CD4 receptor-binding site of the HIV envelope protein gp120.* J Biomol Struct Dyn, 1998. **15**(6): p. 1101-13.
112. Huang, C.C., et al., *Structure of a V3-containing HIV-1 gp120 core.* Science, 2005. **310**(5750): p. 1025-8.
113. McLellan, J.S., et al., *Structure of HIV-1 gp120 V1/V2 domain with broadly neutralizing antibody PG9.* Nature. **480**(7377): p. 336-43.

114. Pancera, M., et al., *Structure of HIV-1 gp120 with gp41-interactive region reveals layered envelope architecture and basis of conformational mobility.* Proc Natl Acad Sci U S A. **107**(3): p. 1166-71.
115. Phogat, S.K., S.M. Kaminsky, and W.C. Koff, *HIV-1 rational vaccine design: molecular details of b12-gp120 complex structure.* Expert Rev Vaccines, 2007. **6**(3): p. 319-21.
116. Wu, X., et al., *Rational design of envelope identifies broadly neutralizing human monoclonal antibodies to HIV-1.* Science. **329**(5993): p. 856-61.
117. Zhou, T., et al., *Structural basis for broad and potent neutralization of HIV-1 by antibody VRC01.* Science. **329**(5993): p. 811-7.
118. Kwong, P.D., et al., *HIV-1 evades antibody-mediated neutralization through conformational masking of receptor-binding sites.* Nature, 2002. **420**(6916): p. 678-82.
119. Allaway, G.P., et al., *Synergistic inhibition of HIV-1 envelope-mediated cell fusion by CD4-based molecules in combination with antibodies to gp120 or gp41.* AIDS Res Hum Retroviruses, 1993. **9**(7): p. 581-7.
120. Ashish, et al., *Global structure of HIV-1 neutralizing antibody IgG1 b12 is asymmetric.* Biochem Biophys Res Commun. **391**(1): p. 947-51.
121. Bhattacharyya, S., et al., *Design of a non-glycosylated outer domain-derived HIV-1 gp120 immunogen that binds to CD4 and induces neutralizing antibodies.* J Biol Chem. **285**(35): p. 27100-10.
122. Braibant, M., et al., *Antibodies to conserved epitopes of the HIV-1 envelope in sera from long-term non-progressors: prevalence and association with neutralizing activity.* AIDS, 2006. **20**(15): p. 1923-30.
123. Burton, D.R., et al., *HIV vaccine design and the neutralizing antibody problem.* Nat Immunol, 2004. **5**(3): p. 233-6.
124. Phogat, S. and R. Wyatt, *Rational modifications of HIV-1 envelope glycoproteins for immunogen design.* Curr Pharm Des, 2007. **13**(2): p. 213-27.
125. Phogat, S., R.T. Wyatt, and G.B. Karlsson Hedestam, *Inhibition of HIV-1 entry by antibodies: potential viral and cellular targets.* J Intern Med, 2007. **262**(1): p. 26-43.
126. Pietzsch, J., et al., *Human anti-HIV-neutralizing antibodies frequently target a conserved epitope essential for viral fitness.* J Exp Med. **207**(9): p. 1995-2002.

127. Seaman, M.S., et al., *Tiered categorization of a diverse panel of HIV-1 Env pseudoviruses for assessment of neutralizing antibodies.* J Virol. **84**(3): p. 1439-52.
128. Li, Y., et al., *Analysis of neutralization specificities in polyclonal sera derived from human immunodeficiency virus type 1-infected individuals.* J Virol, 2009. **83**(2): p. 1045-59.
129. Corti, D., et al., *Analysis of memory B cell responses and isolation of novel monoclonal antibodies with neutralizing breadth from HIV-1-infected individuals.* PLoS One. **5**(1): p. e8805.
130. Moore, J.P. and D.D. Ho, *Antibodies to discontinuous or conformationally sensitive epitopes on the gp120 glycoprotein of human immunodeficiency virus type 1 are highly prevalent in sera of infected humans.* J Virol, 1993. **67**(2): p. 863-75.
131. Visciano, M.L., et al., *Antibodies to the CD4-binding site of HIV-1 gp120 suppress gp120-specific CD4 T cell response while enhancing antibody response.* Infect Agent Cancer, 2008. **3**: p. 11.
132. Pantophlet, R., *Antibody epitope exposure and neutralization of HIV-1.* Curr Pharm Des. **16**(33): p. 3729-43.
133. Wei, X., et al., *Antibody neutralization and escape by HIV-1.* Nature, 2003. **422**(6929): p. 307-12.
134. Rezacova, P., et al., *Structural basis of HIV-1 and HIV-2 protease inhibition by a monoclonal antibody.* Structure, 2001. **9**(10): p. 887-95.
135. Walker, L.M., et al., *A limited number of antibody specificities mediate broad and potent serum neutralization in selected HIV-1 infected individuals.* PLoS Pathog. **6**(8).
136. Scheid, J.F., et al., *Broad diversity of neutralizing antibodies isolated from memory B cells in HIV-infected individuals.* Nature, 2009. **458**(7238): p. 636-40.
137. Kelker, H.C., V.R. Itri, and F.T. Valentine, *A strategy for eliciting antibodies against cryptic, conserved, conformationally dependent epitopes of HIV envelope glycoprotein.* PLoS One. **5**(1): p. e8555.

138. DeVico, A., et al., *Antibodies to CD4-induced sites in HIV gp120 correlate with the control of SHIV challenge in macaques vaccinated with subunit immunogens.* Proc Natl Acad Sci U S A, 2007. **104**(44): p. 17477-82.
139. Douagi, I., et al., *Influence of novel CD4 binding-defective HIV-1 envelope glycoprotein immunogens on neutralizing antibody and T-cell responses in nonhuman primates.* J Virol. **84**(4): p. 1683-95.
140. Li, A., et al., *Synergistic neutralization of a chimeric SIV/HIV type 1 virus with combinations of human anti-HIV type 1 envelope monoclonal antibodies or hyperimmune globulins.* AIDS Res Hum Retroviruses, 1997. **13**(8): p. 647-56.
141. Wu, X., et al., *Focused evolution of HIV-1 neutralizing antibodies revealed by structures and deep sequencing.* Science. **333**(6049): p. 1593-602.
142. Cadogan, M. and A.G. Dalgleish, *Pathogenesis of HIV: non-specific immune hyperactivity and its implications for vaccines.* Clin Med, 2008. **8**(3): p. 267-71.
143. Mikell, I., et al., *Characteristics of the earliest cross-neutralizing antibody response to HIV-1.* PLoS Pathog. **7**(1): p. e1001251.
144. Pancera, M., et al., *Crystal structure of PG16 and chimeric dissection with somatically related PG9: structure-function analysis of two quaternary-specific antibodies that effectively neutralize HIV-1.* J Virol. **84**(16): p. 8098-110.
145. Kwong, P.D., J.R. Mascola, and G.J. Nabel, *Mining the B cell repertoire for broadly neutralizing monoclonal antibodies to HIV-1.* Cell Host Microbe, 2009. **6**(4): p. 292-4.
146. Moore, P.L., et al., *Potent and broad neutralization of HIV-1 subtype C viruses by plasma antibodies targeting a quaternary epitope including residues in the V2 loop.* J Virol.
147. Pejchal, R., et al., *Structure and function of broadly reactive antibody PG16 reveal an H3 subdomain that mediates potent neutralization of HIV-1.* Proc Natl Acad Sci U S A. **107**(25): p. 11483-8.
148. Saphire, E.O., et al., *Crystal structure of a neutralizing human IGG against HIV-1: a template for vaccine design.* Science, 2001. **293**(5532): p. 1155-9.
149. Burton, D.R., et al., *Efficient neutralization of primary isolates of HIV-1 by a recombinant human monoclonal antibody.* Science, 1994. **266**(5187): p. 1024-7.

150. Gauduin, M.C., et al., *Passive immunization with a human monoclonal antibody protects hu-PBL-SCID mice against challenge by primary isolates of HIV-1.* Nat Med, 1997. **3**(12): p. 1389-93.
151. Zwick, M.B., et al., *Molecular features of the broadly neutralizing immunoglobulin G1 b12 required for recognition of human immunodeficiency virus type 1 gp120.* J Virol, 2003. **77**(10): p. 5863-76.
152. Wu, X., et al., *Mechanism of human immunodeficiency virus type 1 resistance to monoclonal antibody B12 that effectively targets the site of CD4 attachment.* J Virol, 2009. **83**(21): p. 10892-907.
153. Allaway, G.P., et al., *Expression and characterization of CD4-IgG2, a novel heterotetramer that neutralizes primary HIV type 1 isolates.* AIDS Res Hum Retroviruses, 1995. **11**(5): p. 533-9.
154. Lagenaur, L.A., et al., *sCD4-17b bifunctional protein: extremely broad and potent neutralization of HIV-1 Env pseudotyped viruses from genetically diverse primary isolates.* Retrovirology. **7**: p. 11.
155. Moore, J.P. and P.J. Klasse, *Thermodynamic and kinetic analysis of sCD4 binding to HIV-1 virions and of gp120 dissociation.* AIDS Res Hum Retroviruses, 1992. **8**(4): p. 443-50.
156. Schon, A., et al., *Some binding-related drug properties are dependent on thermodynamic signature.* Chem Biol Drug Des. **77**(3): p. 161-5.
157. Moore, J.P. and J. Sodroski, *Antibody cross-competition analysis of the human immunodeficiency virus type 1 gp120 exterior envelope glycoprotein.* J Virol, 1996. **70**(3): p. 1863-72.
158. McInerney, T.L., et al., *A human IgG1 (b12) specific for the CD4 binding site of HIV-1 neutralizes by inhibiting the virus fusion entry process, but b12 Fab neutralizes by inhibiting a postfusion event.* Virology, 1997. **233**(2): p. 313-26.
159. Posner, M.R., et al., *Neutralization of HIV-1 by F105, a human monoclonal antibody to the CD4 binding site of gp120.* J Acquir Immune Defic Syndr, 1993. **6**(1): p. 7-14.
160. Wilkinson, R.A., et al., *Structure of the Fab fragment of F105, a broadly reactive anti-human immunodeficiency virus (HIV) antibody that recognizes the CD4 binding site of HIV type 1 gp120.* J Virol, 2005. **79**(20): p. 13060-9.

161. Schon, A., et al., *Thermodynamics of binding of a low-molecular-weight CD4 mimetic to HIV-1 gp120.* Biochemistry, 2006. **45**(36): p. 10973-80.
162. Capon, D.J. and R.H. Ward, *Antiviral effects of CD4 derivatives.* Curr Opin Immunol, 1989. **2**(3): p. 433-8.
163. Byrn, R.A., et al., *Biological properties of a CD4 immunoadhesin.* Nature, 1990. **344**(6267): p. 667-70.
164. Smith, D.H., et al., *Blocking of HIV-1 infectivity by a soluble, secreted form of the CD4 antigen.* Science, 1987. **238**(4834): p. 1704-7.
165. Chamow, S.M., et al., *CD4 immunoadhesins in anti-HIV therapy: new developments.* Int J Cancer Suppl, 1992. **7**: p. 69-72.
166. Capon, D.J., et al., *Designing CD4 immunoadhesins for AIDS therapy.* Nature, 1989. **337**(6207): p. 525-31.
167. Traunecker, A., et al., *Highly efficient neutralization of HIV with recombinant CD4-immunoglobulin molecules.* Nature, 1989. **339**(6219): p. 68-70.
168. Byrn, R.A., et al., *Biological properties of a CD4 immunoadhesin.* Nature, 1990. **344**(6267): p. 667-70.
169. Moore, J.P., et al., *Dissociation of gp120 from HIV-1 virions induced by soluble CD4.* Science, 1990. **250**(4984): p. 1139-42.
170. Manca, F., J.A. Habeshaw, and A.G. Dalgleish, *HIV envelope glycoprotein, antigen specific T-cell responses, and soluble CD4.* Lancet, 1990. **335**(8693): p. 811-5.
171. Fisher, R.A., et al., *HIV infection is blocked in vitro by recombinant soluble CD4.* Nature, 1988. **331**(6151): p. 76-8.
172. Dey, B., C.S. Del Castillo, and E.A. Berger, *Neutralization of human immunodeficiency virus type 1 by sCD4-17b, a single-chain chimeric protein, based on sequential interaction of gp120 with CD4 and coreceptor.* J Virol, 2003. **77**(5): p. 2859-65.
173. Daar, E.S. and D.D. Ho, *Relative resistance of primary HIV-1 isolates to neutralization by soluble CD4.* Am J Med, 1991. **90**(4A): p. 22S-26S.
174. Haim, H., et al., *Soluble CD4 and CD4-mimetic compounds inhibit HIV-1 infection by induction of a short-lived activated state.* PLoS Pathog, 2009. **5**(4): p. e1000360.

175. Clapham, P.R., et al., *Soluble CD4 blocks the infectivity of diverse strains of HIV and SIV for T cells and monocytes but not for brain and muscle cells.* Nature, 1989. **337**(6205): p. 368-70.
176. Smith-Burchnell, C., et al., *Soluble CD4 enhances antiviral activity of anti-HIV serum in vitro.* AIDS, 1991. **5**(8): p. 1030-1.
177. Deen, K.C., et al., *A soluble form of CD4 (T4) protein inhibits AIDS virus infection.* Nature, 1988. **331**(6151): p. 82-4.
178. Kennedy, M.S., et al., *Analysis of synergism/antagonism between HIV-1 antibody-positive human sera and soluble CD4 in blocking HIV-1 binding and infectivity.* AIDS Res Hum Retroviruses, 1991. **7**(12): p. 975-81.
179. Orloff, S.L., et al., *Two mechanisms of soluble CD4 (sCD4)-mediated inhibition of human immunodeficiency virus type 1 (HIV-1) infectivity and their relation to primary HIV-1 isolates with reduced sensitivity to sCD4.* J Virol, 1993. **67**(3): p. 1461-71.
180. Cerutti, N., et al., *Stabilization of HIV-1 gp120-CD4 receptor complex through targeted interchain disulfide exchange.* J Biol Chem, 2010. **285**(33): p. 25743-52.
181. Harris, R.J., K.L. Wagner, and M.W. Spellman, *Structural characterization of a recombinant CD4-IgG hybrid molecule.* Eur J Biochem, 1990. **194**(2): p. 611-20.
182. Langner, K.D., et al., *Antiviral effects of different CD4-immunoglobulin constructs against HIV-1 and SIV: immunological characterization, pharmacokinetic data and in vivo experiments.* Arch Virol, 1993. **130**(1-2): p. 157-70.
183. Ryu, S.E., et al., *Crystal structure of an HIV-binding recombinant fragment of human CD4.* Nature, 1990. **348**(6300): p. 419-26.
184. Ashkenazi, A., et al., *Resistance of primary isolates of human immunodeficiency virus type 1 to soluble CD4 is independent of CD4-rgp120 binding affinity.* Proc Natl Acad Sci U S A, 1991. **88**(16): p. 7056-60.
185. Berger, E.A., T.R. Fuerst, and B. Moss, *A soluble recombinant polypeptide comprising the amino-terminal half of the extracellular region of the CD4 molecule contains an active binding site for human immunodeficiency virus.* Proc Natl Acad Sci U S A, 1988. **85**(7): p. 2357-61.

186. Berger, E.A., J.D. Lifson, and L.E. Eiden, *Stimulation of glycoprotein gp120 dissociation from the envelope glycoprotein complex of human immunodeficiency virus type 1 by soluble CD4 and CD4 peptide derivatives: implications for the role of the complementarity-determining region 3-like region in membrane fusion.* 1991. **88**(18): p. 8082-6.
187. Degar, S., et al., *Replication of primary HIV-1 isolates is inhibited in PM1 cells expressing sCD4-KDEL.* Virology, 1996. **226**(2): p. 424-9.
188. Harris, R.J., et al., *Characterization of a soluble form of human CD4. Peptide analyses confirm the expected amino acid sequence, identify glycosylation sites and demonstrate the presence of three disulfide bonds.* Eur J Biochem, 1990. **188**(2): p. 291-300.
189. Ibegbu, C.C., et al., *Structural features of CD4 required for binding to HIV.* J Immunol, 1989. **142**(7): p. 2250-6.
190. Kahn, J.O., et al., *The safety and pharmacokinetics of recombinant soluble CD4 (rCD4) in subjects with the acquired immunodeficiency syndrome (AIDS) and AIDS-related complex. A phase 1 study.* Ann Intern Med, 1990. **112**(4): p. 254-61.
191. Traunecker, A., W. Luke, and K. Karjalainen, *Soluble CD4 molecules neutralize human immunodeficiency virus type 1.* Nature, 1988. **331**(6151): p. 84-6.
192. Zettlmeissl, G., et al., *Expression and characterization of human CD4:immunoglobulin fusion proteins.* DNA Cell Biol, 1990. **9**(5): p. 347-53.
193. Arthos, J., et al., *Biochemical and biological characterization of a dodecameric CD4-Ig fusion protein: implications for therapeutic and vaccine strategies.* J Biol Chem, 2002. **277**(13): p. 11456-64.
194. *Designing CD4 immunoadhesins for AIDS therapy.* Dis Markers, 1990. **8**(1): p. 35-6.
195. Ashkenazi, A., D.J. Capon, and R.H. Ward, *Immunoadhesins.* Int Rev Immunol, 1993. **10**(2-3): p. 219-27.
196. Allaway, G., P and P.J. Maddon, *Synergistic composition of CD4-based protein and anti-HIV-1 antibody, and methods of using same.* U. S Patent No. 5817767, 1998.

197. Gauduin, M.C., et al., *CD4-immunoglobulin G2 protects Hu-PBL-SCID mice against challenge by primary human immunodeficiency virus type 1 isolates.* J Virol, 1998. **72**(4): p. 3475-8.
198. Trkola, A., et al., *Cross-clade neutralization of primary isolates of human immunodeficiency virus type 1 by human monoclonal antibodies and tetrameric CD4-IgG.* J Virol, 1995. **69**(11): p. 6609-17.
199. Beaudry, G.A. and P.J. Maddon, *CD4-gamma2 and CD4-IgG2 chimeras.* International Publication Number: WO92/13947, Internation Publication Date: 20 August 1992, 1992.
200. Fletcher, C.V., et al., *Nonlinear pharmacokinetics of high-dose recombinant fusion protein CD4-IgG2 (PRO 542) observed in HIV-1-infected children.* J Allergy Clin Immunol, 2007. **119**(3): p. 747-50.
201. Shearer, W.T., et al., *Recombinant CD4-IgG2 in human immunodeficiency virus type 1-infected children: phase 1/2 study. The Pediatric AIDS Clinical Trials Group Protocol 351 Study Team.* J Infect Dis, 2000. **182**(6): p. 1774-9.
202. Jacobson, J.M., et al., *Single-dose safety, pharmacology, and antiviral activity of the human immunodeficiency virus (HIV) type 1 entry inhibitor PRO 542 in HIV-infected adults.* J Infect Dis, 2000. **182**(1): p. 326-9.
203. Shearer, W.T., et al., *Susceptibility of pediatric HIV-1 isolates to recombinant CD4-IgG2 (PRO 542) and humanized mAb to the chemokine receptor CCR5 (PRO 140).* J Allergy Clin Immunol, 2006. **118**(2): p. 518-21.
204. Gauduin, M.C., et al., *Effective ex vivo neutralization of human immunodeficiency virus type 1 in plasma by recombinant immunoglobulin molecules.* J Virol, 1996. **70**(4): p. 2586-92.
205. Trkola, A., et al., *Neutralization sensitivity of human immunodeficiency virus type 1 primary isolates to antibodies and CD4-based reagents is independent of coreceptor usage.* J Virol, 1998. **72**(3): p. 1876-85.
206. Beaudry, G.A. and P.J. Maddon, *CD4-gamma2 and CD4-IgG2 chimeras.* International publication number: WO92/13974. International publication date: 20 August 1992, 1992.
207. Beaudry, G.A. and P.J. Maddon, *Cells expressing a CD4-IgG2 chimeric heterotetramer.* U. S Patent No. 7070991 B2, Date of Patent: 4 July 2006.

208. Norbert, S., W.C. Olson, and C.P. Parkhurst-Lang, *CD4-IgG2 formulations.* Pub. No. US 2005/0142139 A1. Pub. Date: 30 June 2005.
209. Simister, N.E., et al., *An IgG-transporting Fc receptor expressed in the syncytiotrophoblast of human placenta.* Eur J Immunol, 1996. **26**(7): p. 1527-31.
210. Shearer, W.T., et al., *Susceptibility of pediatric HIV-1 isolates to recombinant CD4-IgG2 (PRO 542) and humanized mAb to the chemokine receptor CCR5 (PRO 140).* Journal of Allergy and Clinical Immunology, 2006. **118**(2): p. 518-521.
211. Guex, N. and M.C. Peitsch, *SWISS-MODEL and the Swiss-PdbViewer: an environment for comparative protein modeling.* Electrophoresis, 1997. **18**(15): p. 2714-23.
212. Laemmli, U.K., *Cleavage of structural proteins during the assembly of the head of bacteriophage T4.* Nature, 1970. **227**(5259): p. 680-5.
213. Sattentau, Q.J. and J.P. Moore, *The role of CD4 in HIV binding and entry.* Philos Trans R Soc Lond B Biol Sci, 1993. **342**(1299): p. 59-66.
214. Shearer, W.T., *HIV infection and AIDS.* Prim Care, 1998. **25**(4): p. 759-74.
215. Ashkenazi, A. and S.M. Chamow, *Immunoadhesins as research tools and therapeutic agents.* Curr Opin Immunol, 1997. **9**(2): p. 195-200.
216. Ashorn, P., B. Moss, and E.A. Berger, *Therapeutic strategies employing CD4, the HIV receptor.* Adv Exp Med Biol, 1992. **312**: p. 71-81.
217. Byrn, R.A., et al., *Characterization of in vitro inhibition of human immunodeficiency virus by purified recombinant CD4.* J Virol, 1989. **63**(10): p. 4370-5.
218. Schooley, R.T., et al., *Recombinant soluble CD4 therapy in patients with the acquired immunodeficiency syndrome (AIDS) and AIDS-related complex. A phase I-II escalating dosage trial.* Ann Intern Med, 1990. **112**(4): p. 247-53.
219. Hussey, R.E., et al., *A soluble CD4 protein selectively inhibits HIV replication and syncytium formation.* Nature, 1988. **331**(6151): p. 78-81.
220. Beaudry, G.A. and P.J. Maddon, *CD4-gamma2 and CD4-IgG2 chimeras.* International Publication Number: WO92/13947, 1992.

221. Allaway, G.P. and P.J. Maddon, *Synergistic composition of CD4-based protein and anti-HIV-1 antibody, and methods of using same.* U.S Patent No. 5817767, 1998.
222. Beaudry, G.A. and P.J. Maddon, *Cells expressing a CD4-IgG2 chimeric heterotetramer.* U.S Patent No. 7070991 B2, 2006.
223. Hebert, D.N. and L.M. Gierasch, *The molecular dating game: an antibody heavy chain hangs loose with a chaperone while waiting for its life partner.* Mol Cell, 2009. **34**(6): p. 635-6.
224. Herbert, D.N. and L.M. Gierasch, *The molecular dating game: An antibody heavy chain hangs loose with a chaperone while waiting for its life partner.* Molecular Cell, 2009. **34**: p. 635-636.
225. Vanhove, M., Y.-K. Usherwood, and L.M. Henderson, *Unassembled Ig heavy chains do not cycle from BiP in vitro but require light chains to trigger their release.* Cell press, 2002. **15**: p. 105-114.
226. Chan, C.E., et al., *Optimized expression of full-length IgG1 antibody in a common E. coli strain.* PLoS One. **5**(4): p. e10261.
227. Fan, J.Y., et al., *[Expression of human Fab antibody against keratin in E.coli and its renaturation].* Xi Bao Yu Fen Zi Mian Yi Xue Za Zhi, 2004. **20**(4): p. 441-3.
228. Martineau, P. and J.M. Betton, *In vitro folding and thermodynamic stability of an antibody fragment selected in vivo for high expression levels in Escherichia coli cytoplasm.* J Mol Biol, 1999. **292**(4): p. 921-9.
229. Liu, M., et al., *One-step on-column purification and refolding of a single-chain variable fragment (scFv) antibody against tumour necrosis factor alpha.* Biotechnol Appl Biochem, 2006. **43**(Pt 3): p. 137-45.
230. Simmons, L.C., et al., *Expression of full-length immunoglobulins in Escherichia coli: rapid and efficient production of aglycosylated antibodies.* J Immunol Methods, 2002. **263**(1-2): p. 133-47.
231. Duhamel, R.C., et al., *pH gradient elution of human IgG1, IgG2 and IgG4 from protein A-sepharose.* J Immunol Methods, 1979. **31**(3-4): p. 211-7.
232. Zhou, T., et al., *Structural definition of a conserved neutralization epitope on HIV-1 gp120.* Nature, 2007. **445**(7129): p. 732-7.

233. Jacobson, J.M., et al., *Treatment of advanced human immunodeficiency virus type 1 disease with the viral entry inhibitor PRO 542.* Antimicrob Agents Chemother, 2004. **48**(2): p. 423-9.
234. Chen, B., *SPR biosensor as a tool for screening prion protein binders as potential antiprion leads.* Methods Mol Biol. **627**: p. 147-55.
235. Nanduri, V., et al., *SPR biosensor for the detection of L. monocytogenes using phage-displayed antibody.* Biosens Bioelectron, 2007. **23**(2): p. 248-52.
236. Karlsson, R., *SPR for molecular interaction analysis: a review of emerging application areas.* J Mol Recognit, 2004. **17**(3): p. 151-61.
237. Rich, R.L. and D.G. Myszka, *Spying on HIV with SPR.* Trends Microbiol, 2003. **11**(3): p. 124-33.
238. Adamczyk, M., et al., *Surface plasmon resonance (SPR) as a tool for antibody conjugate analysis.* Bioconjug Chem, 1999. **10**(6): p. 1032-7.
239. Vachali, P., et al., *Surface plasmon resonance (SPR) studies on the interactions of carotenoids and their binding proteins.* Arch Biochem Biophys. **519**(1): p. 32-7.
240. Xie, Z. and J.C. Reed, *Analysis of dimerization of Bcl-2 family proteins by surface plasmon resonance.* Methods Enzymol, 2000. **322**: p. 266-74.
241. Williams, C. and T.A. Addona, *The integration of SPR biosensors with mass spectrometry: possible applications for proteome analysis.* Trends Biotechnol, 2000. **18**(2): p. 45-8.
242. Yuk, J.S. and K.S. Ha, *Proteomic applications of surface plasmon resonance biosensors: analysis of protein arrays.* Exp Mol Med, 2005. **37**(1): p. 1-10.
243. DeVico, A.L., *CD4-induced epitopes in the HIV envelope glycoprotein, gp120.* Curr HIV Res, 2007. **5**(6): p. 561-71.
244. Dey, B., et al., *Structure-based stabilization of HIV-1 gp120 enhances humoral immune responses to the induced co-receptor binding site.* PLoS Pathog, 2009. **5**(5): p. e1000445.
245. Wu, L., et al., *CD4-induced interaction of primary HIV-1 gp120 glycoproteins with the chemokine receptor CCR-5.* Nature, 1996. **384**(6605): p. 179-83.
246. Xiang, S.H., et al., *Epitope mapping and characterization of a novel CD4-induced human monoclonal antibody capable of neutralizing primary HIV-1 strains.* Virology, 2003. **315**(1): p. 124-34.

Chapter 7: Appendices

Appendix 1: Nucleic acid analyses reagents and protocols

1.1 LB Broth

Ten grams of tryptone (Oxoid, Cambridge, England) was combined with 10 g of yeast extract (Biolab, South Africa), 15 g of NaCl (Merck, Darmstadt, Germany) and dissolved in 1 L of dH_2O. The broth was autoclaved at 121 °C for 20 minutes and used when it had cooled to a temperature of 20 °C.

1.2 LB agar plates

Thirty-five grams of LB agar powder (Sigma-Aldrich; St. Louis, USA) was dissolved in 1 L of sterile dH_2O. The dissolved agar powder was autoclaved at 121 °C for 20 minutes and used once it had cooled to 20 °C. Ten millilitres of the dissolved LB agar was poured in sterile petri dishes (available in our laboratory). The plates were used once the LB agar had solidified.

1.3 Ampicillin

One hundred milligrams of ampicillin (available in our laboratory) was dissolved in 1 mL of 75% solution of absolute ethanol (Merck; Darmstadt, Germany). This solution was filtered using a 0.22 micron filter (Millipore; Massauchusetts, USA) and regarded as the 1000X stock. The stock solution was stored at -20 °C when not in use.

1.8 70% Isopropanol

Seventy millilitres of absolute isopropanol (Saarchem; South Africa) was added to 30 mL of sterile dH_2O and mixed thoroughly.

1.9 70% ethanol

Seventy millilitres of absolute ethanol (Merck; Darmstadt, Germany) was added to 30 mL of sterile dH_2O and mixed thoroughly.

1.10 50X TAE buffer

In 1L of sterile dH_2O; 242 g of tris (Sigma-Aldrich; St. Louis, USA), 51 mL of glacial acetic acid (Merck; Darmstadt; Germany) and 100 mL of 0.5 M sodium-EDTA was dissolved. The solution was corrected to have a pH of 8 using concentrated HCl (Merck, Darmstadt; Germany).

1.11 0.7% agarose gel

To make a 0.7% agarose gel, 0.7 g of agarose powder (Sigma-Aldrich; St. Louis, USA) was added to 100 mL of 1X TAE buffer (refer to 1.10). The mixture was heated in a microwave until all the powder had dissolved. When the solution had cooled to approximately 40 °C, 5 µg of ethidium bromide (Promega; Madison, USA) was added to the agarose solution. The solution was then cast and used once it had solidified.

1.12 6X loading buffer

Six times loading was made by adding 25 mg bromophenol blue (Fluka chemika, Buchs, Switzerland) and 3 mL glycerol (Saarchem; Wadeville, South Africa) to 10 mL of dH_2O. DNA samples were diluted with loading buffer to give a final volume of 15 µL before they were loaded in the wells of agarose gel.

Appendix 2: Protein expression and characterisation related reagents

2.1 DMEM additives

DMEM (Sigma-Aldrich; St. Louis, USA) was supplemented with 10 mM of Glutamax™ L-glutamine (Invitrogen; California, USA) and 10% fetal bovine serum (FBS) (Sigma-Aldrich; St. Louis, USA), unless otherwise stated.

2.2 SFM II additives

SFM II was supplement with 10 mM of Glutamax™ L-glutamine (Invitrogen; California, USA) only.

2.3 SDS-PAGE reagents and protocol

4X stacking gel buffer

Three grams of tris (Sigma-Aldrich; St. Louis, USA) was added to 40 mL of ddH_2O and the solution was adjusted to have a pH of 6.8 with concentrated HCl (Merck; Darmstadt, Germany). Fifty millilitres of sterile dH_2O were added thereafter and the solution was stored for up to 3 months in the dark when not used.

4X running gel buffer

To make the 4X running gel buffer, 36.3 g of tris (Sigma-Aldrich; St. Louis, USA) was added to 150 mL of sterile dH_2O. The solution was adjusted to have a pH of 8. 8 with HCl (Merck; Darmstadt, Germany), topped up with ddH_2O to a final solution of 200 mL and then stored at 4 °C for up to 3 months in the dark when not used.

10% SDS solution

Five grams of SDS (Merck; Darmstadt, Germany) was added to 45 mL of ddH_2O and the solution was stored at room temperature for up to 6 month if not used.

10% (W/V) ammonium persulphate solution

An amount of 0.1 g of ammonium persulphate (Sigma-Aldrich; St. Louis, USA) was added to 900 µL of ddH_2O. The solution was used on the day it made and not stored.

Running gel overlay

Absolute isopropanol (Merk, Darmstadt, Germany) was used as the running gel overlay.

2X treatment buffer

One and a half millilitres of 2X stacking gel buffer, 4 mL of 10% of SDS solution, 2 mL of glycerol (Merck; Darmstadt, Germany), 2 mg of bromophenol blue (Fluka chemika, Buchs, Switzerland) and 1.5 mL of sterile dH2O were mixed together to make 2X treatment buffer. For reducing SDS-PAGE conditions, 100 µL of beta-mercaptoethanol (Sigma-Aldrich, St. Louis, USA) was added per 900 µL of 4X treatment buffer. The treatment buffer was made in 500 µL aliquots and thawed to 20 °C before. Unused 2X treatment buffer was kept at -20 °C.

Tank Buffer

To make one litre of tank buffer; 3.3 g of tris (Sigma-Aldrich, St. Louis, USA), 28.8 g of glycine (Saarchem; Wadeville, South Africa) and 2 g of SDS (Merk, Darmstadt, Germany) were dissolved in 1 L of sterile dH_2O.

Coomassie stain solution

Five hundred millilitres of absolute methanol (Merck; Darmstadt, Germany), 100 mL of acetic acid (Sigma-Aldrich, St. Louis, USA) and 400 mL of sterile dH_2O were combined, then 0.25 g of coomassie R-250 (Fluka chemika, Buchs, Switzerland) was dissolved in the solution.

Destain solution

To make destain solution; one adds 50 mL of absolute ethanol (Merk, Darmstadt, Germany) to 70 mL of acetic acid and 880 mL of sterile dH_2O.

Protocol

To make 60 mL of running gel solution for two 1.5 mm thick SDS-PAGE gels; 8.75 mL of monomer solution (Sigma-Aldrich; St. Louis, USA), 15 mL of 4X running gel buffer (refer to appendix 2.3), 0.6 mL of 10% SDS (refer to appendix 2.3) and 26.6 mL of sterile dH_2O were combined and mixed. To commence polymerisation of the acrylamide, 300 µL of 10% (w/v) ammonium persulphate (Sigma-Aldrich; St. Louis, USA) and 20 µL of TEMED (Sigma-Aldrich; St. Louis, USA) were added consecutively to the running gel solution and mixed thoroughly. The running gel solution was cast in Bio-Rad plates (Bio-Rad; Hercules, USA) for polymerisation for approximately 45 minutes till they had solidified.

To make 30 mL of stacking gel solution for two 1.5 mm thick SDS-PAGE gels; 2.66 mL of monomer solution (Sigma-Aldrich; St. Louis, USA), 5 mL of stacking

gel buffer (refer to appendix 2.3), 0.2 mL of 10% SDS solution (refer to appendix 2.3) and 12 mL of sterile dH_2O were combined and mixed thoroughly. To commence polymerisation of the acrylamide, 100 µL of 10% (w/v) ammonium persulphate (Sigma-Aldrich; St. Louis, USA) and 10 µL of TEMED (Sigma-Aldrich; St. Louis, USA) were added consecutively to the stacking gel solution. The stacking gel solution was then cast in Bio-Rad plates (Bio-Rad; Hercules, USA) for a minimum of 45 minutes until they had solidified.

2.4 Western blotting reagents

10 X TBS

Ten grams of NaCl (Merk, Darmstadt, Germany), 30 g of tris (Sigma-Aldrich, St. Louis, USA) and 2 g of KCl (Calbiochem; California, USA) were dissolved in 900 mL of sterile dH_2O. The pH of the solution was adjusted to 7.4 with HCl (Merk, Darmstadt, Germany) before 100 mL of sterile dH_2O was added to complete the solution.

1 X TTBS

One hundred millilitres of 10X TBS (Appendix 2.4) was added to 900 mL of sterile dH_2O. To complete the solution, 1 mL of tween-20 (Sigma-Aldrich, St. Louis, USA) was then dissolved in the solution.

Transfer buffer

Each litre of transfer buffer contains 800 mL of tank buffer (Appendix 2.3) and 200 mL of absolute methanol (Merck, Darmstadt, Germany).

Primary antibody: MT310 (Santa Cruz Biotechnology INC; California, USA)

Three microlitres of stock MT310 (Santa Cruz Biotechnology INC; California, USA) was diluted in 3 mL of 1X TTBS (Appendix 2.4) and poured onto the surface of nitrocellulose membrane and allowed to incubate away from light, undisturbed for a 1 hour.

Secondary antibody: anti-mouse Ig horseradish peroxidase-linked whole antibody (GE Healthcare; Buckinghamshire, England)

Three microlitres of stock anti-mouse Ig horseradish peroxidase-linked whole antibody (GE Healthcare; Buckinghamshire, England) was diluted in 3 mL of 1X TTBS (Appendix 2.4) and poured onto the surface of nitrocellulose membrane and allowed to incubate away from light, undisturbed for a 1 hour.

2.5 Protein-A agarose beads (Bio-Rad; Hercules, USA)

The Protein-A agarose beads (Bio-Rad; Hercules, USA) were stored in 1X PBS (Sigma-Aldrich; St. Louis, USA) containing 0.1% sodium azide (Sigma-Aldrich; St. Louis, USA). Before use, the beads were washed thoroughly with 1X PBS (Sigma-Aldrich; St. Louis, USA) without sodium azide (Sigma-Aldrich; St. Louis, USA).

2.6 Binding buffer (0.02 M sodium phosphate pH 6.5)

Binding buffer was made combining 37.5 mL of 0.1 M sodium phosphate (di-sodium salt) solution (Fluka chemika, Buchs, Switzerland) with 62.5 mL of sodium phosphate (mono-sodium salt) (Sigma-Aldrich; St. Louis, USA) solution and dissolving the two combined solutions in 400 mL of sterile dH_2O. The solution was filtered using a 0.22 micron Millipore filter (Millipore; Massauchusetts, USA) before use. Unused buffer was stored at 4 °C for up to 1 month.

2.7 Elution buffer (0.1 M citric acid buffer at pH 3.5)

The elution buffer was made by combining 31.5 mL of trisodium citrate dehydrate (Merck; Darmstadt, Germany) solution with 68.5 mL of sodium citrate monohydrate (Sigma-Aldrich; St. Louis, USA) solution. The solution was filtered using a 0.22 micron Millipore filter (Millipore; Massauchusetts, USA) before use. Unused buffer was stored at 4 °C for up to 1 month.

2.8 Neutralisation solution (1M tris-HCl at pH 9)

A mass of 6.057 g of tris (Sigma-Aldrich; St. Louis, USA) was dissolved into 50 mL of sterile dH_2O and the pH of solution was corrected to a value of 9 using concentrated HCl (Merck; Darmstadt, Germany).

2.9 Regeneration buffer (50 mM NaCl and 50 mM NaOH)

To make the regeneration solution; 0.14 g of NaCl (Sigma-Aldrich; St. Louis, USA) and 0.1 g of NaOH (Sigma-Aldrich; St. Louis, USA) were dissolved together in 500 mL of sterile dH_2O.

2.10 Anti-gp120 antibody cocktail

The ID6, Chessie supernatant and NEA antibodies were diluted in a 1: 1000 with 1X TTBS (Appendix 2.4), applied to the nitrocellulose blot on a flat surface and allowed to incubate undisturbed for 1 hour.

2.11 HBS

HBS was made by combining 10 M hepes (Sigma-Aldrich, St. Louis, USA), 150 mM NaCl (Sigma-Aldrich, St. Louis, USA), 3 mM EDTA (Calbiochem, Germany) and 0.01% tween-20 (Sigma-Aldrich, St. Louis, USA) in 2 L of sterile ddH_2O. The pH of the buffer was adjusted to a value of 7. 4. The buffer was

filtered using a 0.22 micron Millipore filter (Millipore; Massauchusetts, USA) before use.